PAUL SCHERRER INSTITUT

PSI

Wir schaffen Wissen – heute für morgen

Muon Spin Rotation (μSR) technique and its applications in magnetism and superconductivity

Zurab Guguchia
Laboratory for Muon Spin Spectroscopy
Paul Scherrer Institut

Muon is a Local Magnetic Probe

Muon probes the local magnetism from within the unit cell

Muon probes the local magnetic response of a superconductor (Meissner screening or flux line lattice)

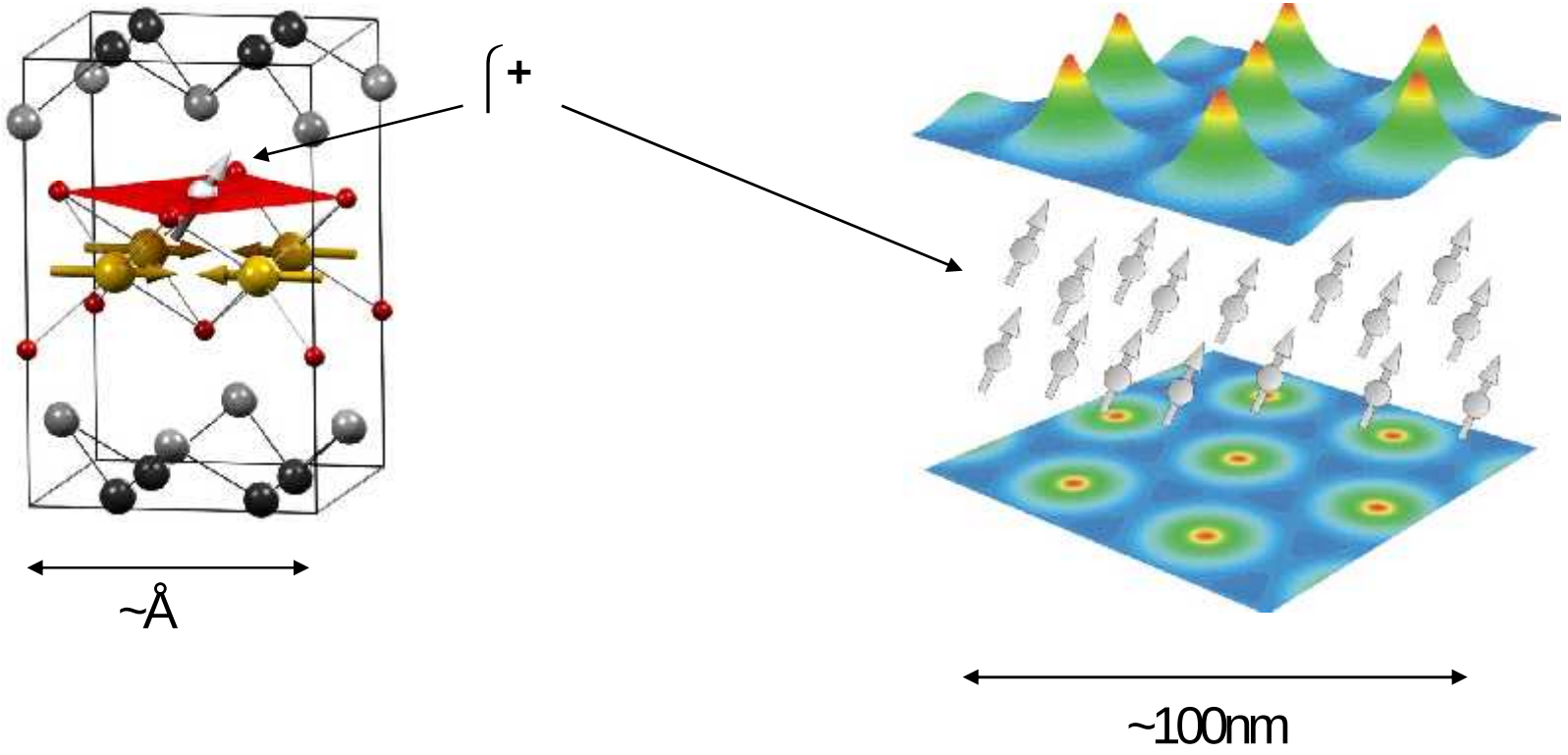

PAUL SCHERRER INSTITUT

Outline

1. Muon Properties

- Pion decay
- Muon decay
- Parity violation
- Muon spin precession

2. Muon Spin Rotation / Relaxation (⌠SR)

- Facilities around the world
- Muon production at PSI
- ⌠SR instruments at PSI
- ⌠SR principle
- Muon thermalization / Muon stopping sites / Muon stopping ranges
- Measurement geometries

3. Muon Spin Rotation / Relaxation on Magnetic Materials

- Different static depolarization functions and examples
- Magnetic phase separation / coexistence of different magnetic phases
- Magnetic fluctuations

4. Muon Spin Rotation on Superconducting Materials

- Using low energy μSR to study the Meissner state of superconductors
- Using bulk μSR to study the Vortex state of superconductors
- Superfluid density and the symmetry of the superconducting gap
- Magnetic and superconducting phase diagrams of Fe-based materials

5. Summary

PAUL SCHERRER INSTITUT

PSI

Muon Properties

PAUL SCHERRER INSTITUT

What is a Muon? Cosmics

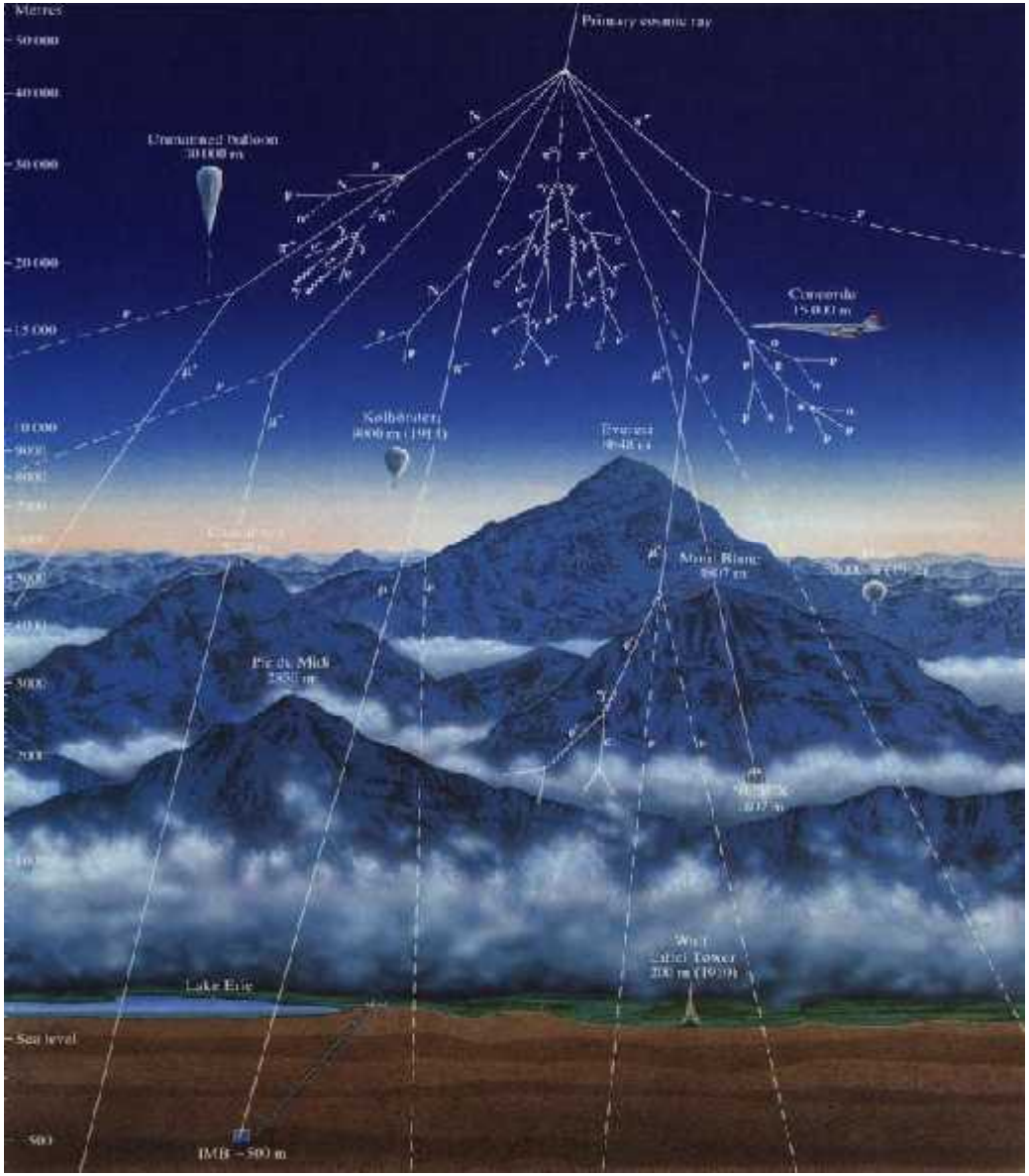

Muon Flux at sea level:
~ 1 Muon/Minute/cm²

Mean Energy:
~ 2 GeV

Elementary particle/antiparticle:

mass:	< 200 x electron mass (105.6MeV/c^2) < 1/9 x proton mass
charge:	+ e, oder - e
spin:	1/2
magnetic moment :	3.18 x μ_p (8.9 x μ_N), g H 2.00
gyromagnetic ratio:	85.145 kHz/G
unstable particle:	**mean lifetime: 2.2 µs** **N(t) = N(0)exp(-t/ ⎜)**

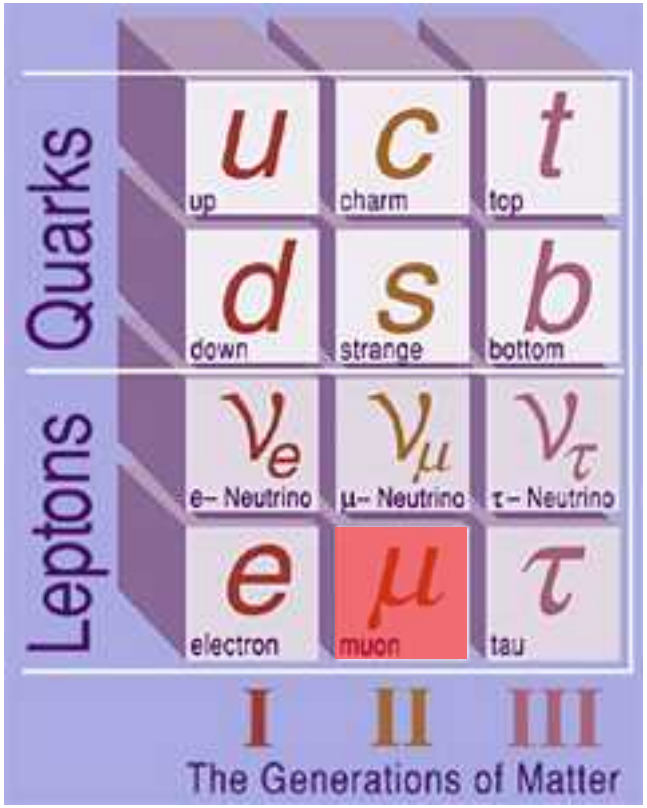

Muon production and polarised beams

Pions as intermediate particles

Protons of 600 to 800 MeV kinetic energy interact with protons or neutrons of the nuclei of a light element target to produce pions.

$$p + p \rightarrow \pi^+ + p + n$$

Pions are unstable (lifetime 26 ns).
They decay into muons (and neutrinos):

$$\pi^+ \rightarrow \mu^+ + \nu_\mu$$

The muon beam is 100 polarised with S_μ antiparallel to P_μ.

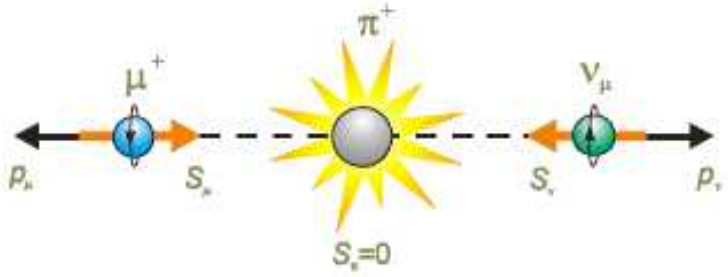

Momentum: P_μ=29.79 MeV/c. Kinetic energy: E_μ=4.12 MeV.

Muon as Result of Pion Decay

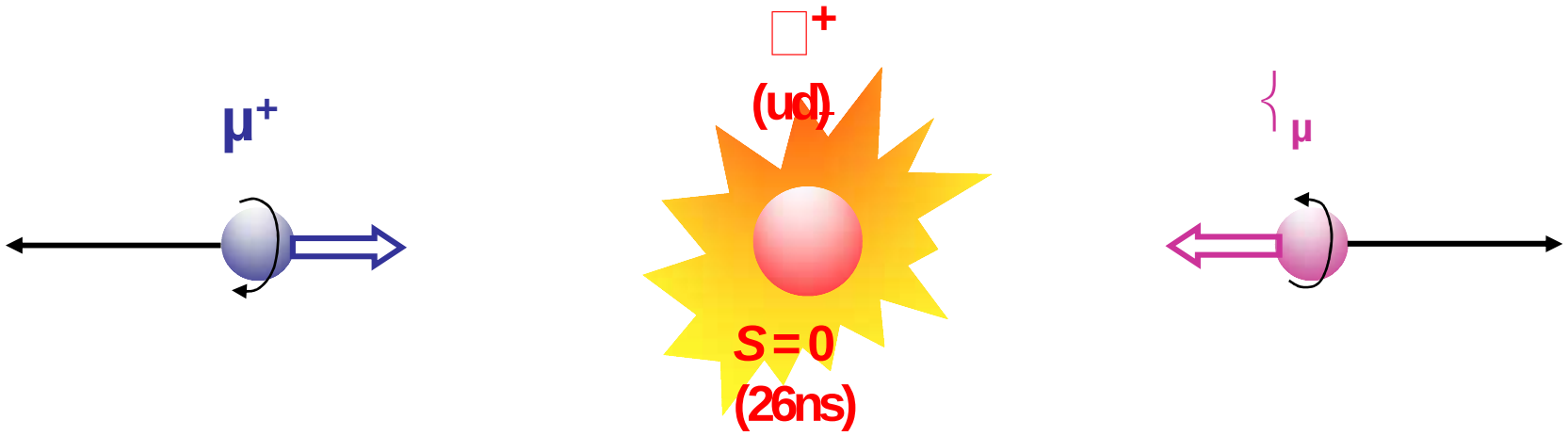

Two-body decay	▶	muon has always the energy 4.1 MeV in the reference frame of the pion (assuming $m_\nu = 0$)
Spin pion = 0	▶	Muon has a spin 1/2 and is 100% polarized (as only left-handed neutrinos are produced)

Muon Decay

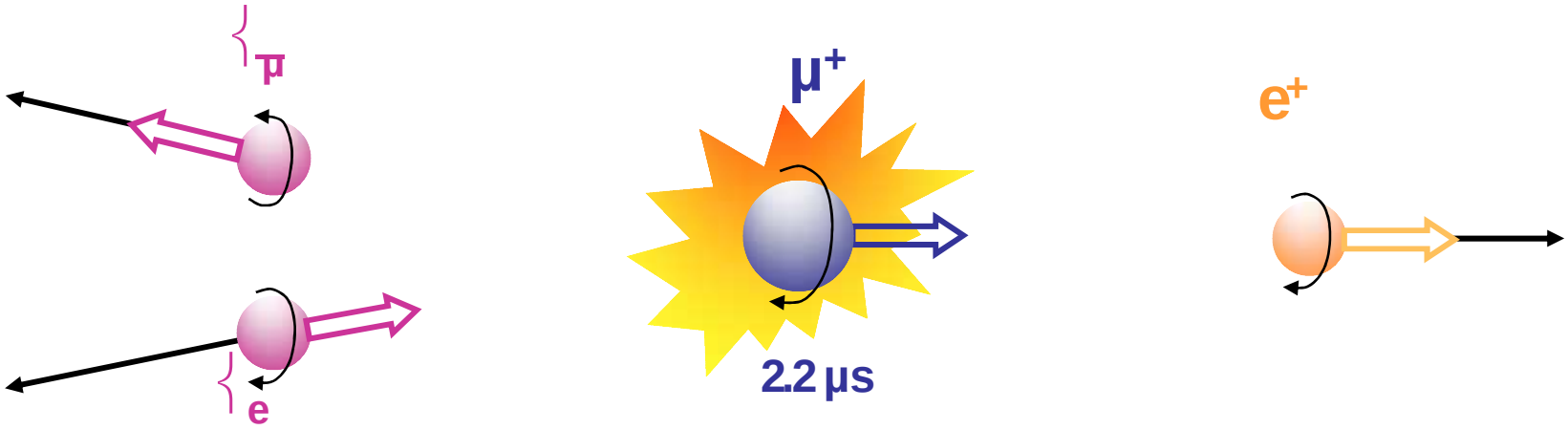

Three-body decay	▶	Distribution of positrons energies
Weak-decay of muon	▶	Parity-violation leading to positrons emitted anisotropically

Measuring P(t): Muon Decay $\mu^+ \rightarrow e^+ + \bar{\nu}_\mu + \nu_e$

- Muon decay (life time 2.2. μs) violates parity conservation

→ asymmetric decay

- Positrons preferentially emitted along muon spin (along polarization vector of muon ensemble)

$$\frac{dN_{e^+}(\theta)}{d\Omega} \propto (1+\frac{1}{3}P\cos\theta) = (1+\frac{1}{3}\vec{P}\cdot\vec{n})$$

$\vec{n}$: direction of observation (detector position)

- Measuring positrons allows to observe time evolution of the polarization P(t) of the muon ensemble
- Positron intensity as a function of time after implantation:

$$N_{e^+}(t) = N_0\left[1+A_0P(t)\right]e^{-\frac{t}{\tau_\mu}} \qquad P(t) = \vec{P}(t)\cdot\vec{n}$$

- A_0: Maximum observable asymmetry
  theoretically: A_0=1/3
  practically it depends on setup (average over solid angle, absorption in materials): A_0 = 0.25 - 0.30
- $A_0P(t)$ is called asymmetry: A(t)

For $P = 1$:

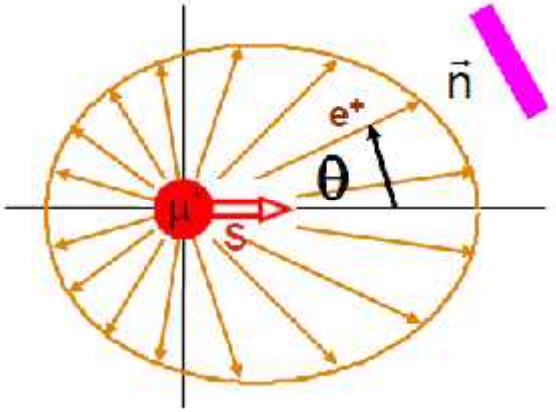

$$\frac{dN_{e^+}(0)}{d\Omega} \propto (1+\frac{1}{3}P\cos\theta)$$

θ : angle between spin (polarization) and positron direction

Anisotropic Muon Decay

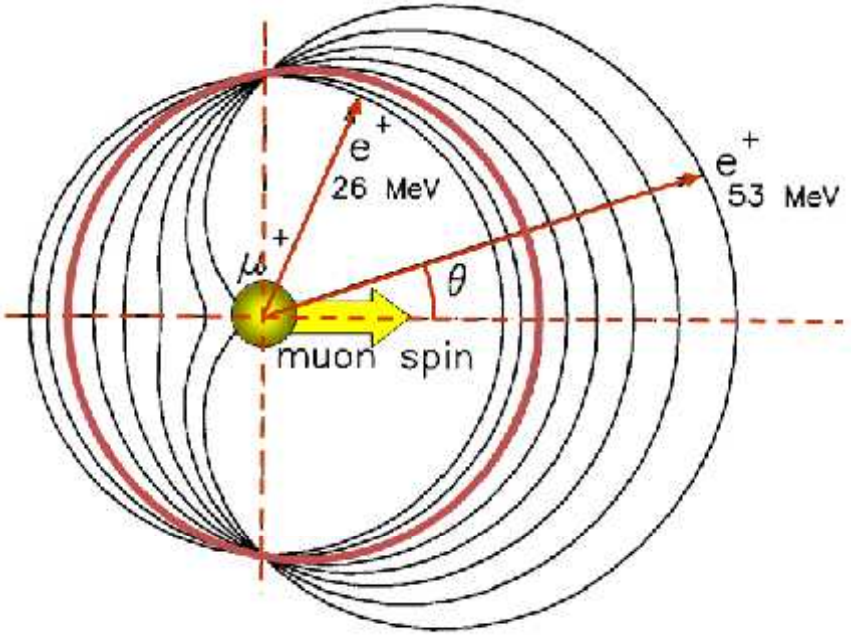

Angular distribution of positrons from the parity violating muon decay:

$$W(E,\theta) = 1 + a(E)\cos(\theta)$$

The asymmetry parameter $a = 1/3$ when all positron energies E are sampled with equal probability.

Positrons preferentially emitted along direction of muon spin at decay time

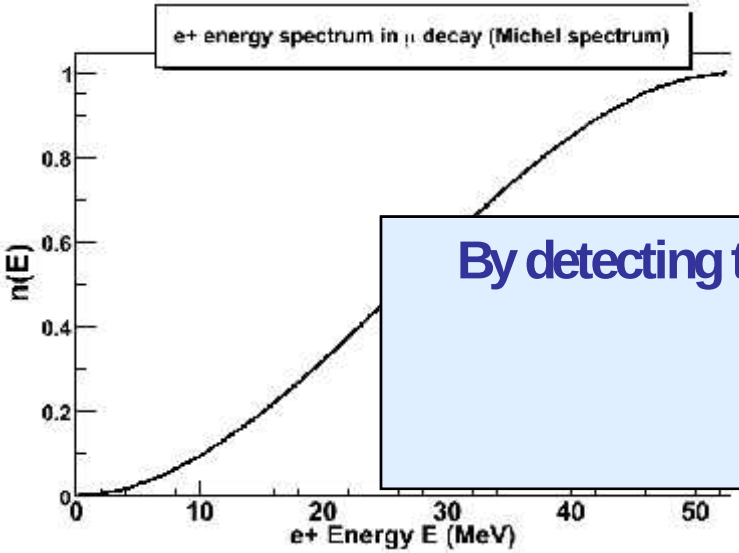

By detecting the spatial positron emission as a function of time

▼

time evolution of muon spin !!!

Muon Spin Precession – Larmor frequency

$$|\psi\rangle = |\uparrow\rangle$$

$$\chi = \begin{pmatrix} 1 \\ 0 \end{pmatrix}$$

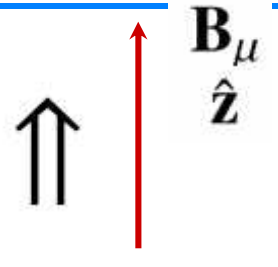

- Field axis: quantization axis
- Spin-state eigenvalue of S_z
- Stationary state

Muon Spin Precession – Larmor frequency

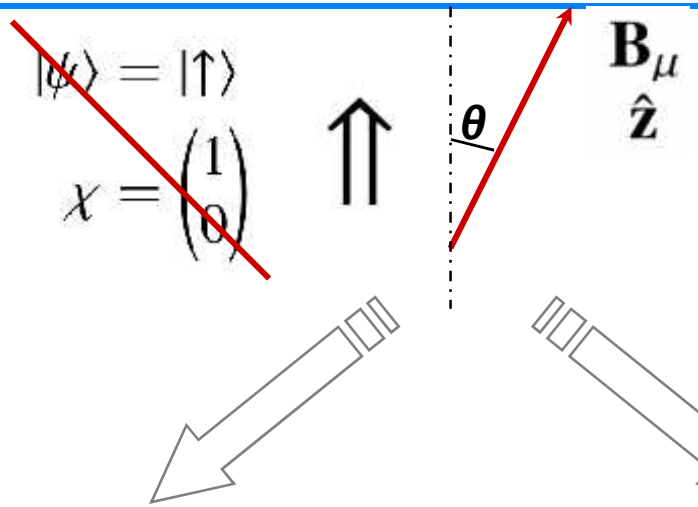

- Field axis: quantization axis
- ~~Spin state eigenvalue of S_z~~
- ~~Stationary state~~

Quantum Mechanics:

$\mathbf{B}_\mu$ quantization axis

χ in the new base $\Rightarrow \chi = \begin{pmatrix} \cos\frac{\theta}{2} \\ \sin\frac{\theta}{2} \end{pmatrix}$

Calculation of $\chi(t)$

with time dependent Schrödinger Eq.

Calculation expectation values of S_α

$\langle S_\alpha \rangle = \chi^\dagger S_\alpha \chi$

Project back to the ref. frame of the lab.

Classically:

Torque: $\boldsymbol{\tau} = \mathbf{m} \times \mathbf{B}_\mu = \gamma_\mu \mathbf{S} \times \mathbf{B}_\mu$

Euler's Eq.: $\frac{d\mathbf{S}}{dt} = \boldsymbol{\tau}$

$\Rightarrow \frac{d\mathbf{S}}{dt} = \gamma_\mu \mathbf{S} \times \mathbf{B}_\mu$

Muon Spin Precession – Larmor frequency

$$\mathbf{P} = \frac{\langle \mathbf{S} \rangle}{\frac{\hbar}{2}}$$

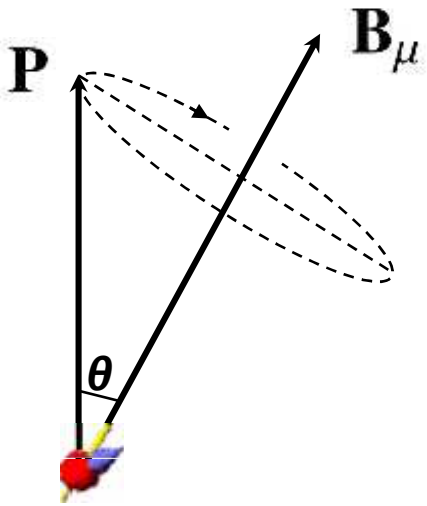

Classically:

Torque: $\boldsymbol{\tau} = \mathbf{m} \times \mathbf{B}_\mu = \gamma_\mu \mathbf{S} \times \mathbf{B}_\mu$

Euler's Eq.: $\frac{d\mathbf{S}}{dt} = \boldsymbol{\tau}$

$\Rightarrow \frac{d\mathbf{S}}{dt} = \gamma_\mu \mathbf{S} \times \mathbf{B}_\mu$

Larmor precessions with angular velocity: $\omega_L = \gamma_\mu B_\mu$

with $\gamma_\mu = \frac{e}{2m_\mu} g_\mu = 8.51615 \times 10^8$ rad/sT

Frequency: $\frac{\gamma_\mu}{2\pi} = 135.539$ MHz/T

Muon Spin Precession - Bloch Equation

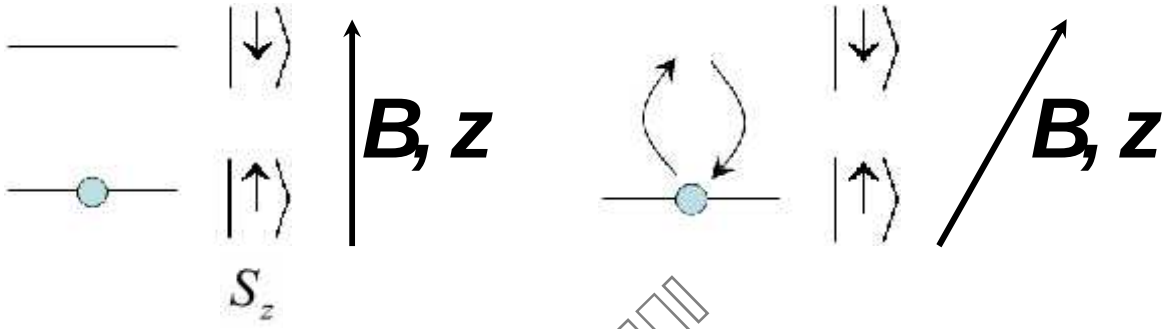

Rabi Oscillations

$\langle S_x \rangle$ and $\langle S_y \rangle$ precess with the Larmor frequency ω_L

Ehrenfest Theorem

Bloch Equation

$$\frac{d\vec{m}}{dt} = \gamma \vec{m} \cdot \vec{B}$$

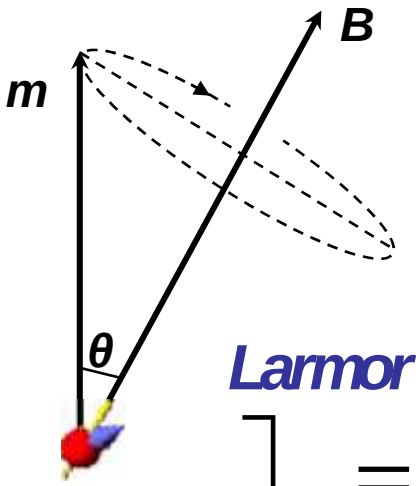

Larmor frequency

$$\omega_L = \gamma \left| \vec{B} \right|$$

Summary - Muon Properties

The three key properties making ⌈SR possible:

1. The muon is 100% spin polarized.
2. The decay positron is preferentially emmitted along the muon spin direction.
3. The muon spin precesses in a magnetic field.

PAUL SCHERRER INSTITUT

PSI

Muon Spin Rotation / Relaxation

μSR Facilities around the World

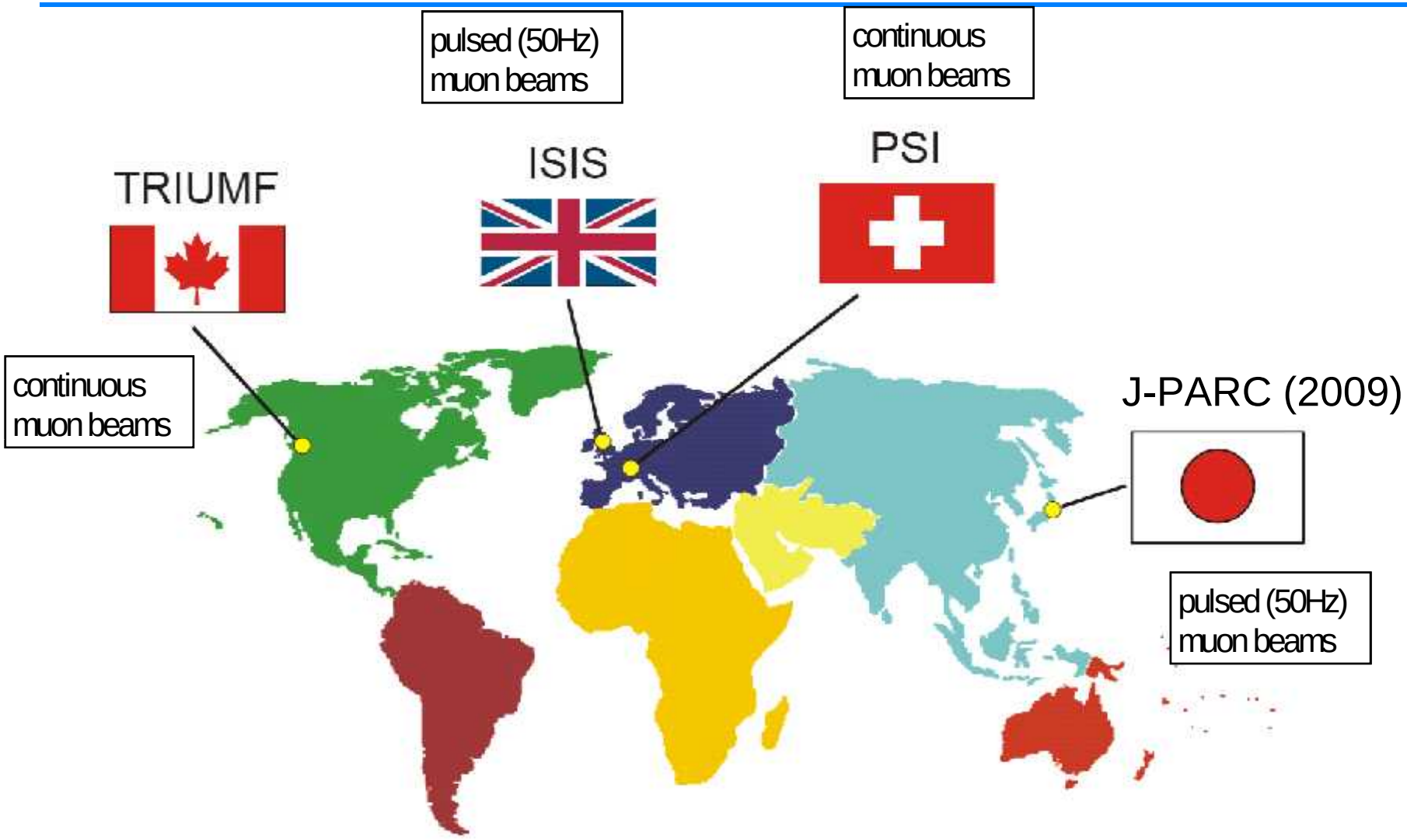

Facilities under study in South Corea, China, US

From "μSR brochure" by J.E Sonier, Simon-Fraser-Univ., Canada, 2002. http://musr.org/intro/musr/muSRBrochure.pdf

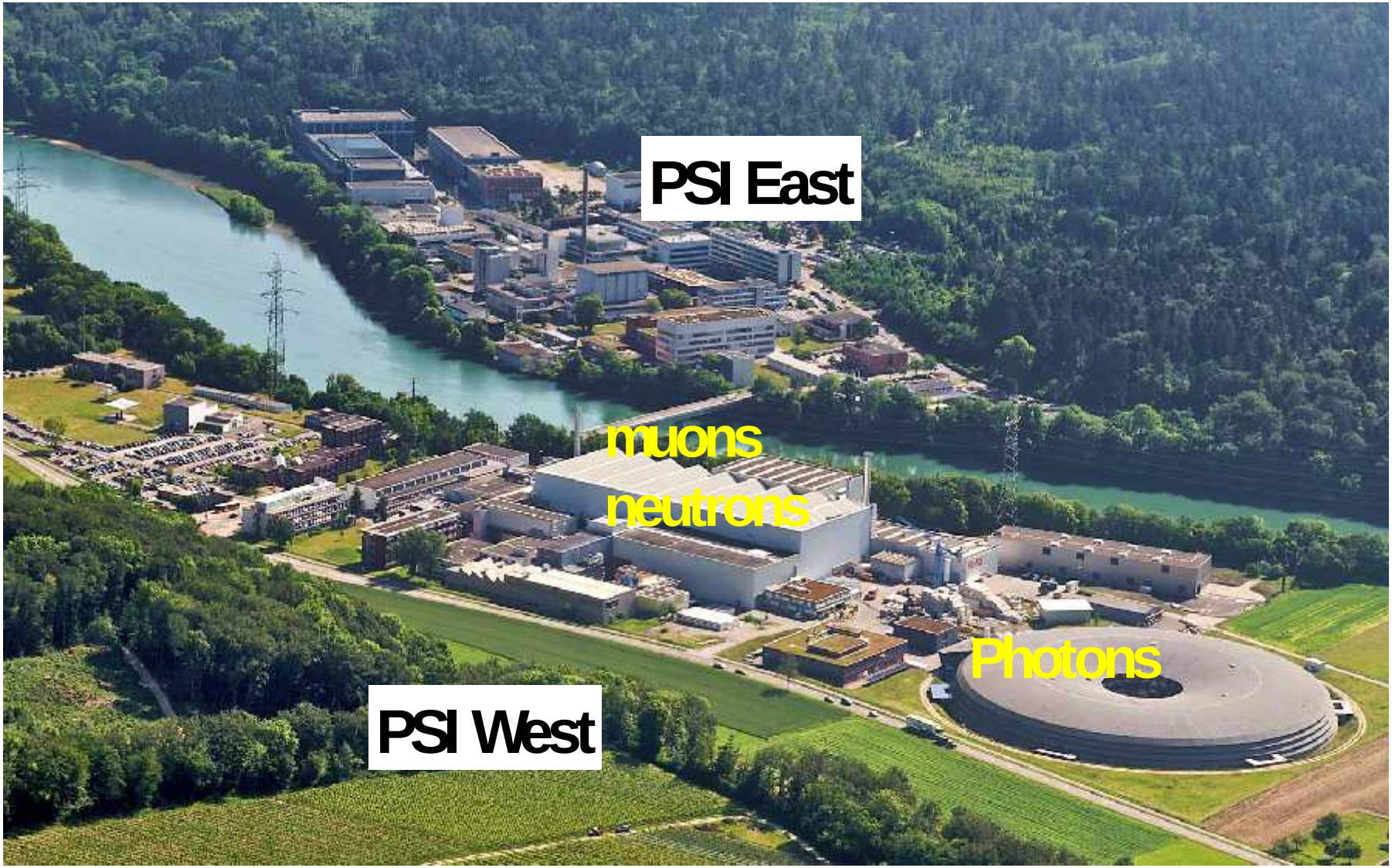
PSI East
muons
neutrons
Photons
PSI West

PAUL SCHERRER INSTITUT

Generation of polarized muons (μ^+)

2.2 mA ≅ 1.4 10^{16} Protons/sec

with 600 MeV

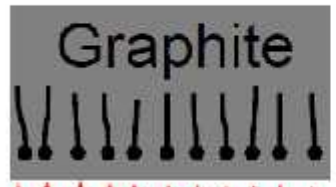

Production Target

π^+

$p + C \rightarrow \pi^+ \pi^- p\ n \ldots$

μ^+

„Surface“ muons

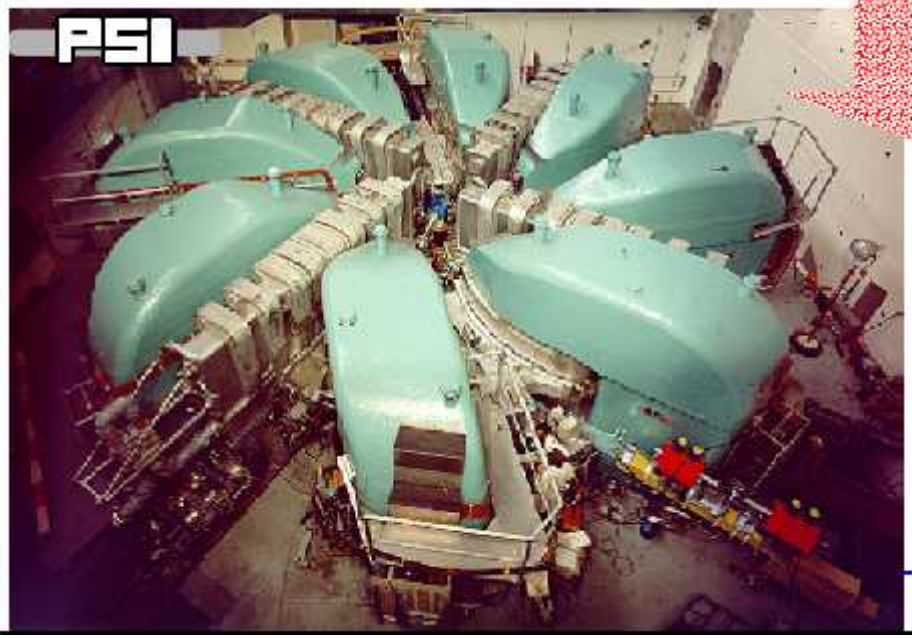

~10^7- 10^8 μ^+/sec

100 % pol.

~ 4 MeV

generally used for “bulk” condensed matter studies

For thin film studies: eV-30 keV

Muon Production at PSI

600 MeV Proton Cyclotron at PSI:

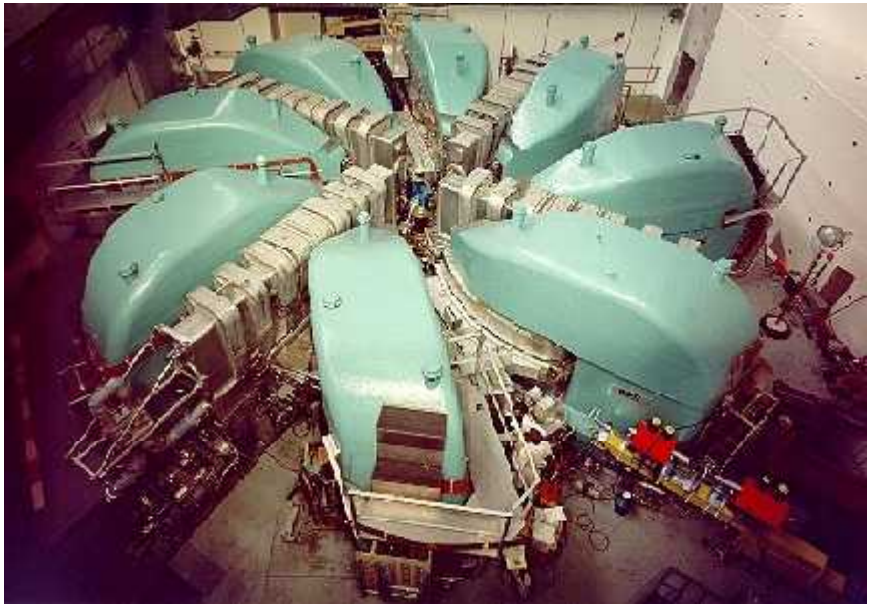

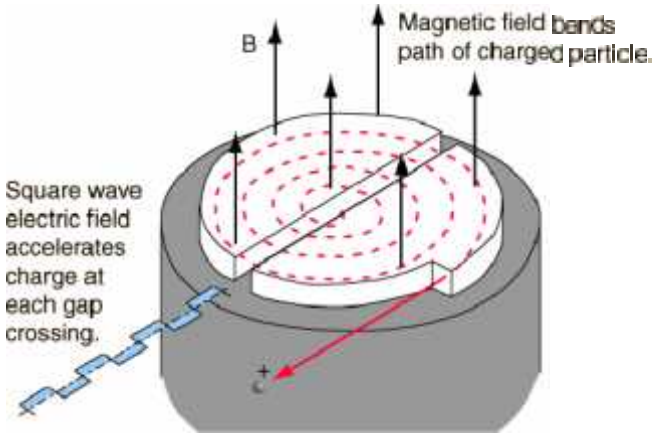

Muons from Pion Decay:

$$\pi^+ \rightarrow \mu^+ + \nu_\mu$$

$$\pi^- \rightarrow \mu^- + \bar{\nu}_\mu$$

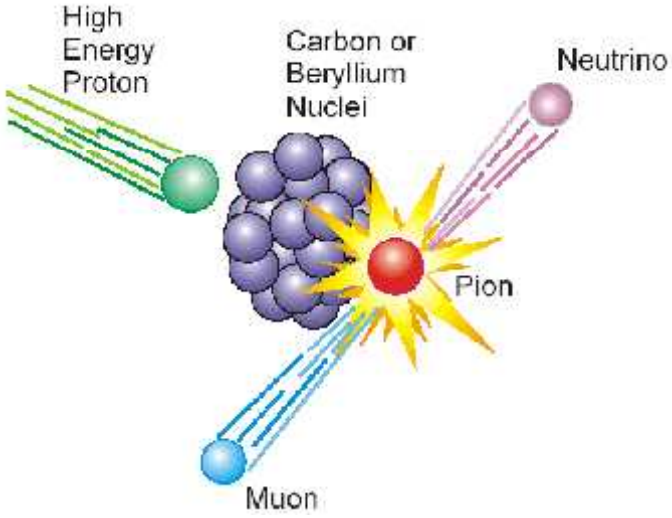

Muon kinetic energy: 4 MeV

PSI Experimental Hall

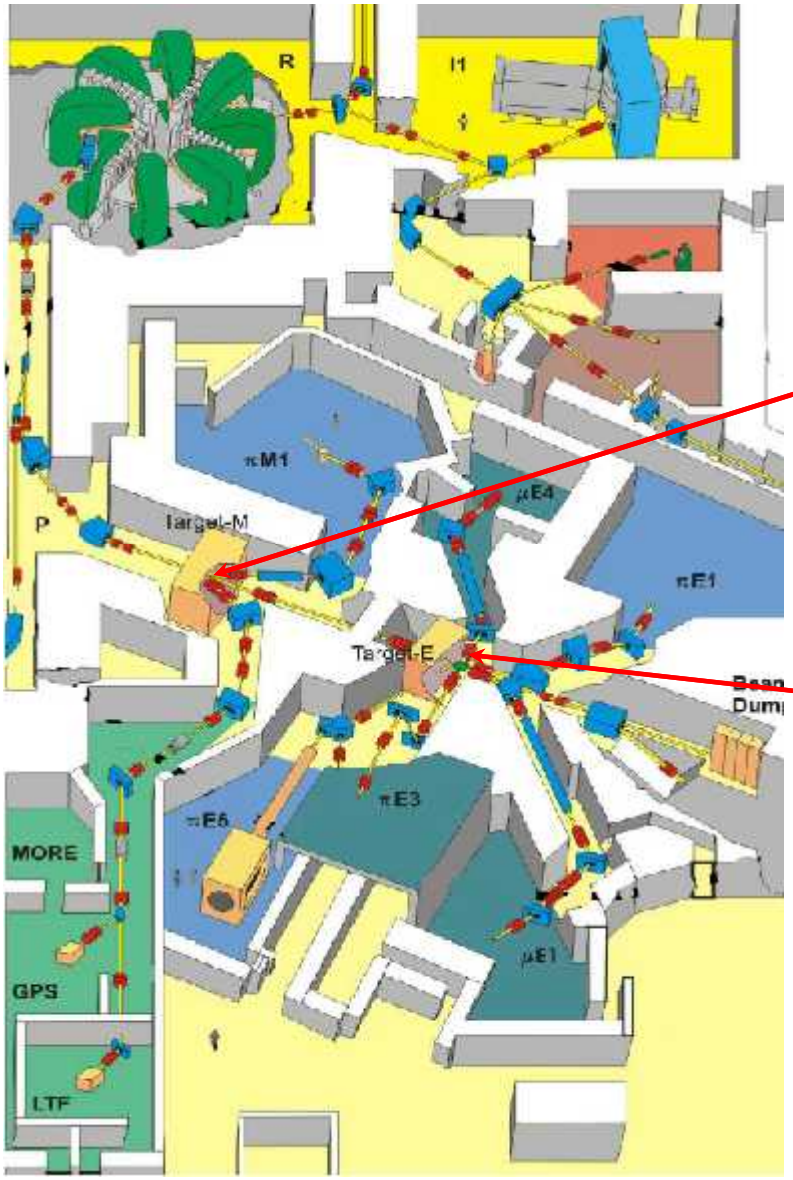

Target M
Thin graphite (5 mm)

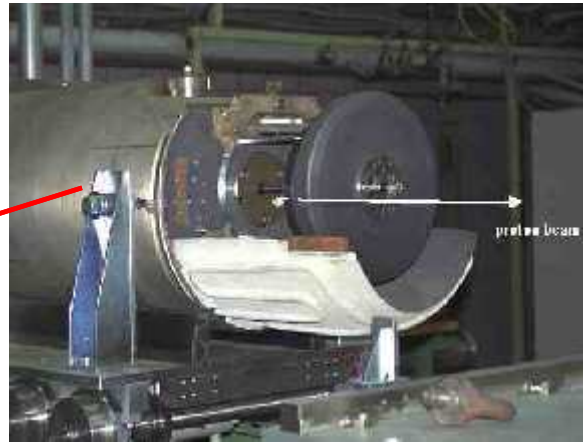

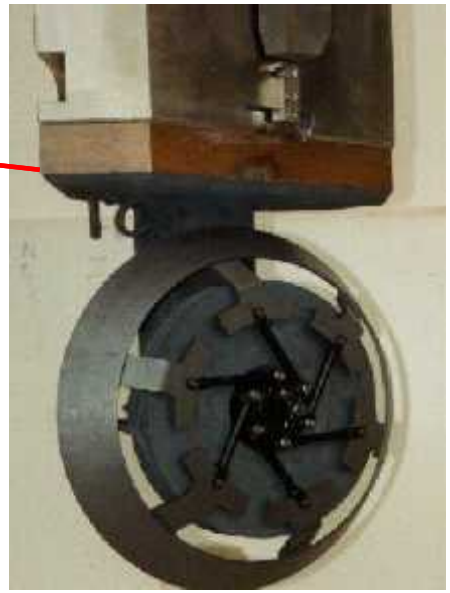

Target E
4cm graphite

"necessary component to expand proton beam before SINQ"

SμS – The Swiss Muon Source

High Field μSR

Muon energy:
4.2 MeV (μ^+)

9.5T, 20mK

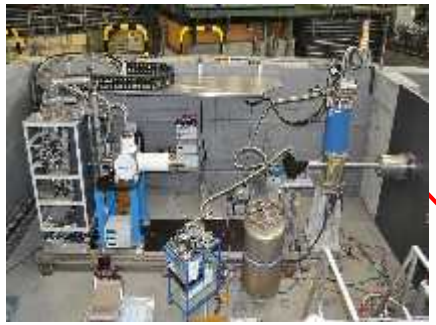

GPS

General Purpose Surface Muon Instrument
Muon energy: 4.2 MeV (μ^+)

0.6T, 1.8K

Shared Beam Surface Muon Facility
(Muon On REquest)

LTF

Low Temperature Facility
Muon energy: 4.2 MeV (μ^+)

3T, 20mK- 4K

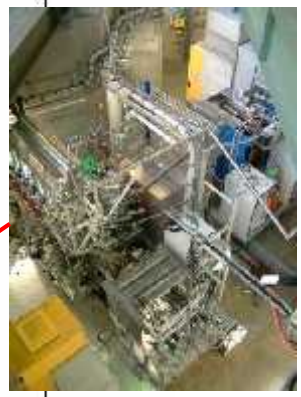

LEM

Low-energy muon beam and instrument , tunable energy (0.5-30 keV, μ^+), *thin-film, near-surface and multi-layer studies (1-300 nm)*

0.3T, 2.9K

DOLLY

General Purpose Surface Muon Instrument
Muon energy: 4.2 MeV (μ^+)

0.5T, 300mK

GPD

General Purpose Decay Channel Instrument
Muon energy: 5 - 60 MeV (μ^+ or μ^-)

0.5T, 300mK
2.8GPa

Principle of a ⌠SR Experiment

Implantation of muons into the sample

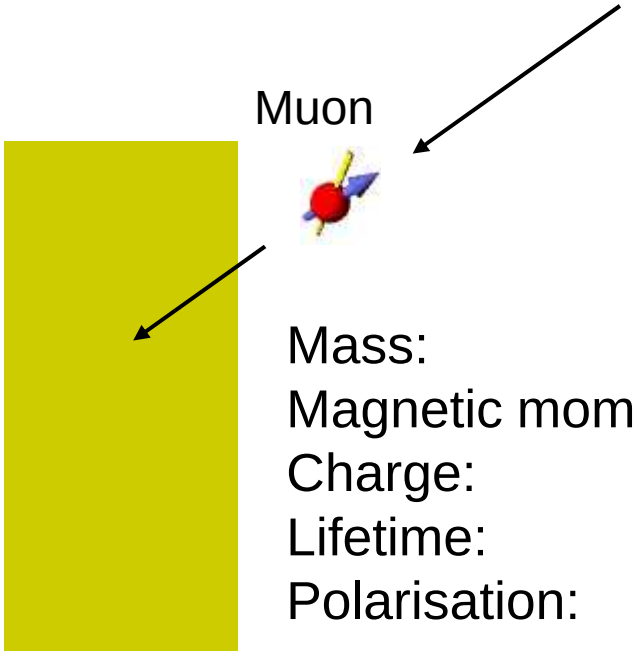

Mass:	$m_{\lceil}$ H 207 m_e H 1/9 m_p
Magnetic moment:	$\lceil_{\lceil}$ H 3 $\lceil_p$
Charge:	+e
Lifetime:	$t_{\lceil}$ H 2.2 ⌠s
Polarisation:	100 %

Principle of a ⌠SR Experiment

Detection of the decay positron

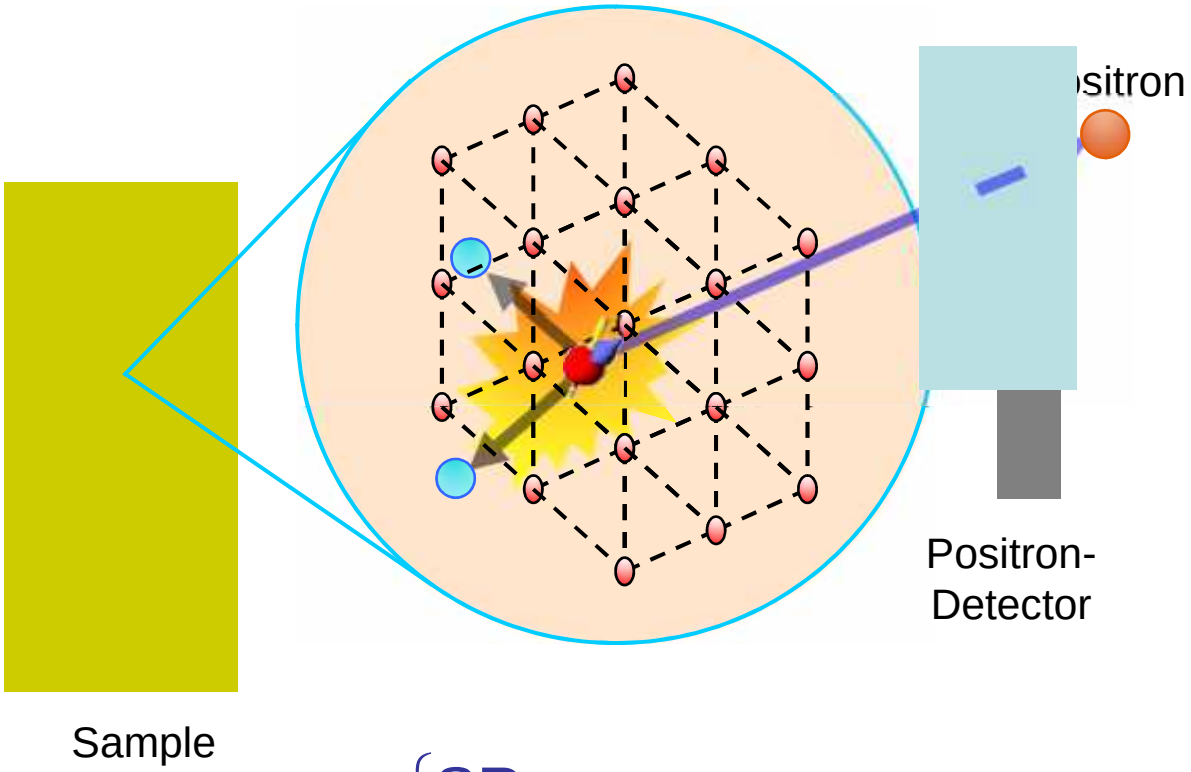

⌠SR

2 ⌠s

Static field distribution
Sensitivity: 10^{-3} – 10^{-4} ⌠B

Fluctuation rates
(10^{5} – 10^{9} Hz)

Muons stopping in matter:

4.1-MeV μ^+, $v \sim 0.27 \cdot c$

↓

ionization of atoms, 10^5-10^6 excess e^-

↓

2 – 3 keV, $v \sim 0.007 \cdot c$

↓

Muonium formation (μ^+e^-), successive e^- capture and loss

↓

100 eV, $v \sim 0.0013 \cdot c$

↓

mainly elastic collisions, stop at intersitial site

- Total stopping time in condensed matter: < 0.1 ns
- Only electrostatic processes
  ➡ no loss of polarization
- Penetration: ~0.1 mm

μSR – Muons Stopping in Matter

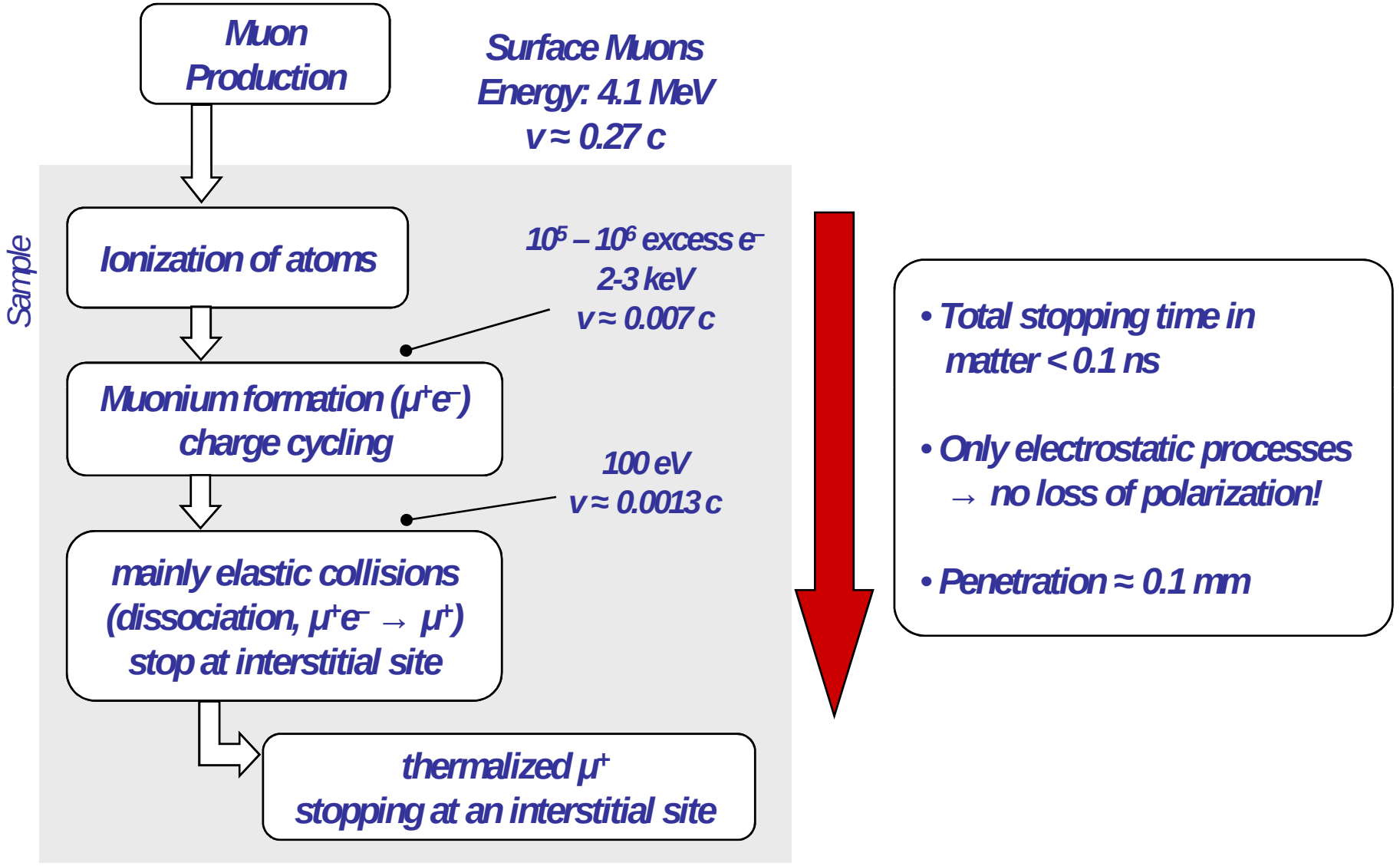

Interstitial Muon Stopping Sites

Electrostatic potential map:

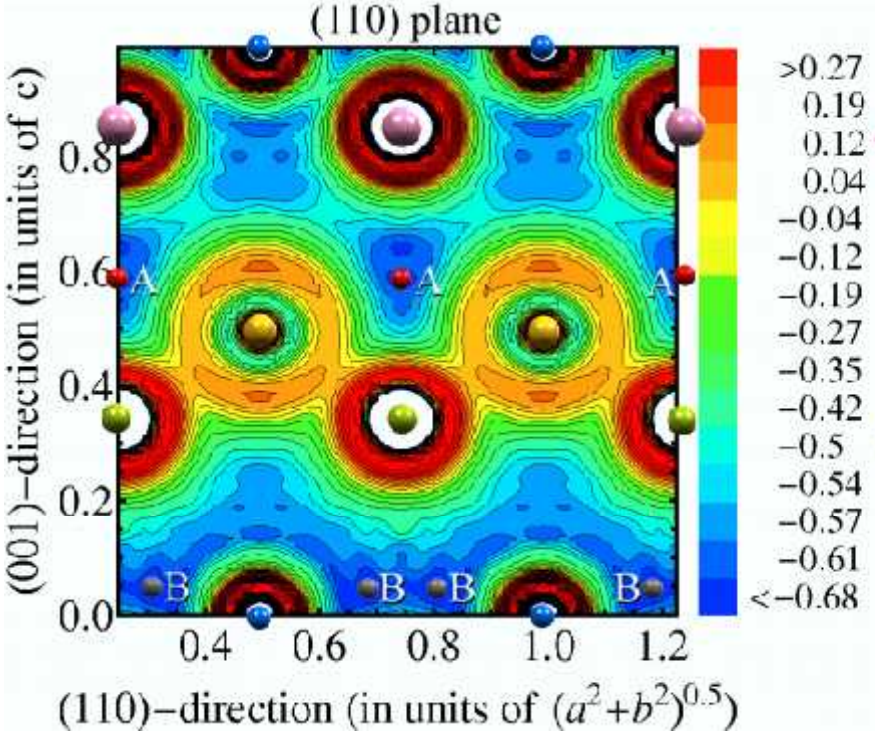

CeOFeAs structure:

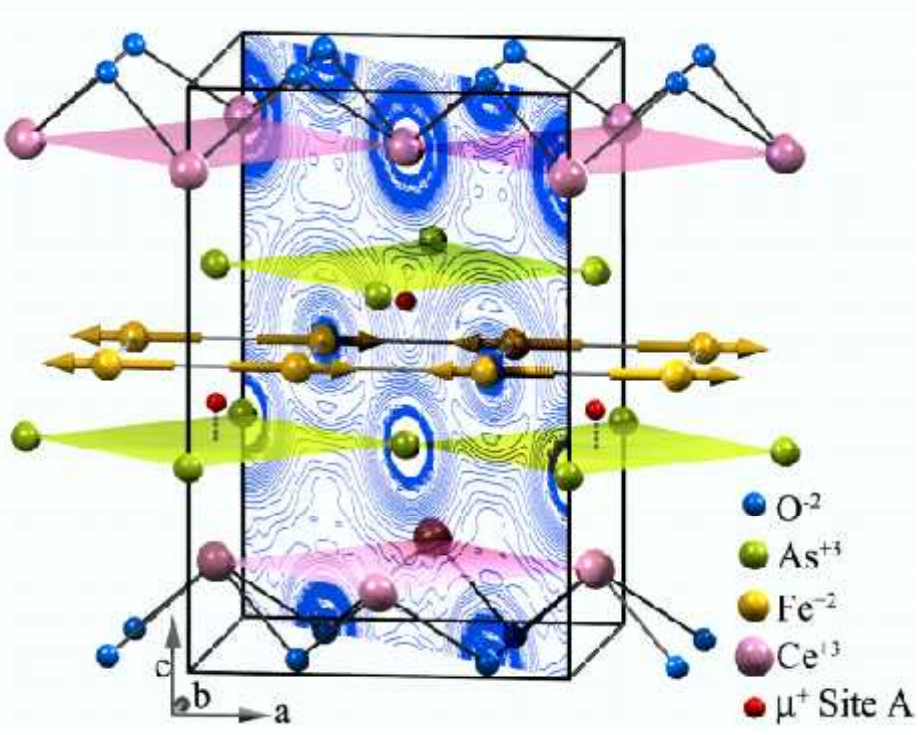

Positive muon likes to stop:

- In the potential minimum
- High symmetry sites
- Near negative ions (e.g. O^{2-}, As^{3-}) (muon hydrogen bond like in OH with ~1 A bond length)
- Large spaces in the crystal structure

Muon Implantation Depth

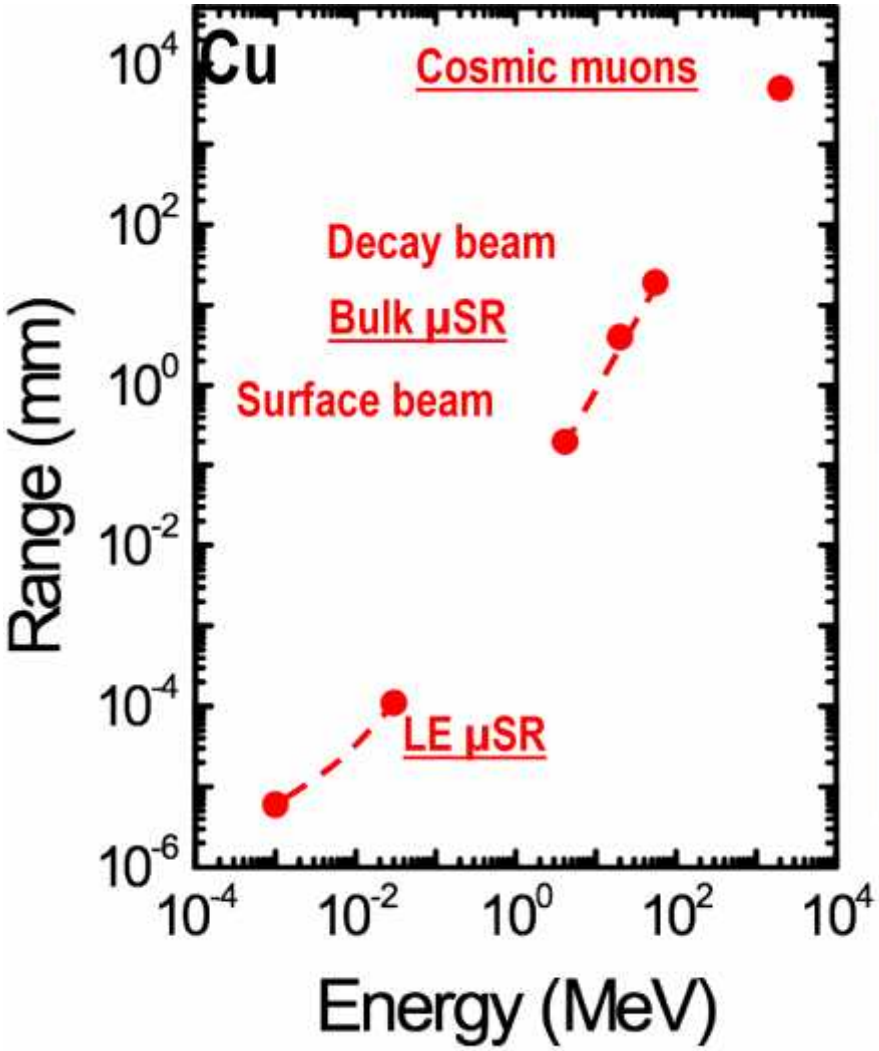

Bulk μSR:

- *"Normal" samples (sub-mm)*
- *Bulky samples + samples in containers or pressure cells*

LE-μSR:

- *Depth-selective investigations (1–200 nm)*

PAUL SCHERRER INSTITUT

μSR

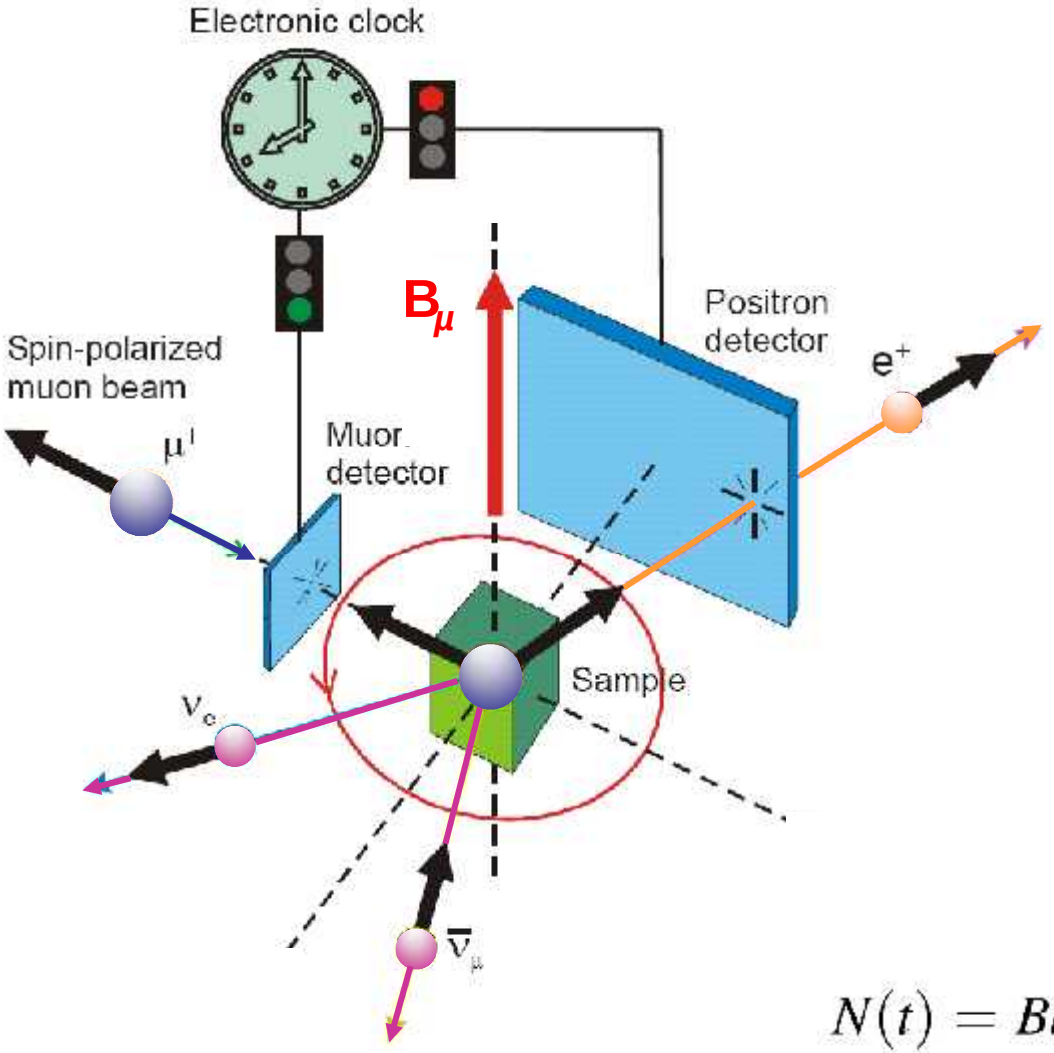

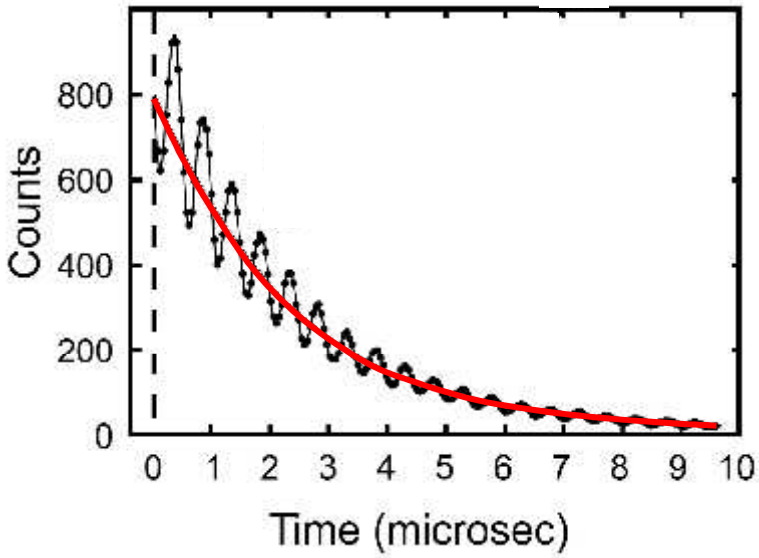

$$N(t) = Bkg + N_0 \exp(-t/\tau_\mu)$$

B_μ internal or external field

$\hat{\mathbf{n}}$: direction of detector

μSR Spectra

$$N(t) = Bkg + N_0 \exp(-t/\tau_\mu)\left[1 + a\,\hat{\mathbf{n}}\cdot\mathbf{P}(t)\right]$$

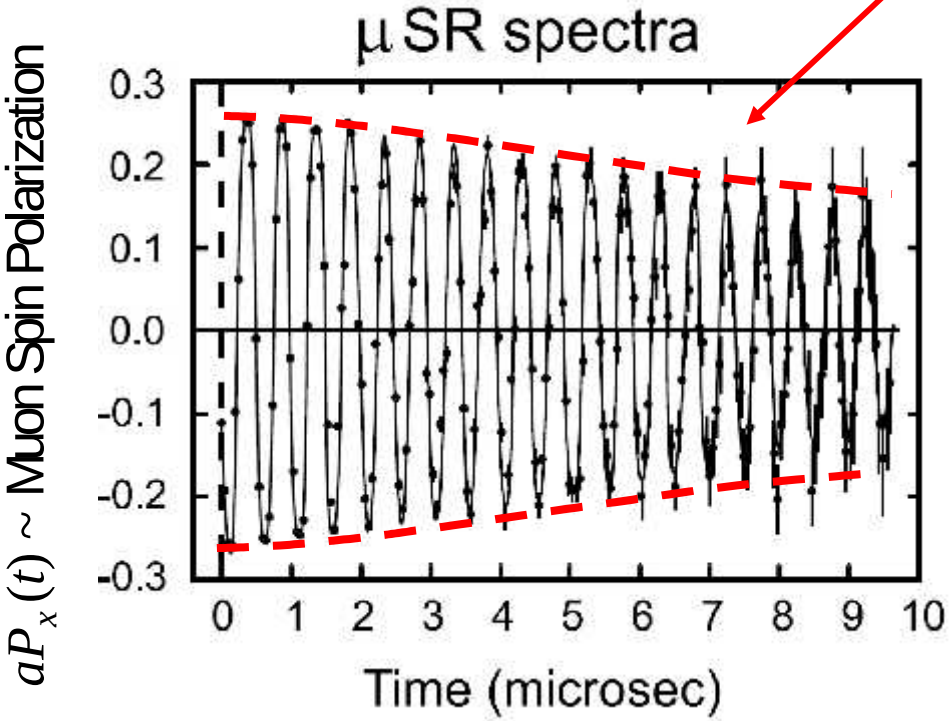

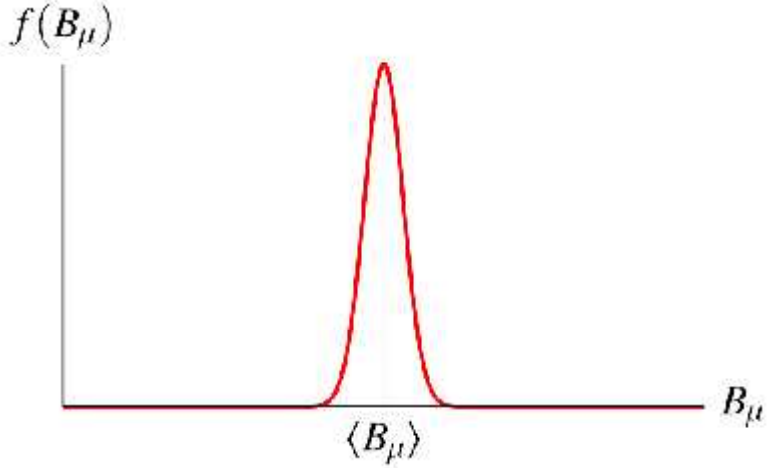

Frequency ▶ *Value of field at muon site* ($\omega_L = \gamma_m B_m$)

Damping ▶ *Field distribution and/or dynamics*

Field Direction -- Field Distribution

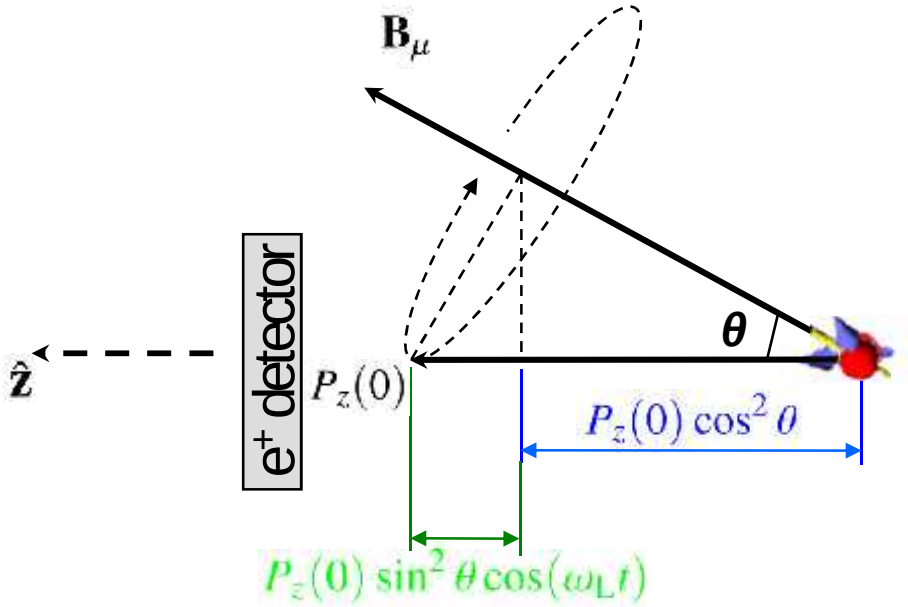

$$P_z(t) = \cos^2\theta + \sin^2\theta\cos(\gamma_\mu B_\mu t) \;)\;]d\mathbf{B}_\mu$$

- Static part
- Oscillating part

θ angle between magnetic field and muon polarization at $t = 0$

Different Measurement Geometries

ZF and LF: Zero field and Longitudinal Field geometry

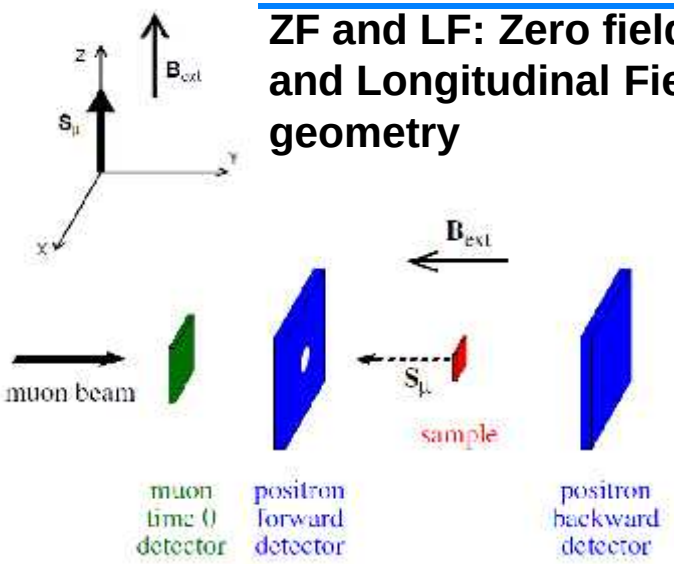

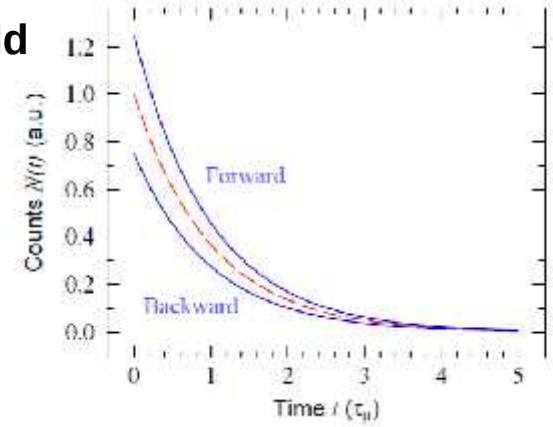

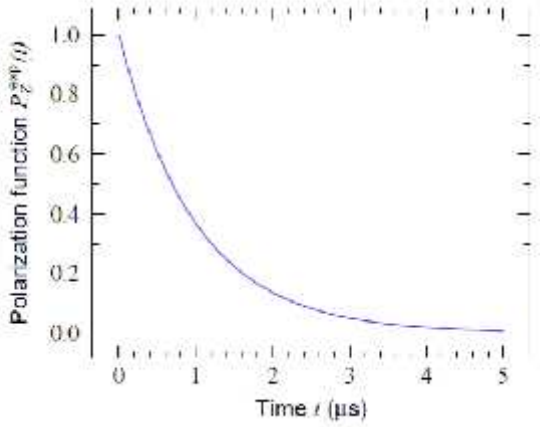

Typically used for the study of:

- Static magnetism
  - Temperature dependence of the magnetic order parameter
  - Determination of the magnetic transition temperature
  - Homogeneity of the sample
- Dynamic magnetism
  - Determination of magnetic fluctuation rates
  - Slowing down of fluctuations near phases transitions

Different Measurement Geometries

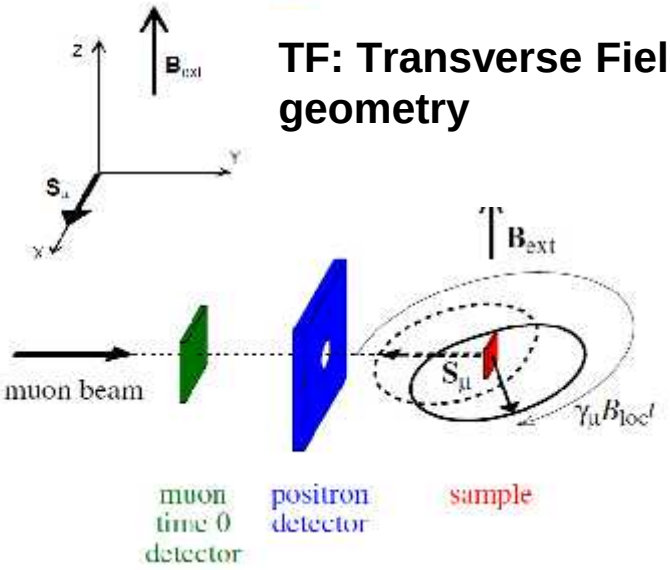

TF: Transverse Field geometry

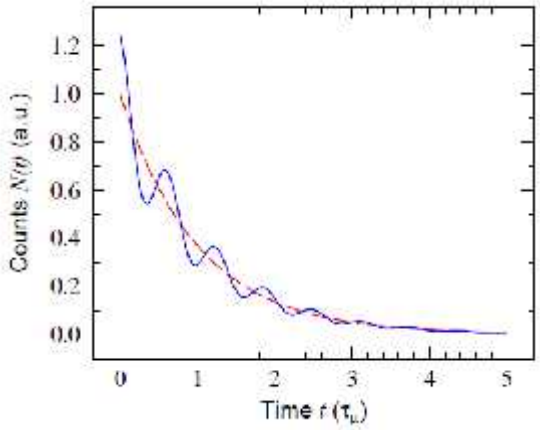

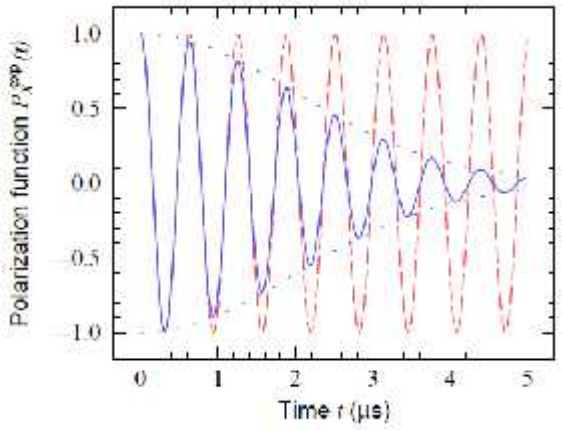

Typically used for the study of:

- Magnetism
  - Determination of the magnetic transition temperature
  - Homogeneity of the sample
  - Knight shift (local susceptibillity)
- Superconductivity
  - Absolute value and temperature dependence of the London penetration depth
  - Coherence length, votex structure, vortex dynamics, …

Local field in magnetic materials

Internal field : generally sum of dipolar :

$$\vec{B}_{dip}(\vec{r}) - \frac{\mu_0}{4\pi}\frac{3(\vec{\mu}_i \cdot \vec{r}_{i\mu})\cdot r_{i\mu} - \vec{\mu}_i r_{i\mu}^2}{r_{i\mu}^5}$$

$$B_{dip} \approx \frac{\mu_0}{4\pi}\frac{\mu_i}{r_{i\mu}^3} \approx \frac{\mu_i[\mu_B]}{d^3[A^3]}\,T \approx 0.1T$$

and contact field (spin density at muon site):

$$\vec{B}_{hf}(\vec{r}_\mu) \quad \frac{2\mu_0}{3}\mu_B \rho_{spin}(\vec{r}_\mu) \simeq \frac{2\mu_0}{3}\mu_B \left|\varphi(\vec{r}_\mu)\right|^2 < \vec{s} >$$

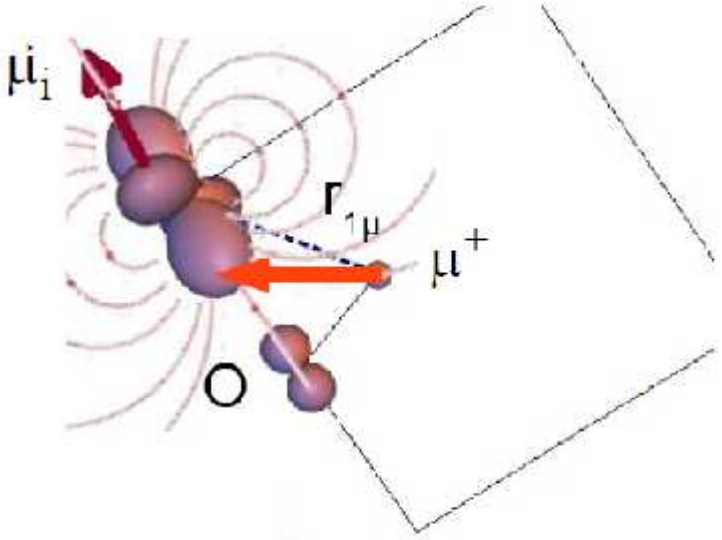

High sensitivity:

μSR time window 10-20 μs

$\rightarrow \nu_\mu \simeq 50$ kHz detectable

$$\rightarrow B = \frac{2\pi}{\gamma_\mu}\nu_\mu \approx 0.1\text{mT (Gauss)}$$

(corresponds to $0.001\mu_B$ or nuclear moments μ_n)

PAUL SCHERRER INSTITUT

PSI

The μSR technique has a unique time window for the study of magnetic flcutuations in materials that is complementary to other experimental techniques.

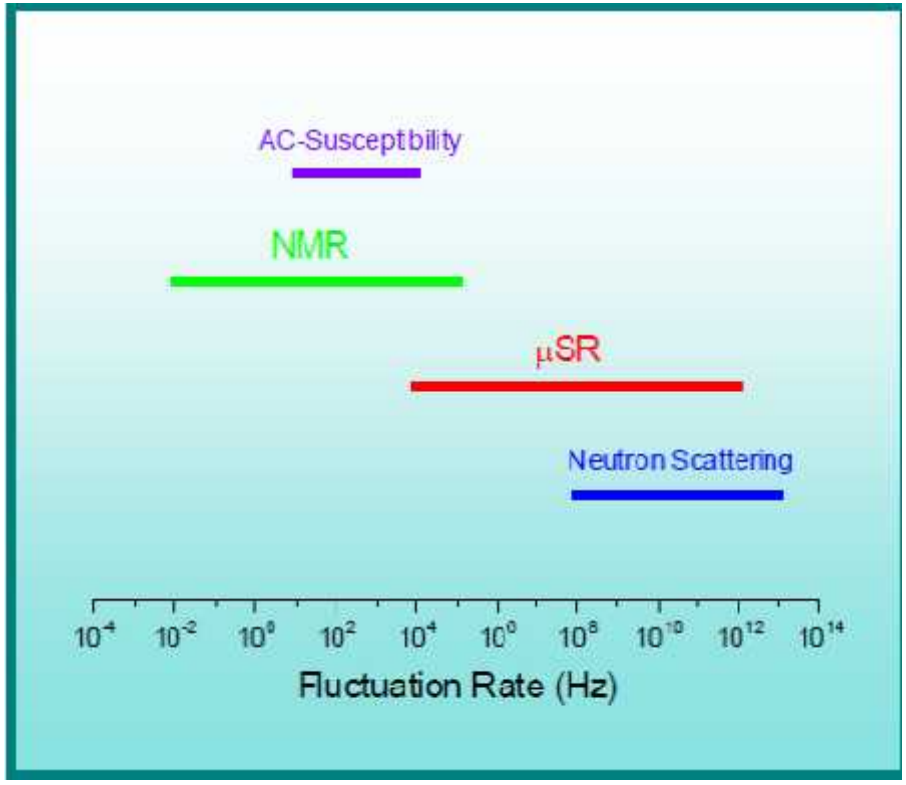

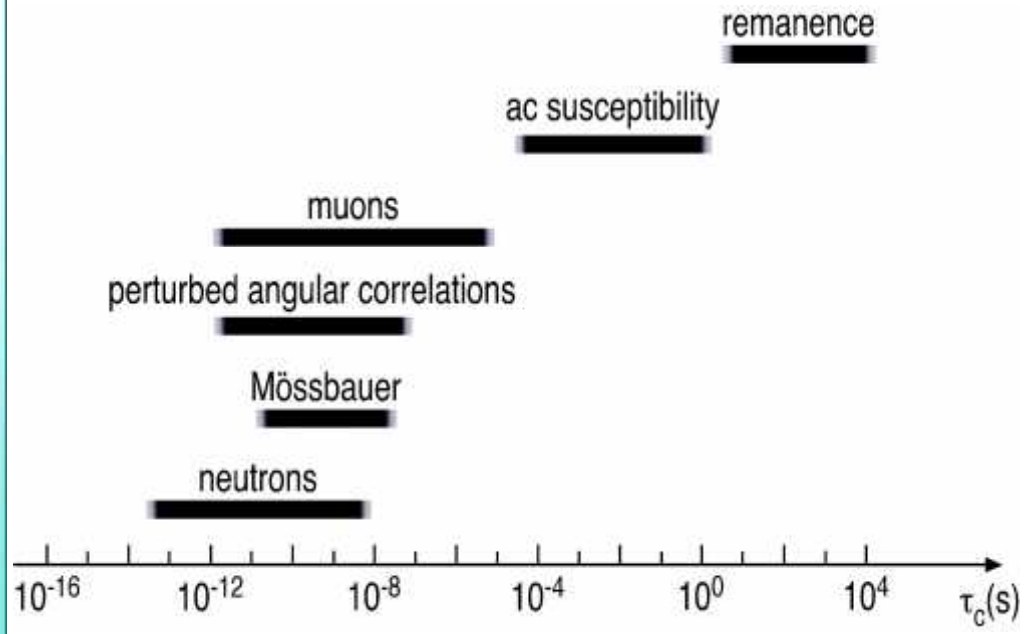

PAUL SCHERRER INSTITUT

PSI

Muon Spin Rotation / Relaxation on Magnetic Materials

Zurab Guguchia

Magnetism

Magnetism

Paramagnetism

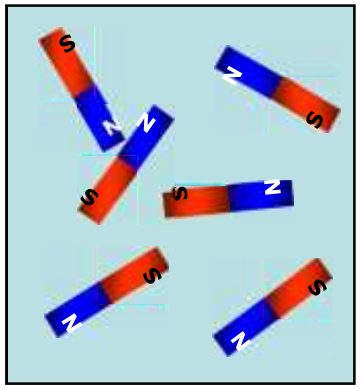

fluctuating
$T>T_C$

Ferromagnetism

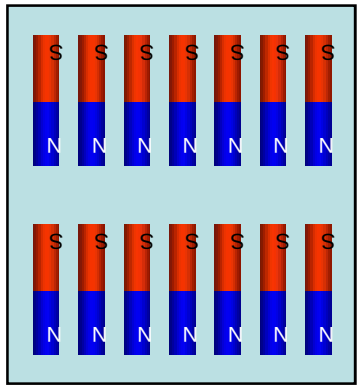

static
$T<T_C$

The interesting property of magnetically ordered system is the size and temperature dependence of the magnetic moment.

How do you measure this?

Macroscopic techniques (average over the hole sample):

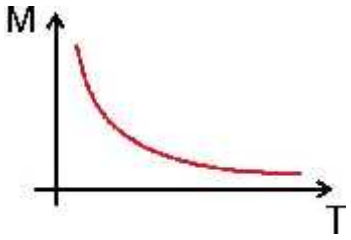

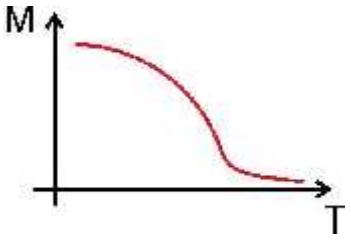

SQUID, PPMS, …

Magnetism

Paramagnetism

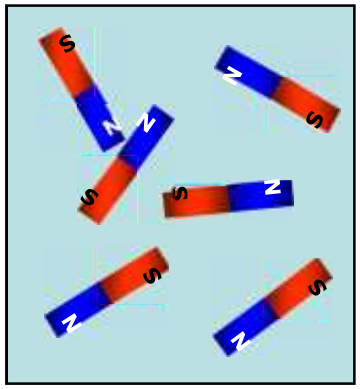

fluctuating
$T>T_C$

Ferromagnetism

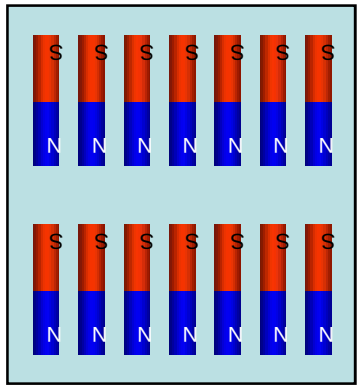

static
$T<T_C$

Antiferromagnetism

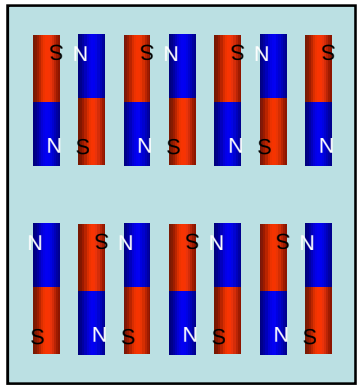

static
$T<T_N$

The interesting property of magnetically ordered system is the size and temperature dependence of the magnetic moment.

How do you measure this?

Macroscopic techniques (average over the hole sample):

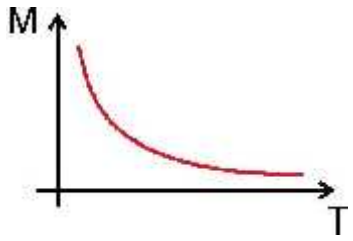

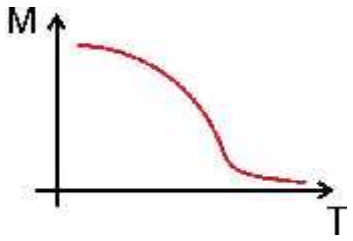

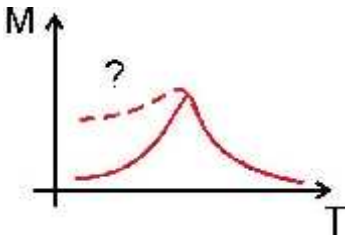

Magnetism

Scattering techniques:
(neutrons, X-rays)

Local probes:
(μSR, NMR, …)

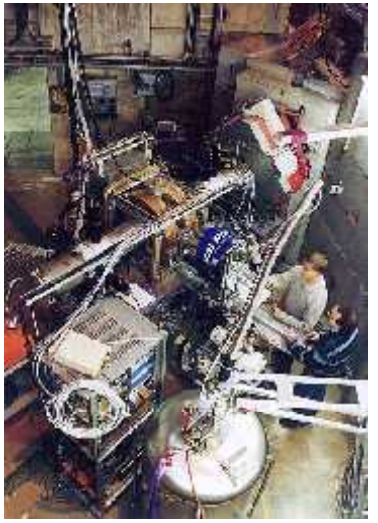

Strength of muon spin rotation / relaxation:

Investigation of magnetically inhomogeneous materials:

- Chemical inhomogeneity (“dirty samples”)
- **Competing interactions, coexistence of different magnetic orders, short range order, magnetic frustration**
- **Magnetism and superconductivity (competition and coexistence)**

Magnetically Inhomogeneous Materials

Homogen:

M_{hom}

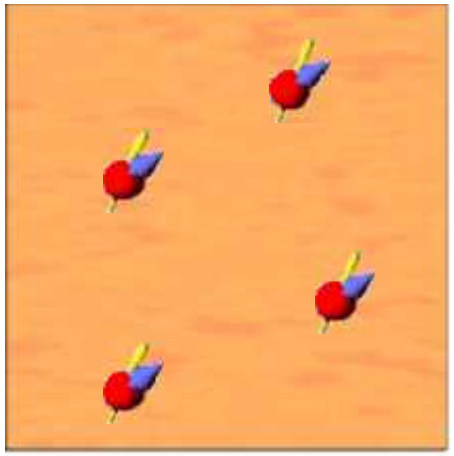

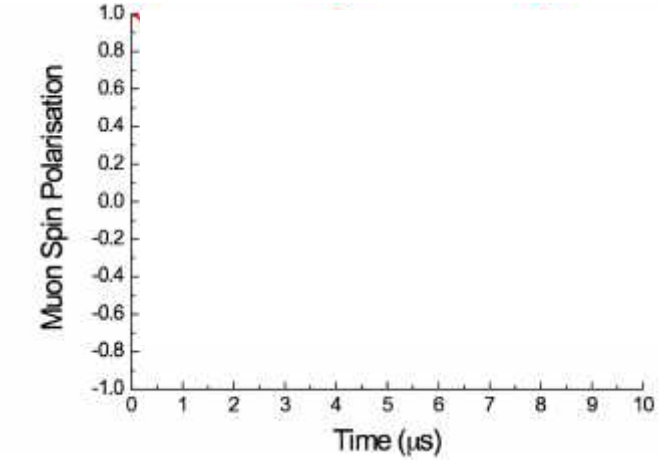

Inhomo-
geneous:

$M_{inhom} = M_{hom}$

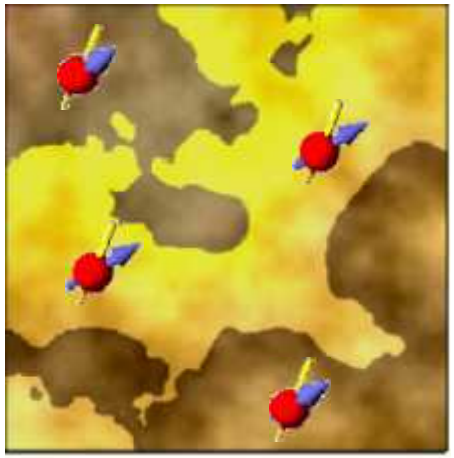

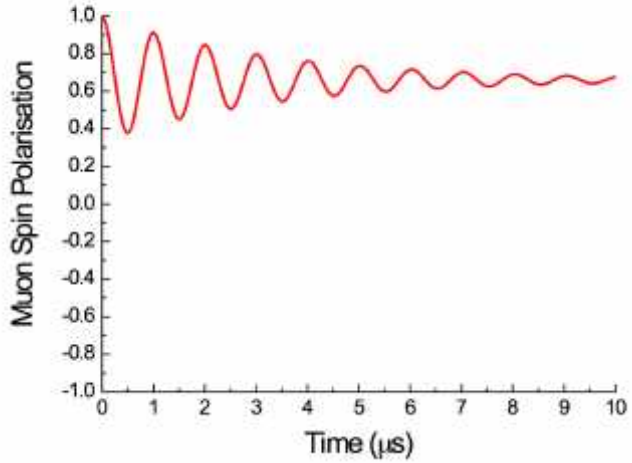

Amplitude = Magnetic volume fraction
Frequency = Size of the magnetic moments (order parameter)
Damping = Inhomogeneity within the magnetic areas

Sensitivity of the Technique

Internal field at the muon site:

$$\mathbf{B}_\mu = \mathbf{B}_c + \mathbf{B}_{\text{dip}}$$

- Contact field $\propto e|\Psi(\mathbf{r}_\mu)|^2$
- Dipolar contribution

$$\mathbf{B}_{\text{dip}} = \sum_i \frac{1}{r_i^3}\left[\frac{(3\mathbf{m}_i \cdot \mathbf{r}_i)}{r_i^2}\mathbf{r}_i - \mathbf{m}_i\right]$$

$$B_{\text{dip}} \simeq \frac{m}{r^3}$$

For $m = 1\,\mu_B$ and $r = 1\,\text{Å} \Rightarrow \quad B_{\text{dip}} \simeq 1\,\text{T}$

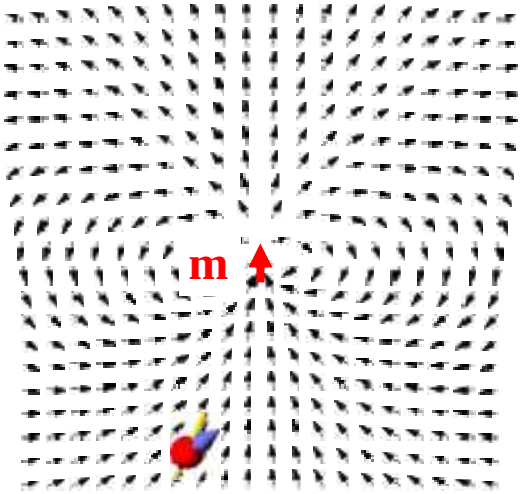

➡ *static moments as low as 0.001 μ_B can be detected by μSR*

μSR time window: 10-20 μsec

➡ Frequencies down to 50 kHz detectable
Fields of few Gauss (10^{-4} T)

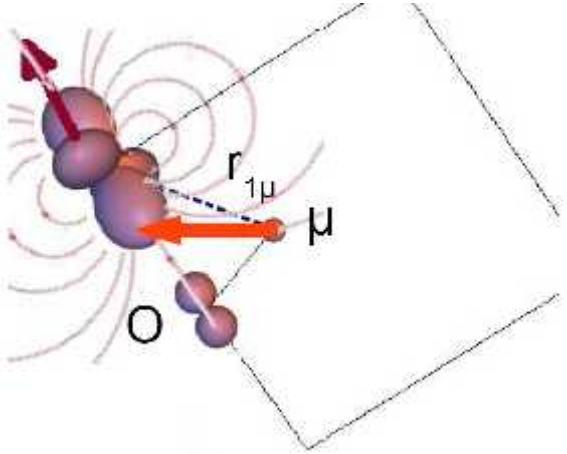

Advantages of μSR

Muons are **purely magnetic** probes (I = ½, no quadrupolar effects).

→

Local information, **interstitial** probe → complementary to NMR.

→

Large magnetic moment: $\mu_\mu = 3.18\ \mu_p = 8.89\ \mu_n$ → **sensitive** probe.

Particularly suitable for:
Very weak effects, small moment magnetism ~ 10^{-3} μ_B/Atom
Random magnetism (e.g. spin glasses).
Short range order (where neutron scattering is not sensitive).
Independent determination of **magnetic moment** and of **magnetic volume fraction.**

→

Determination of magnetic/non magnetic/superconducting fractions.

→

Full polarization in zero field, independent of temperature → unique measurements without disturbance of the system.

Different Depolarization Functions

ferro antiferro dilute

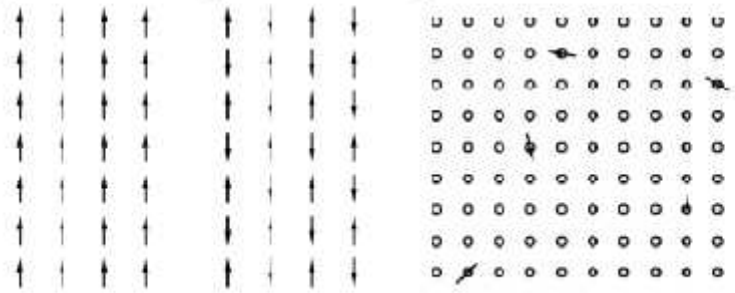

helical

spiral

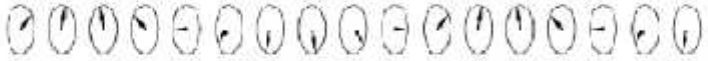

- various spin structures
- spin glasses (randomness)
- variety of field distributions

- nuclear moments
- electronic moments

- static moments
- fluctuating moments

PAUL SCHERRER INSTITUT

PSI

Magnetism of Single Crystals

Simple Magnetic Sample – Single Crystal

$$P_z(t) = \int f(\mathbf{B}_\mu)\left[\cos^2\theta + \sin^2\theta\cos(\gamma_\mu B_\mu t)\right] d\mathbf{B}_\mu$$

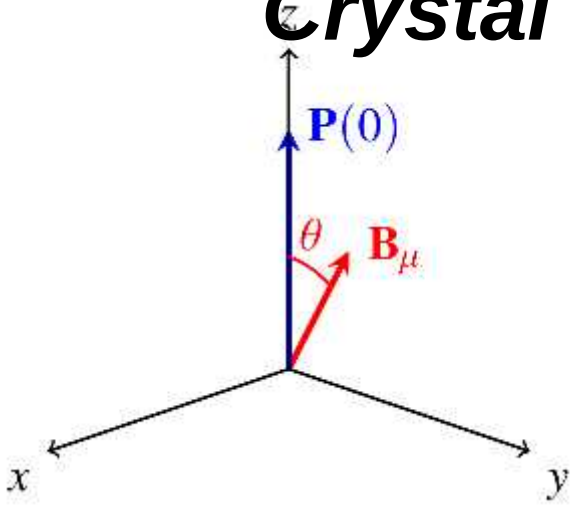

Single Crystal with $\theta = \pi/2$

$$P_z(t) = \cos(\gamma_\mu B_\mu t)$$

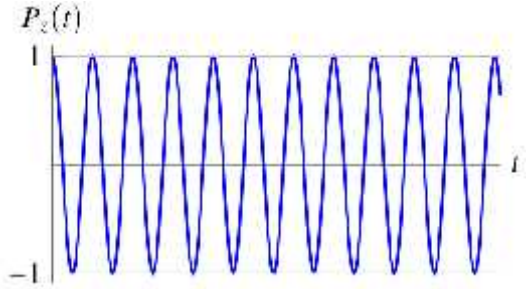

Single Crystal with $\theta \neq \pi/2$

$$P_z(t) = \cos^2\theta + \sin^2\theta\cos(\gamma_\mu B_\mu t)$$

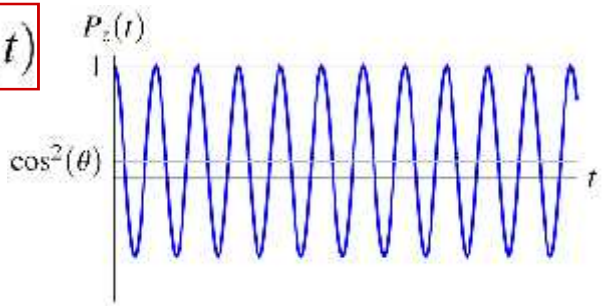

Þ in a single crystal the amplitude of the oscillatory component indicates the direction of the internal field

PAUL SCHERRER INSTITUT

PSI

Example:
Single Crystalline UGe_2

Single Crystalline UGe_2

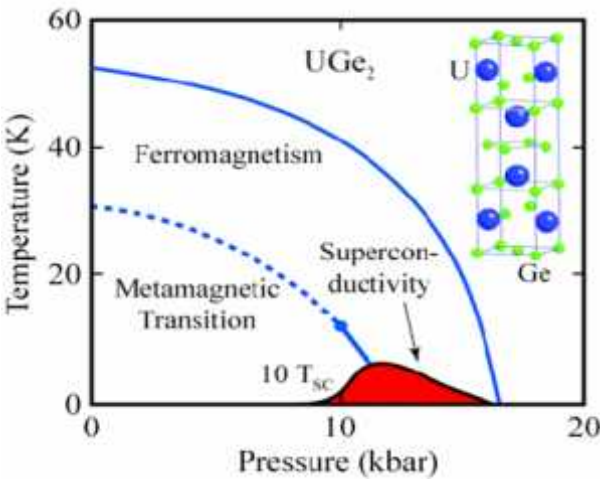

Cavendish Lab.

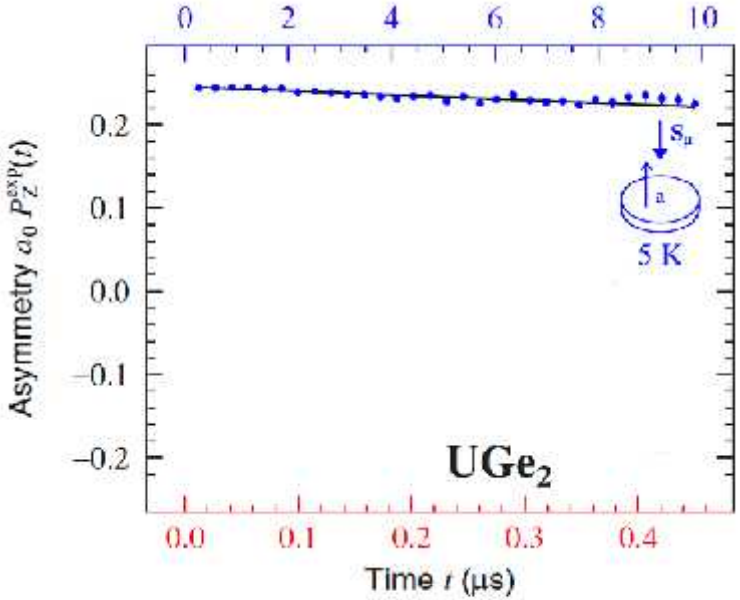

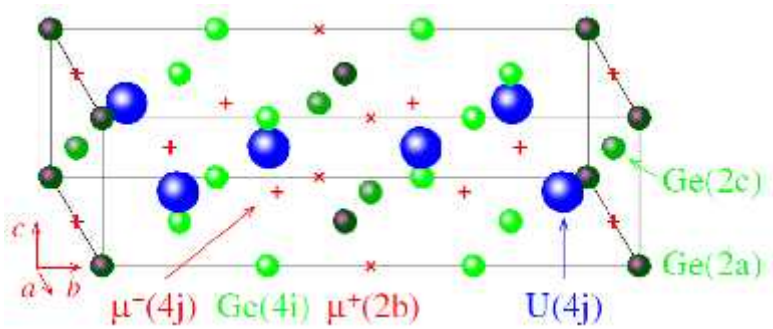

- Two magnetically inequivalent muon stopping sites
- No oscillations for $\mathbf{P}(0)$ pointing along *a*-axis
  Þ Internal fields parallel to *a*-axis ($\theta = 0$)
- Oscillations around zero
  Þ because single crystal

S. Sakarya et al., Phys. Rev. B 81, 024429 (2010)

PAUL SCHERRER INSTITUT

PSI

Magnetism of Polycrystals (Powders)

Simple Magnetic Sample – Polycrystal

$$P_z(t) = \int f(\mathbf{B}_\mu)\left[\cos^2\theta + \sin^2\theta\cos(\gamma_\mu B_\mu t)\right] d\mathbf{B}_\mu$$

Polycrystal (powder)

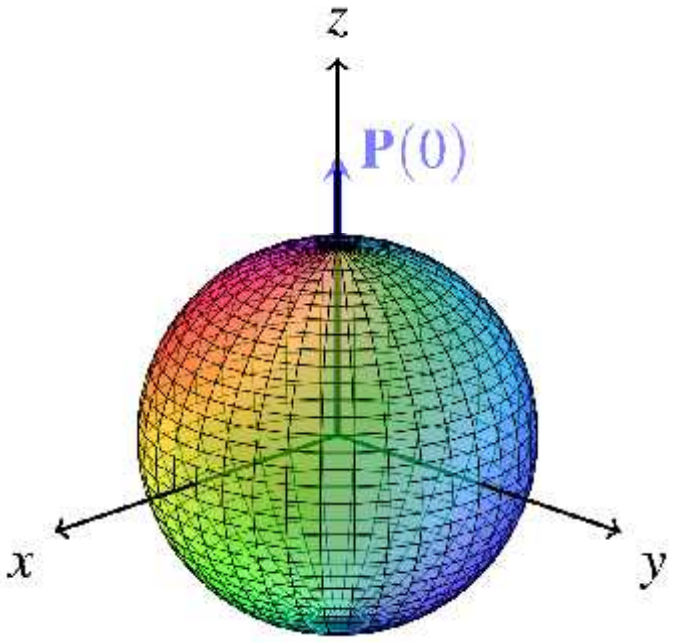

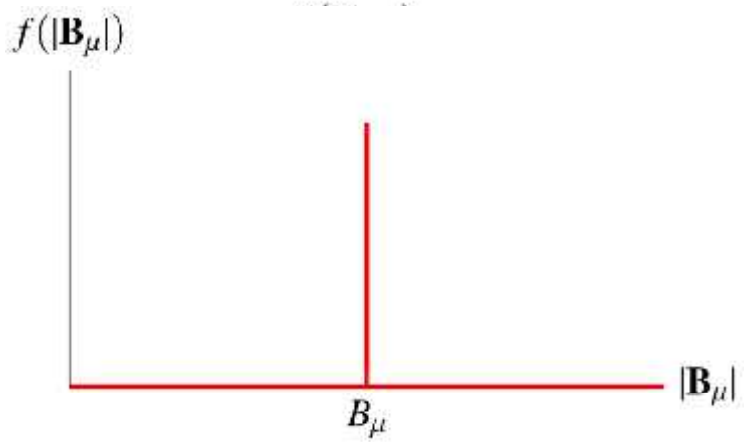

If isotropic:

$$f(|\mathbf{B}_\mu|) = f(\mathbf{B}_\mu)\, 4\pi B_\mu^2$$

$$f(\mathbf{B}_\mu)\, d\mathbf{B}_\mu = \frac{f(|\mathbf{B}_\mu|)}{4\pi}\sin(\theta)\, d\theta\, d\phi\, dB_\mu$$

$$P_z(t) = \frac{1}{3} + \frac{2}{3}\cos(\gamma_\mu B_\mu t)$$

Simple Magnetic Sample – Polycrystal

$$P_z(t) = \int f(\mathbf{B}_\mu)\left[\cos^2\theta + \sin^2\theta\cos(\gamma_\mu B_\mu t)\right] d\mathbf{B}_\mu$$

Polycrystal: Ideal Case

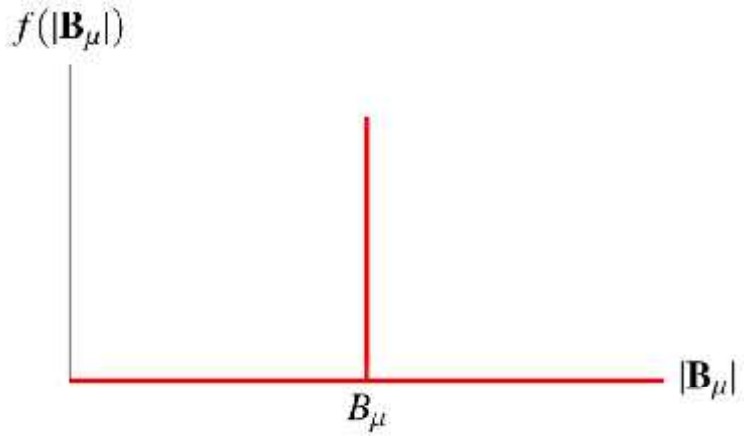

$$P_z(t) = \frac{1}{3} + \frac{2}{3}\cos(\gamma_\mu B_\mu t)$$

Simple Magnetic Sample – Polycrystal

$$P_z(t) = \int f(\mathbf{B}_\mu)\left[\cos^2\theta + \sin^2\theta\cos(\gamma_\mu B_\mu t)\right] d\mathbf{B}_\mu$$

Polycrystal: Ideal Case

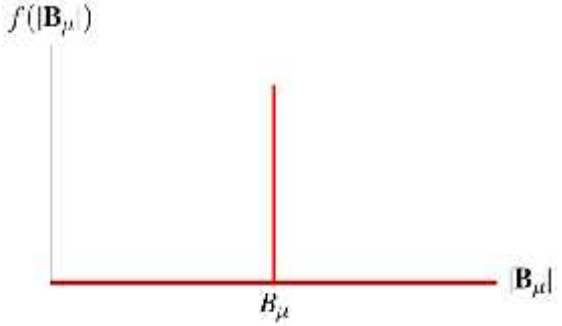

$$P_z(t) = \frac{1}{3} + \frac{2}{3}\cos(\gamma_\mu B_\mu t)$$

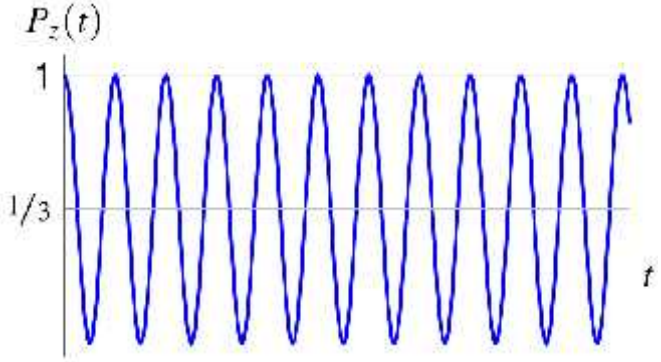

Polycrystal: Real Case

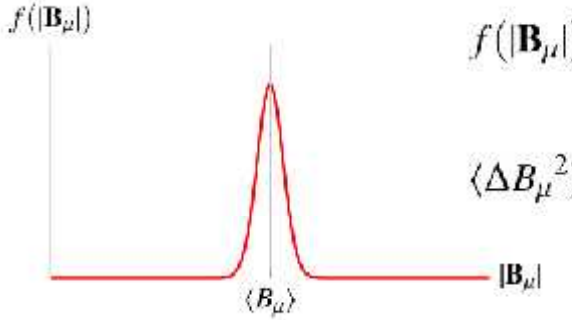

$$f(|\mathbf{B}_\mu|) = \frac{1}{\sqrt{2\pi\langle \Delta B_\mu^2 \rangle}} \exp\left[-\frac{(B_\mu - \langle B_\mu \rangle)^2}{2\langle \Delta B_\mu{}^2 \rangle}\right]$$

$$\langle \Delta B_\mu{}^2 \rangle = \int (B_\mu - \langle B_\mu \rangle)^2 f(|\mathbf{B}_\mu|) dB_\mu$$

$$P_z(t) = \frac{1}{3} + \frac{2}{3}\exp\left[-\frac{1}{2}\gamma_\mu^2 \langle \Delta B_\mu{}^2 \rangle t^2\right]\cos\left[\gamma_\mu \langle B_\mu \rangle t\right]$$

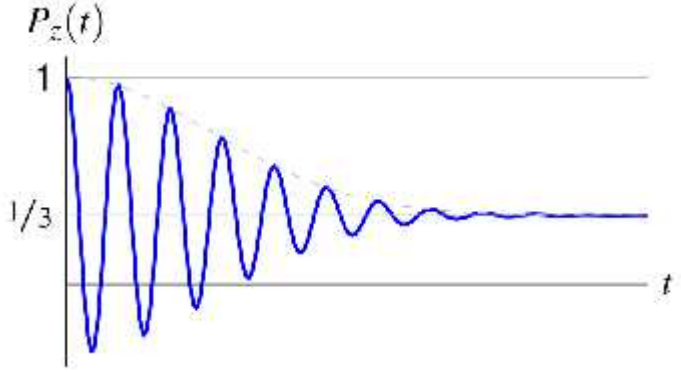

PAUL SCHERRER INSTITUT

Example:
Magnetism of Polycrystalline $EuFe_2(As_{1-x}P_x)_2$

AFe_2As_2(A=Ba,Sr,Ca,Eu)

T_{SDW}(Fe) = 190 K

Eu^{2+} $4f^7$, S = 7/2

$T_{AFM}(Eu^{2+})$ = 19 K

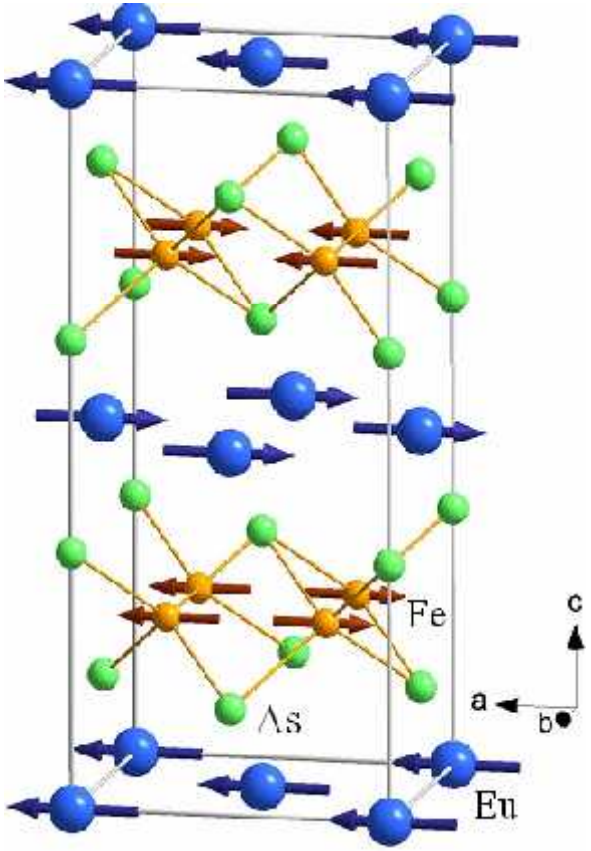

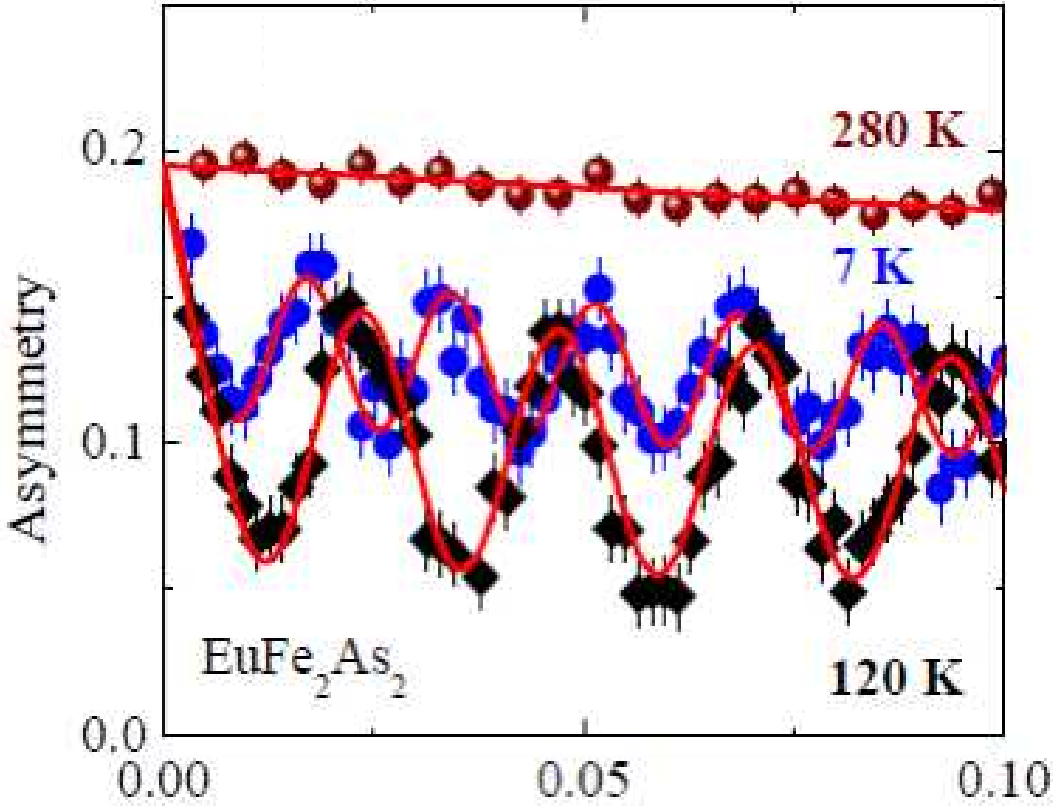

Guguchia *et.al,* PRB **83**, 144516 (2011).

Magnetic structure of $EuFe_2As_2$ at 2.5 K

AFe_2As_2(A=Ba,Sr,Ca,Eu)

$Eu^{2+} \rightarrow 4f^7$, S = 7/2

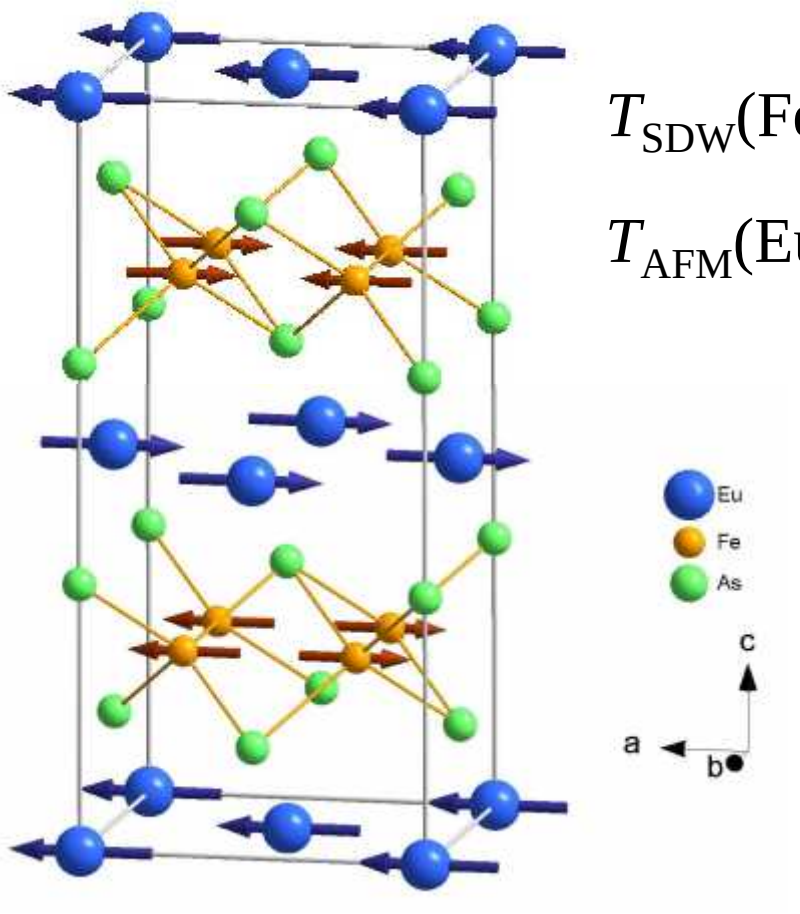

T_{SDW}(Fe) = 190 K

$T_{AFM}(Eu^{2+})$ = 19 K

Y.Xiao *et al.*, PRB 80, 174424 (2009).

Raffius *et al.*, J. Phys. Chem. Solids 54, 13 (1993)

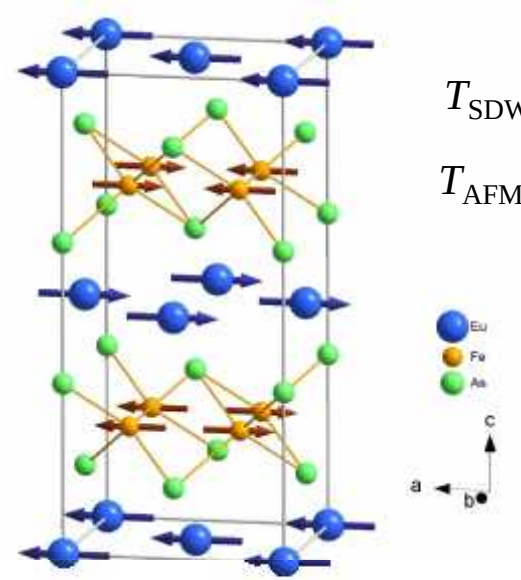

$T_{SDW}(Fe) = 190$ K

$T_{AFM}(Eu^{2+}) = 19$ K

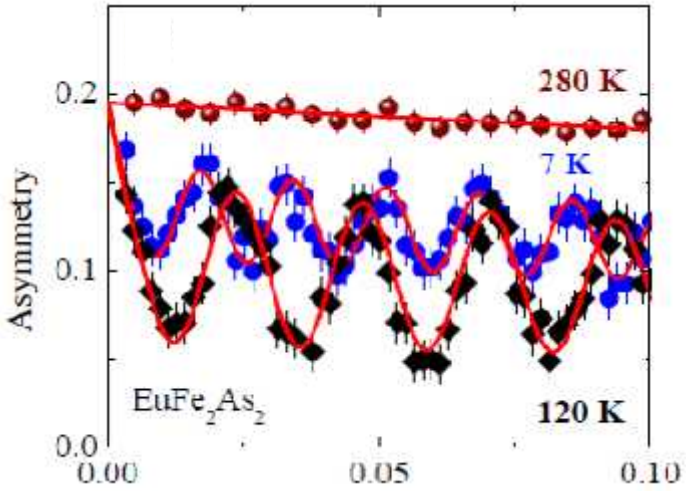

Y. Xiao *et al*., PRB 80, 174424 (2009).

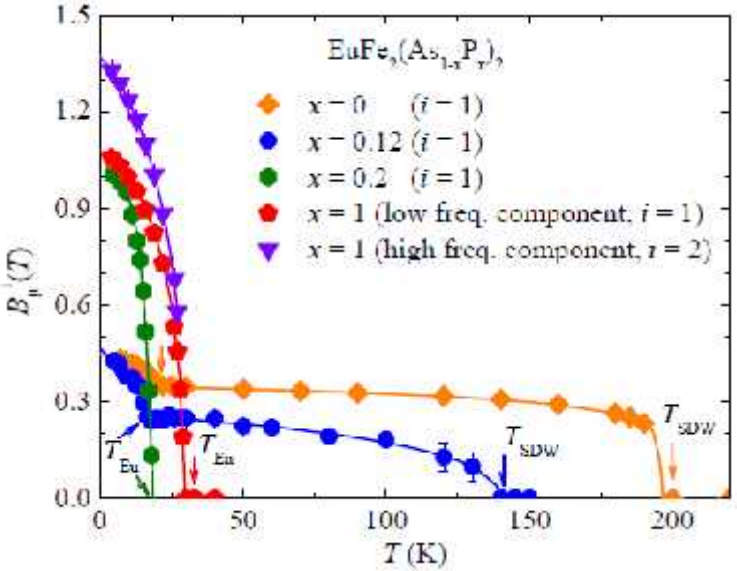

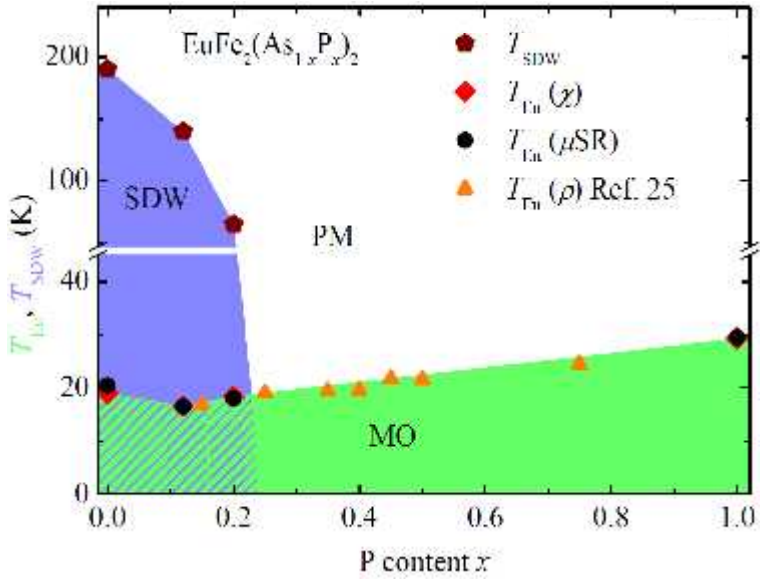

Z. Guguchia *et. al.,* Phys. Rev. B **83**, 144516 (2011).

Z. Guguchia, A. Shengelaya *et. al*., arXiv:1205.0212v1.

Temperature-pressure phase diagram for $EuFe_2(As_{0.88}P_{0.12})_2$

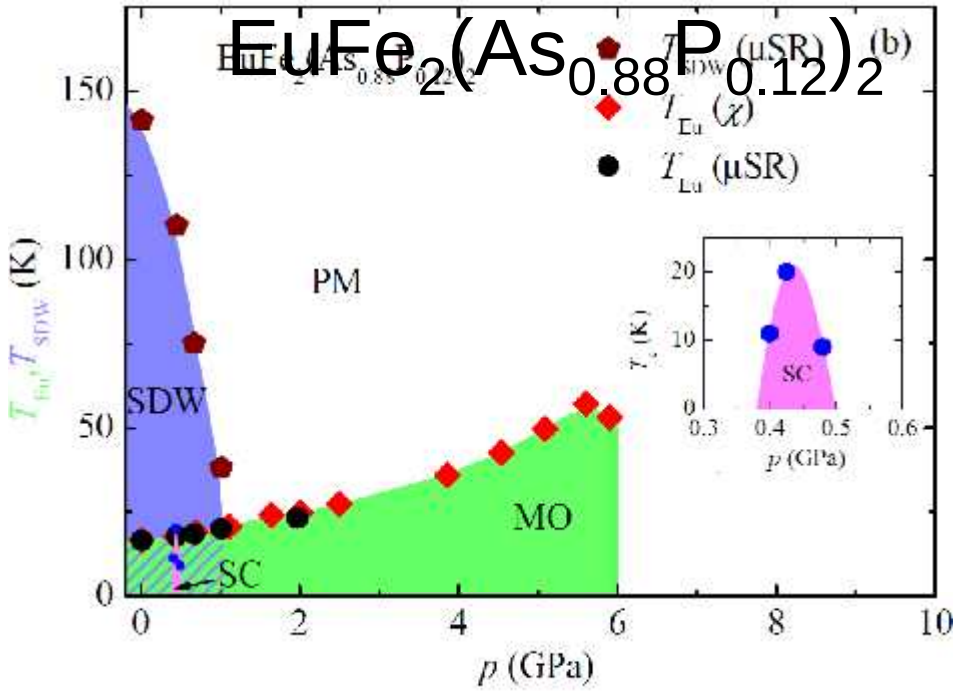

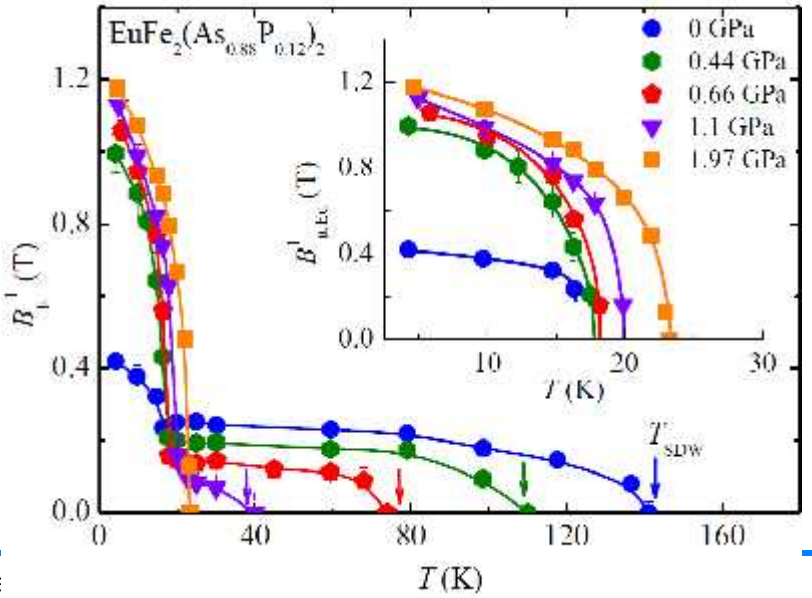

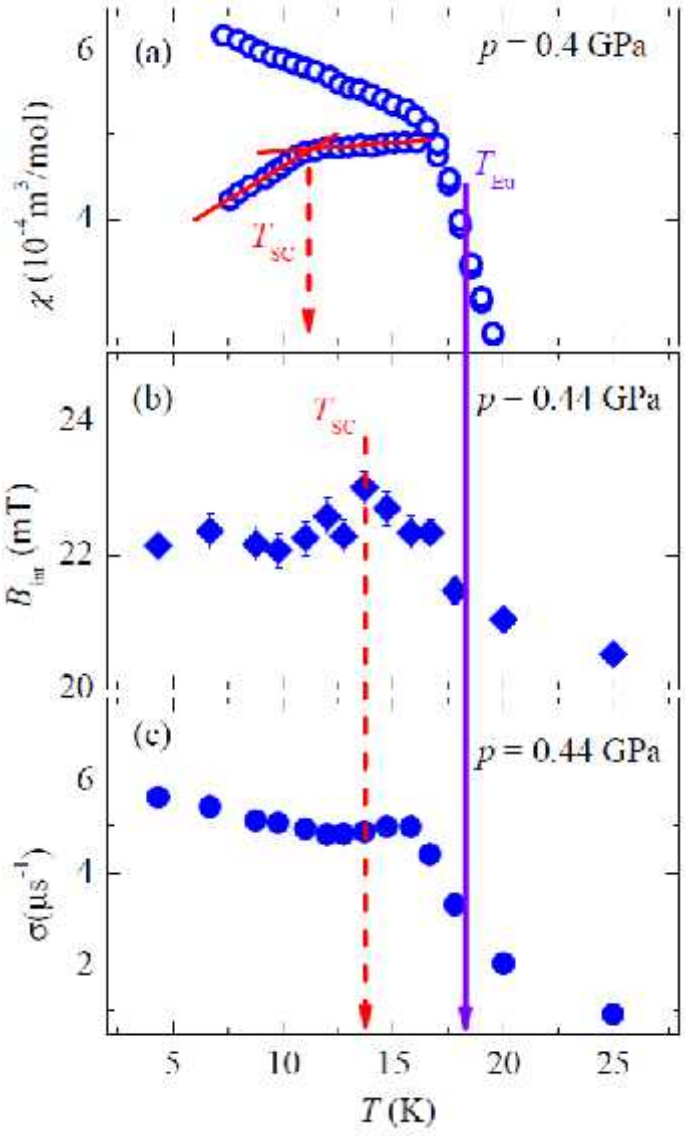

Z. Guguchia *et. al.*, arXiv:1205.0212v1.

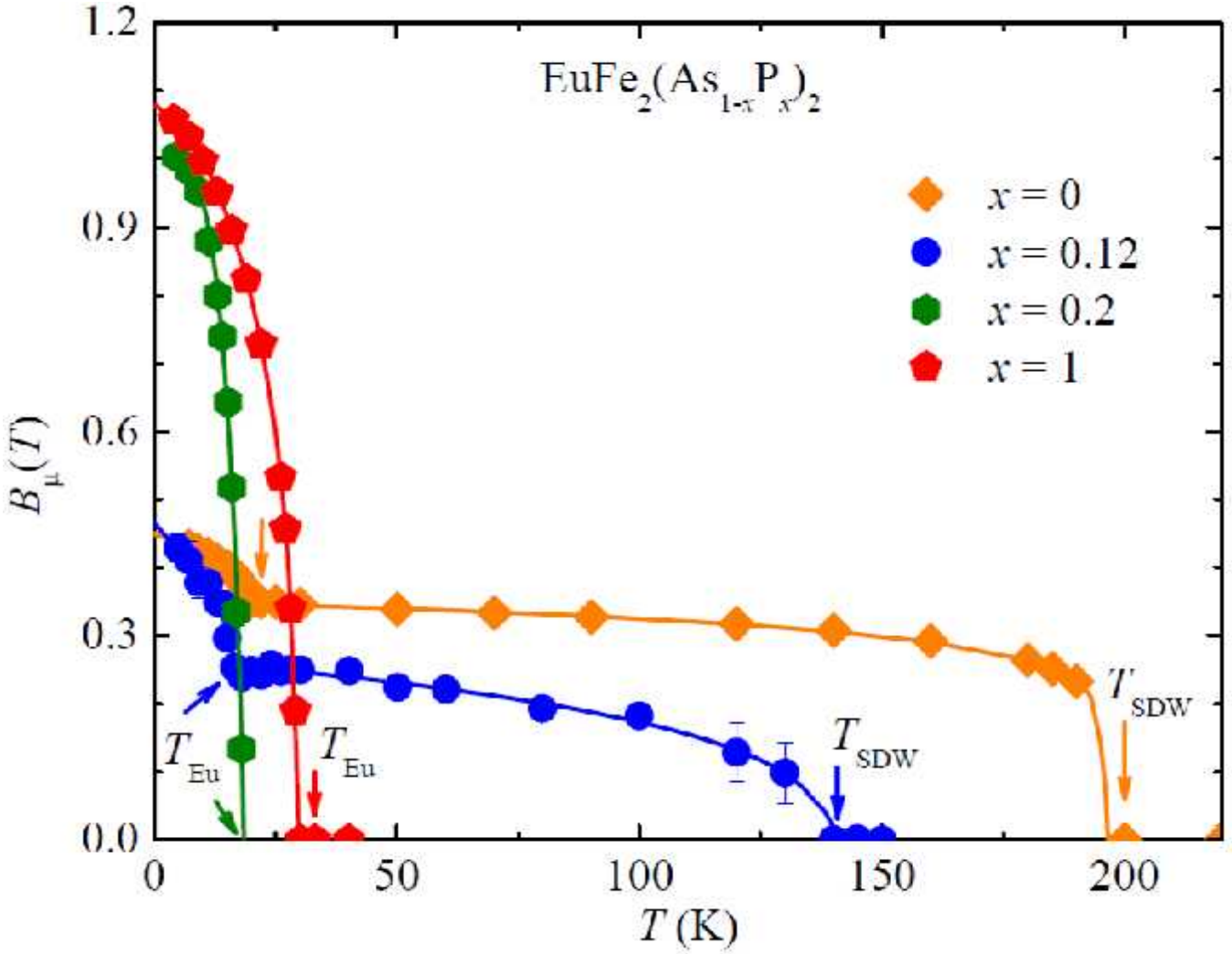

Guguchia *et al,* JSNM **26**, 285 (2013).

Temperature-doping phase diagram

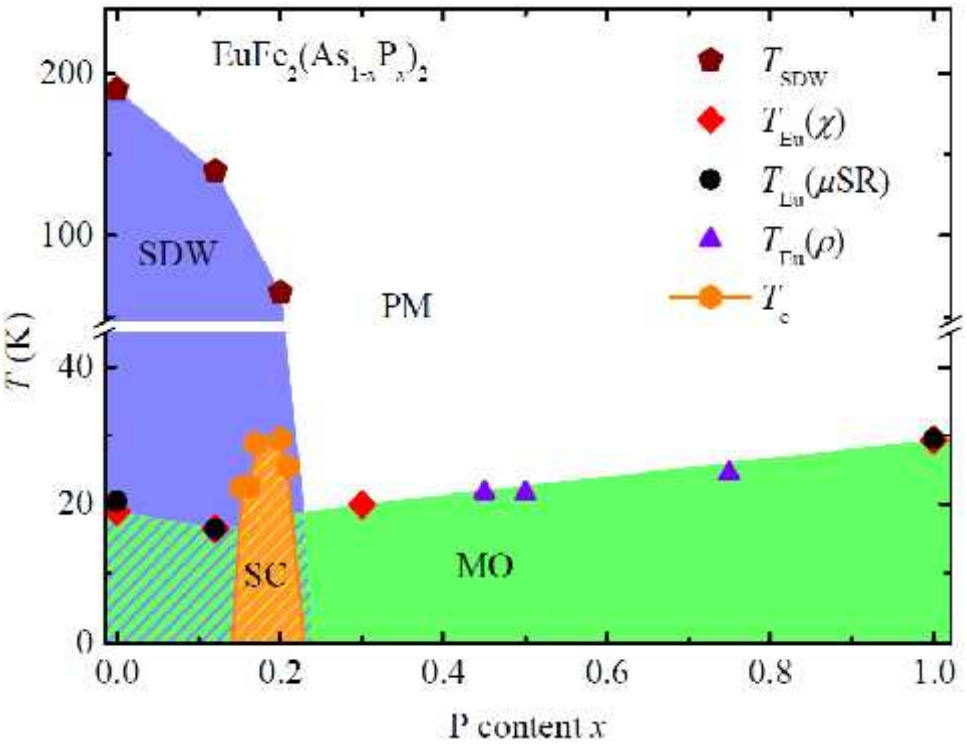

Temperature-pressure phase diagram

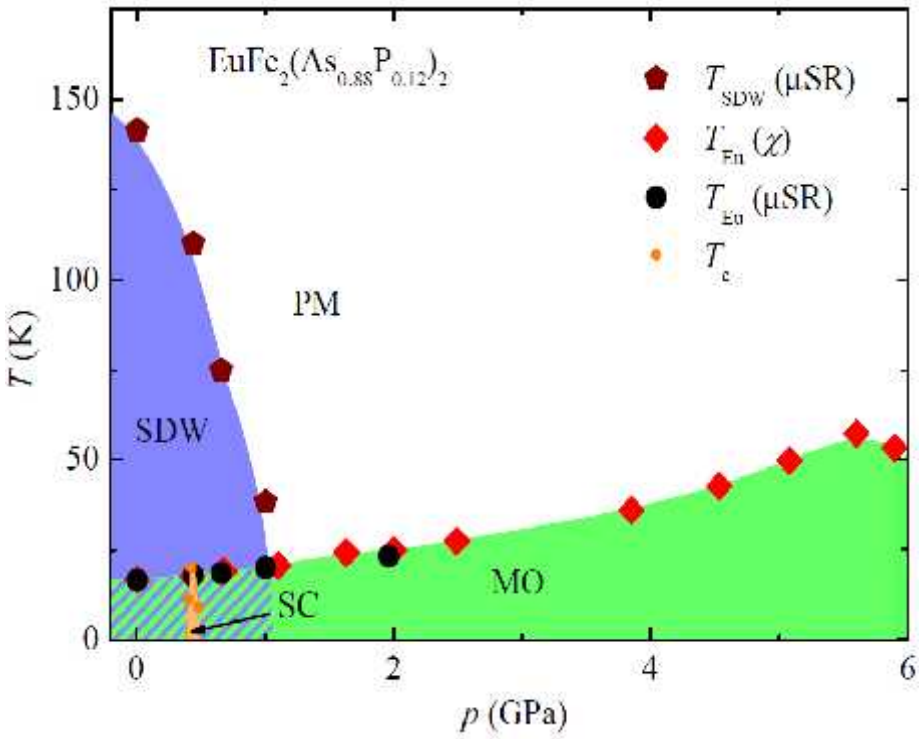

Guguchia *et al,* JSNM **26**, 285 (2013).

PAUL SCHERRER INSTITUT

PSI

Example:
Magnetism of Polycrystalline $La_{1.875}Ba_{0.125}CuO_4$

OIE effect on T_{so} and magnetic fraction V_m

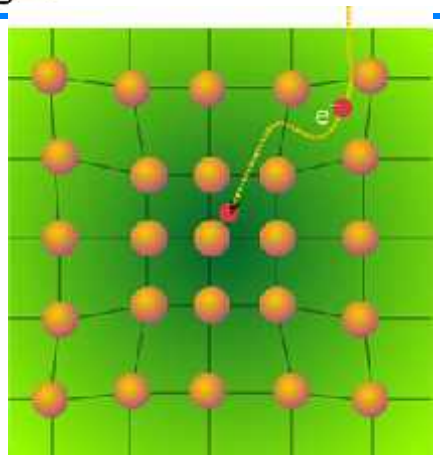

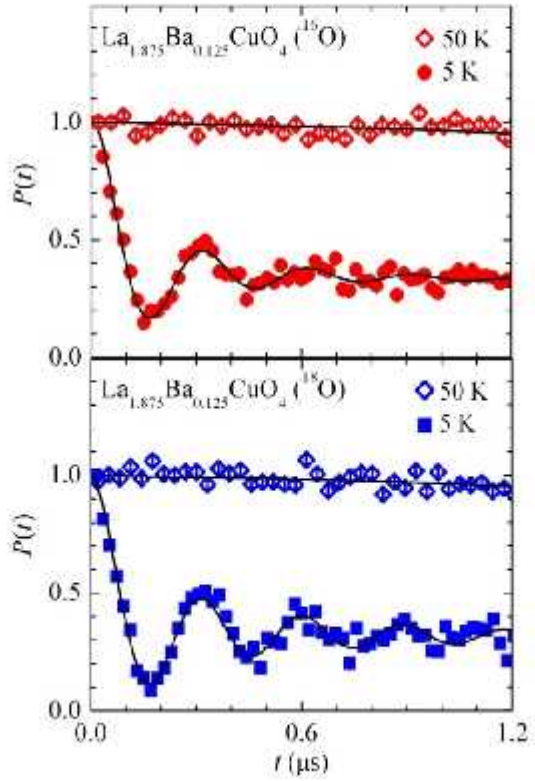

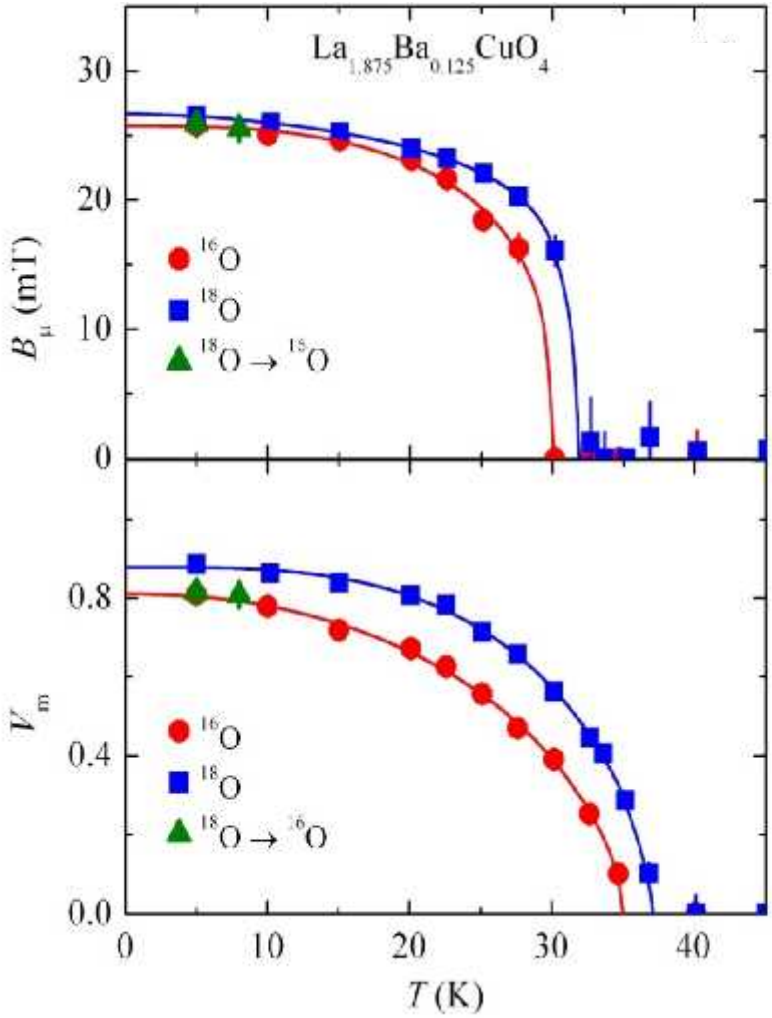

Z. Guguchia *et al.*, Phys. Rev. Lett. 113, 057002 (2014).

PAUL SCHERRER INSTITUT

PSI

Example:
Magnetism of Polycrystalline LaOFeAs

Polycrystalline LaOFeAs

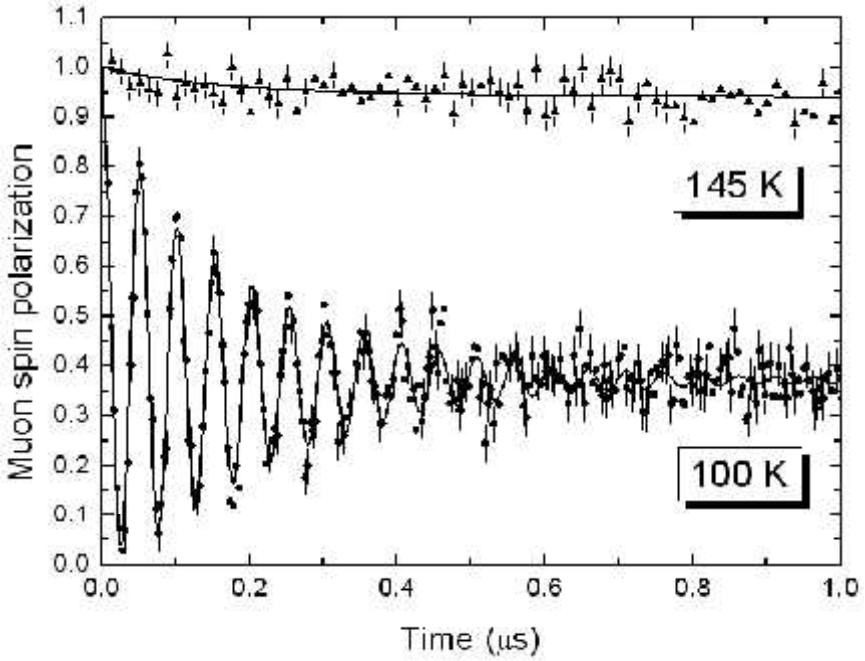

- **Zero Field Muon Spin Rotation**
  - Static commensurate magnetic order

Polycrystalline LaOFeAs

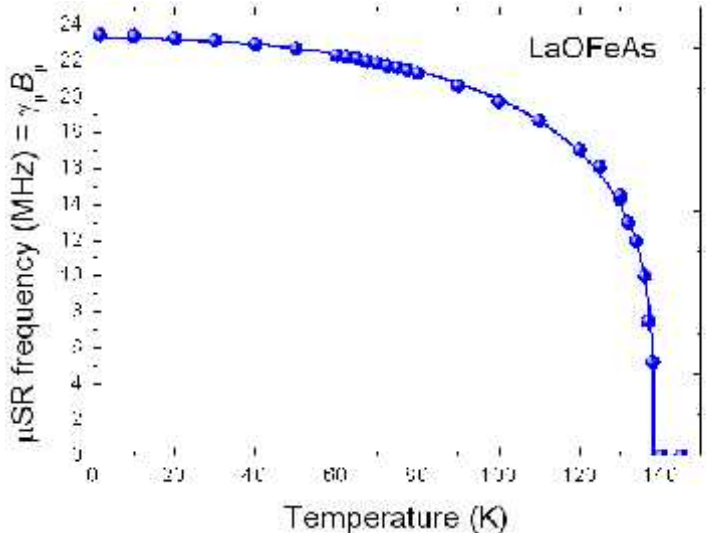

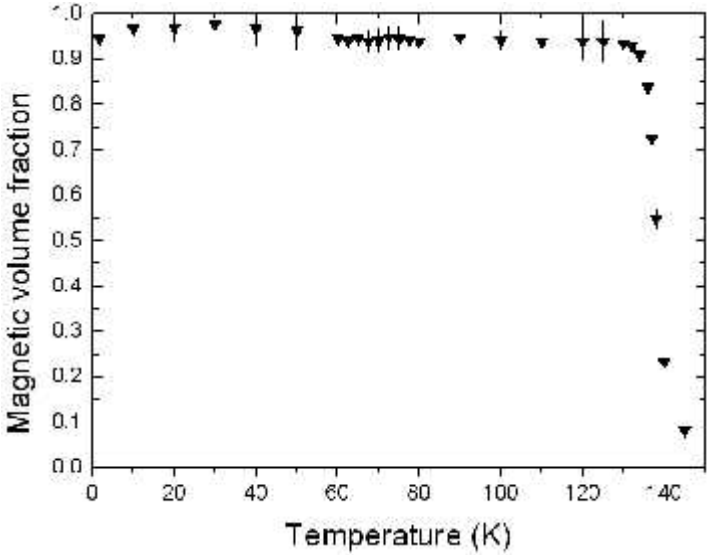

- **Zero Field Muon Spin Rotation**
  - Static commensurate magnetic order
  - T-dependence of the Fe magnetization with high precision, $T_N = 138$ K
  - 100% magnetic volume fraction

Polycrystalline LaOFeAs

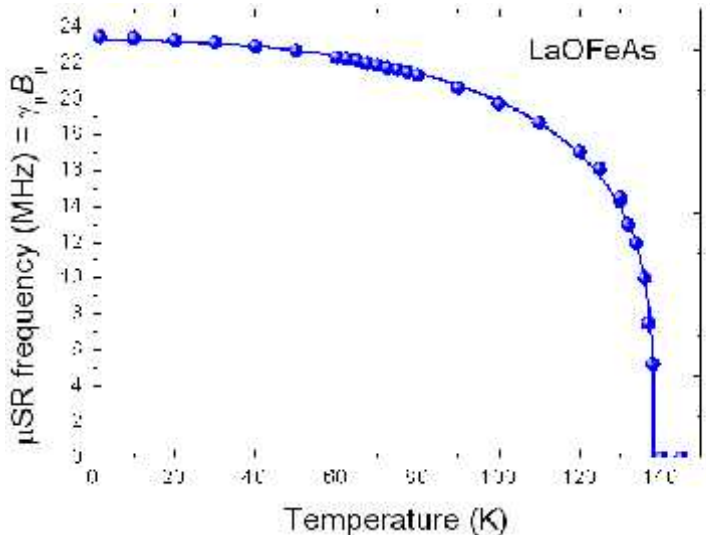

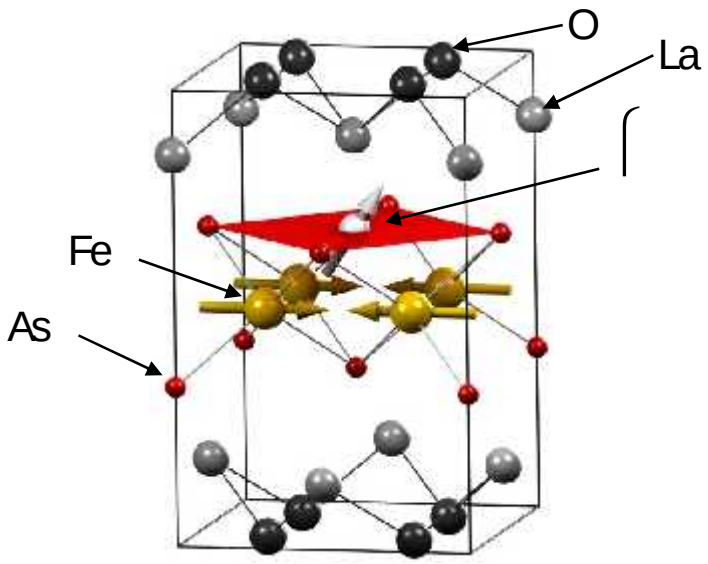

- **Zero Field Muon Spin Rotation**
  - Static commensurate magnetic order
  - T-dependence of the Fe magnetization with high precision, $T_N = 138$ K
  - 100% magnetic volume fraction

Polycrystalline LaOFeAs

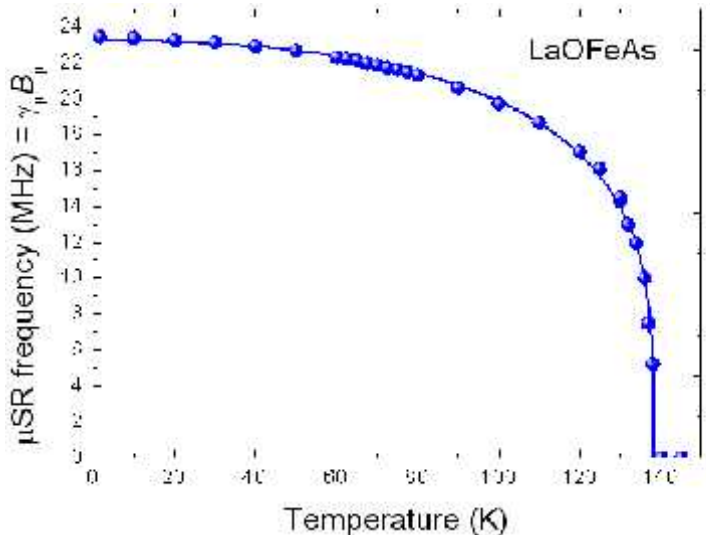

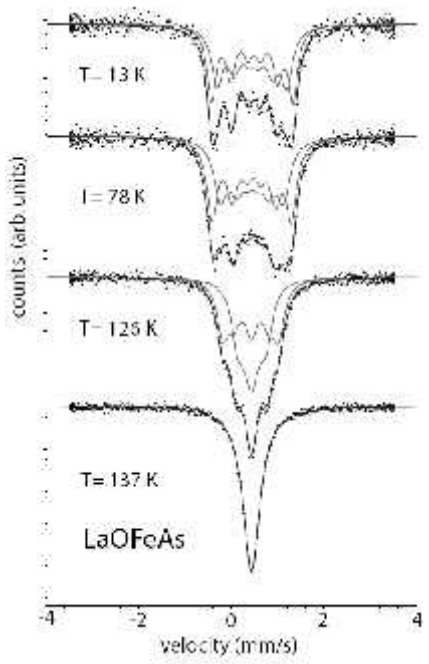

- **Zero Field Muon Spin Rotation**
  - Static commensurate magnetic order
  - T-dependence of the Fe magnetization with high precision, $T_N = 138$ K
  - 100% magnetic volume fraction

$$B_\mu = B_{\mathrm{dip}} + B_c + \cdots$$

contact field $\propto e|\Psi(x_\mu)|^2$

$$B_{\mathrm{dip}} = \sum_i \frac{1}{r_i^3}\left[\frac{(3\boldsymbol{m}_i \cdot \boldsymbol{r}_i)}{r_i^2}\boldsymbol{r}_i - \boldsymbol{m}_i\right]$$

- **Mössbauer spectroscopy**
  - Hyperfine field $B_{hf}(0) = 4.86(5)$ T
    =>
    Saturation moment ⌠ = 0.25 - 0.32 ⌠$_B$

Polycrystalline LaOFeAs

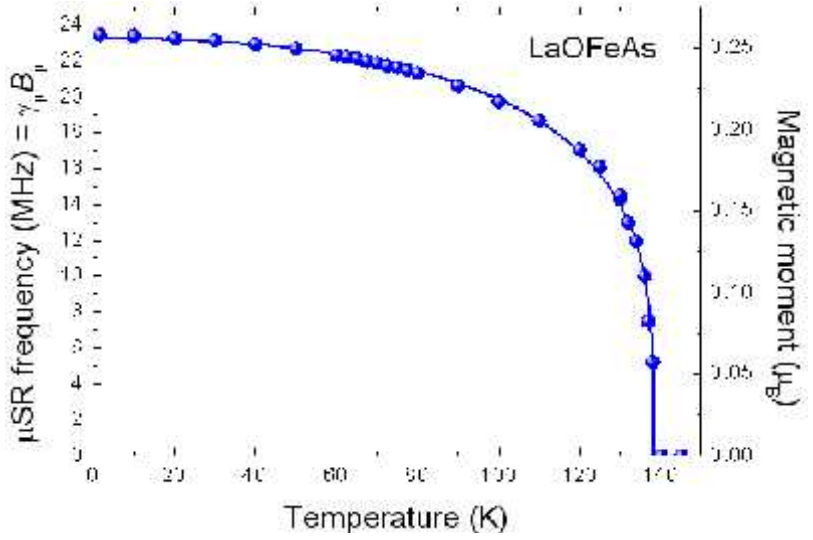

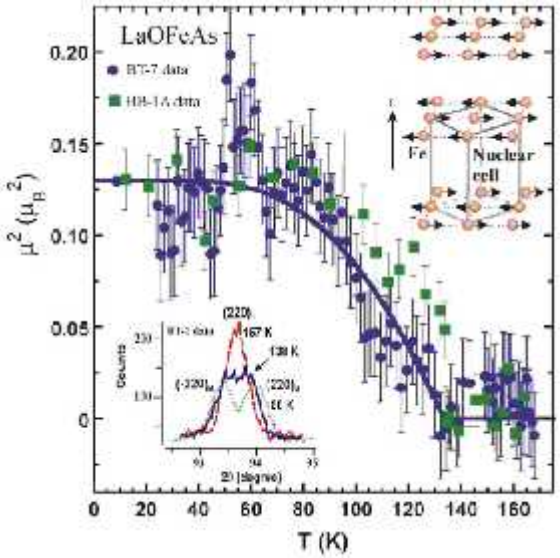

C. de la Cruz *et al.*, Nature 453, 899 (2008)

- **Zero Field Muon Spin Rotation**
  - Static commensurate magnetic order
  - T-dependence of the Fe magnetization with high precision, $T_N = 138$ K
  - 100% magnetic volume fraction

$$B_\mu = B_{\rm dip} + B_{\rm c} + \cdots$$

contact field $\propto e|\Psi(x_\mu)|^2$

$$B_{\rm dip} = \sum_i \frac{1}{r_i^3}\left[\frac{(3\boldsymbol{m}_i \cdot \boldsymbol{r}_i)}{r_i^2}\boldsymbol{r}_i - \boldsymbol{m}_i\right]$$

- **Mössbauer spectroscopy**
  - Hyperfine field $B_{\rm hf}(0) = 4.86(5)$ T
    =>
    Saturation moment **= 0.25 - 0.32 μ_B**

- **Neutron scattering**
  - Saturation moment **= 0.36(5) μ_B**

PAUL SCHERRER INSTITUT

PSI

Randomly Oriented Magnetic Moments

-

Short Range Magnetism

-

Magnetic Disorder

Randomly Oriented Moments

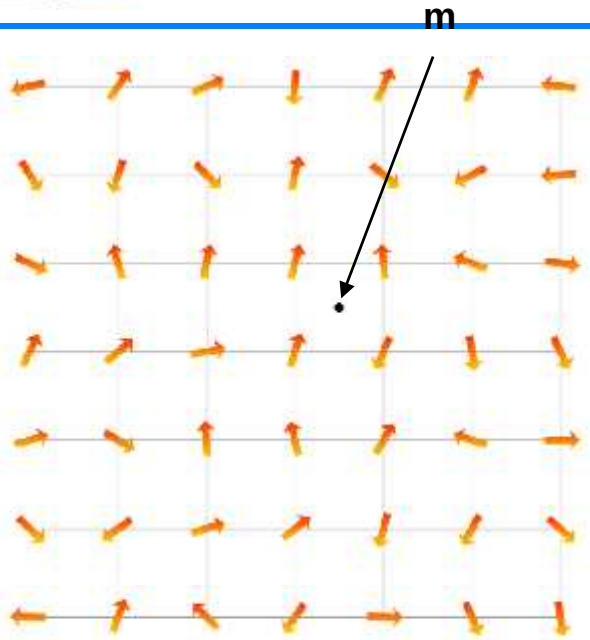

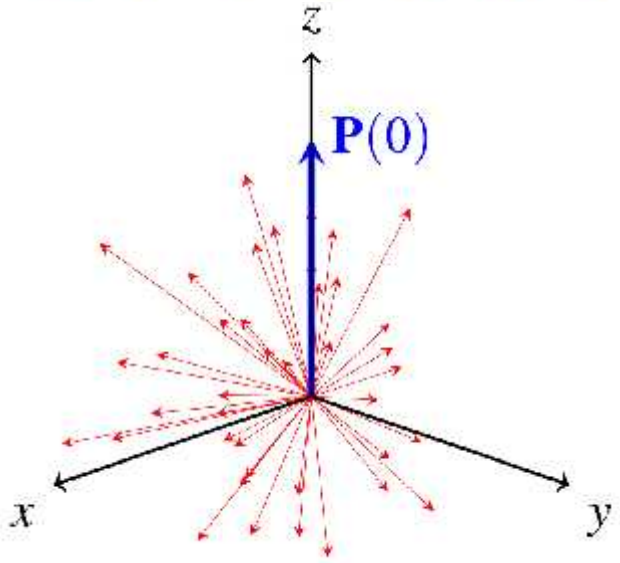

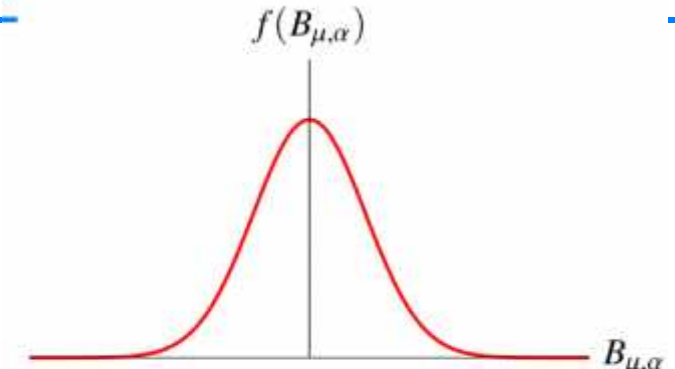

$$f(B_{\mu,\alpha}) = \frac{1}{\sqrt{2\pi\langle\Delta B_\mu^2\rangle}} \exp\left[-\frac{B_{\mu,\alpha}^2}{2\langle\Delta {B_\mu}^2\rangle}\right]$$

If isotropic:

$$f(|\mathbf{B}_\mu|) = f(\mathbf{B}_\mu)\, 4\pi B_\mu^2$$

Maxwell distribution:

$$f(|\mathbf{B}_\mu|) = \frac{1}{\sqrt{2\pi\langle\Delta B_\mu^2\rangle^3}} 4\pi B_\mu^2 \exp\left[-\frac{B_\mu^2}{2\langle\Delta B_\mu^2\rangle}\right]$$

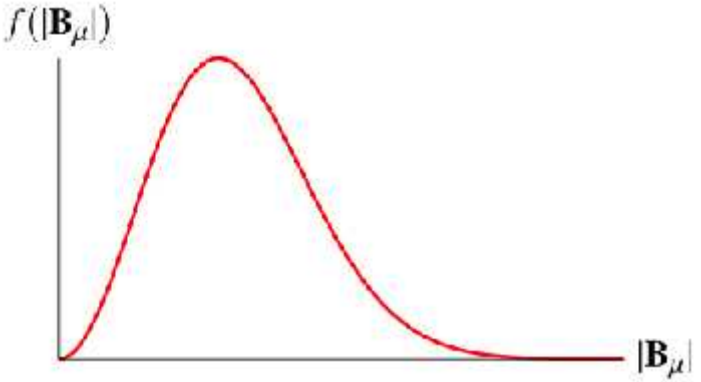

Randomly Oriented Moments

$$P_z(t) = \int f(\mathbf{B}_\mu)\left[\cos^2\theta + \sin^2\theta\cos(\gamma_\mu B_\mu t)\right] d\mathbf{B}_\mu$$

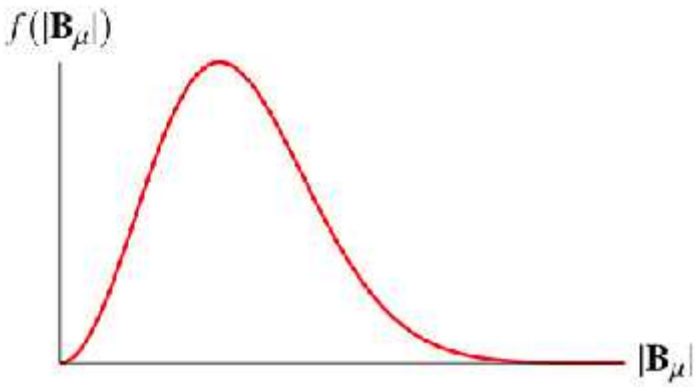

Kubo-Toyabe function

$$P_z(t) = \frac{1}{3} + \frac{2}{3}\left[1 - \gamma_\mu^2\langle\Delta B_\mu^2\rangle t^2\right]\exp\left[-\frac{\gamma_\mu^2\langle\Delta B_\mu^2\rangle t^2}{2}\right]$$

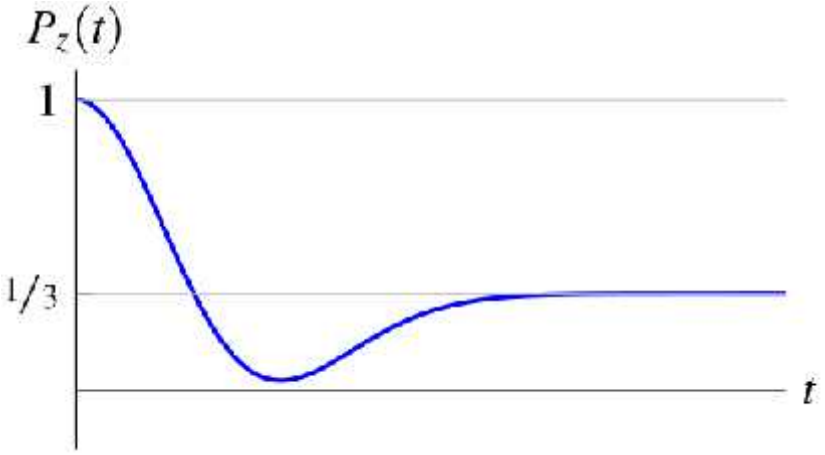

PAUL SCHERRER INSTITUT

PSI

Example:
Kubo-Toyabe depolarization due to nuclear moments
InN and MnSi

InN & MnSi

InN
Semiconductor
Study of the hydrogen-related defect chemistry

Y.G. Celebi et al., Physica B 340-342, 385 (2003)

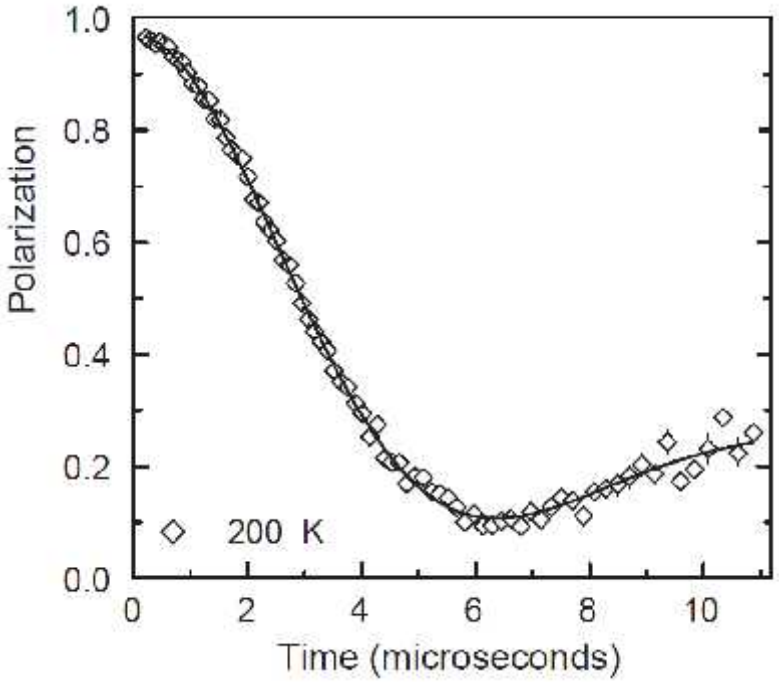

MnSi
system lacking inversion symmetry
itinerant-electron magnet MnSi

R.S. Hayano et al., Phys. Rev. B 20, 850 (1979)

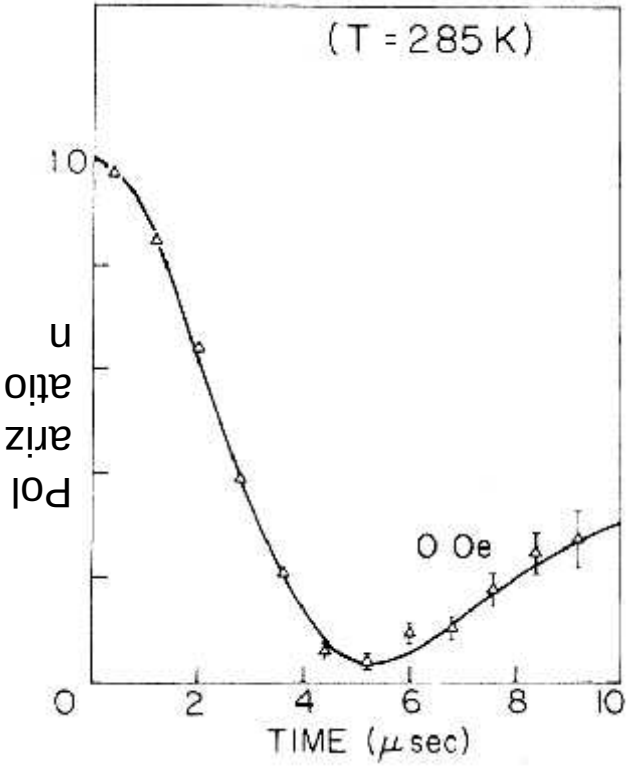

In the paramagnetic state, a KT function is very often observed reflecting the small field distribution created by the nuclear moments

PAUL SCHERRER INSTITUT

PSI

Detection of Magnetic Phase Separation

-

Coexistence of Different Magnetic Phases

Zurab Guguchia

PAUL SCHERRER INSTITUT

PSI

Example:
Helical magnetic order in MnAs

Experiments in Zero Field

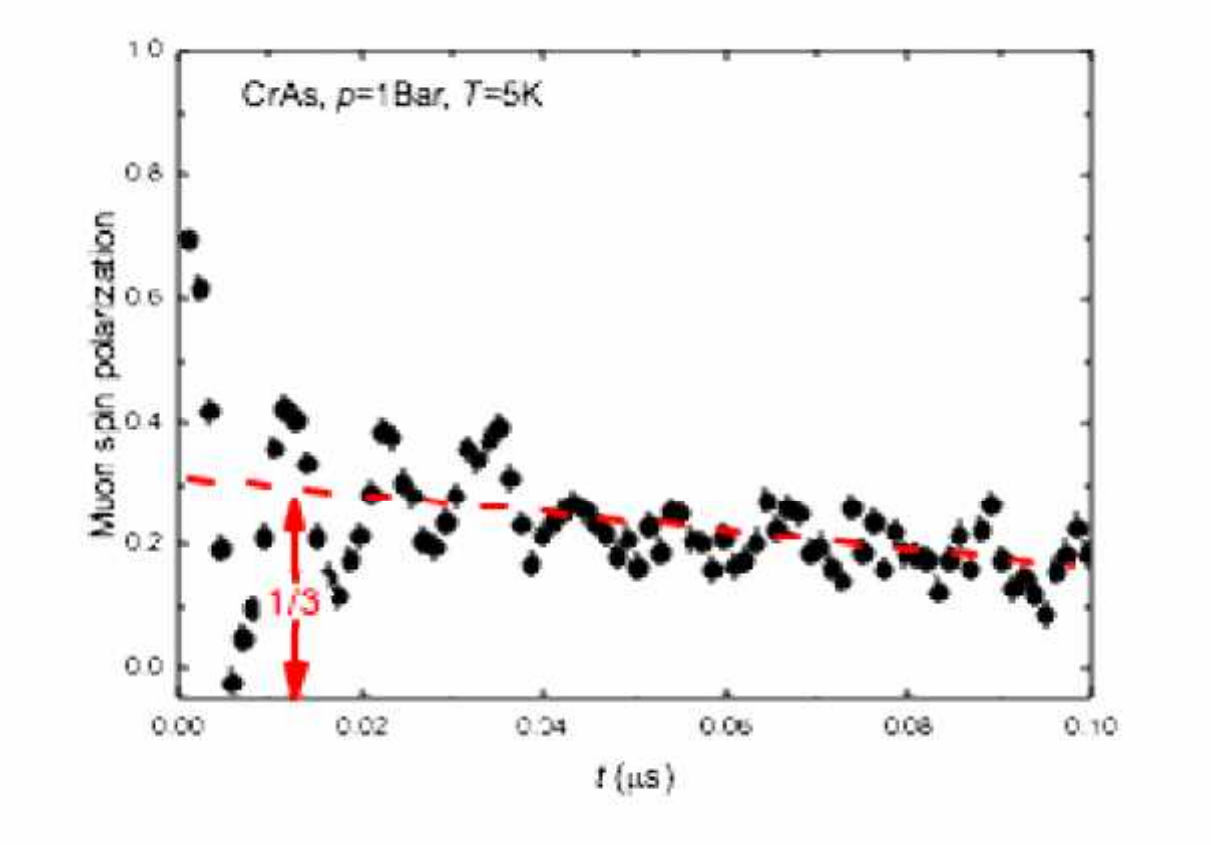

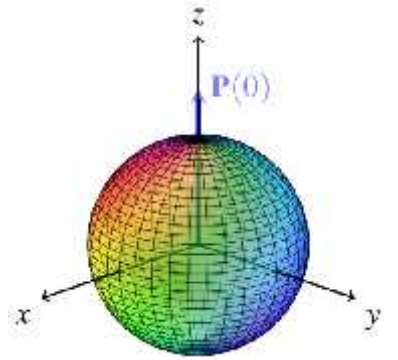

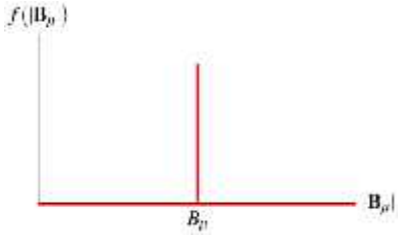

$$P_z(t) = \frac{1}{3} + \frac{2}{3}\cos(\gamma_\mu B_\mu t)$$

At ambient pressure CrAs is 100% magnetic!

Helical magnetic order

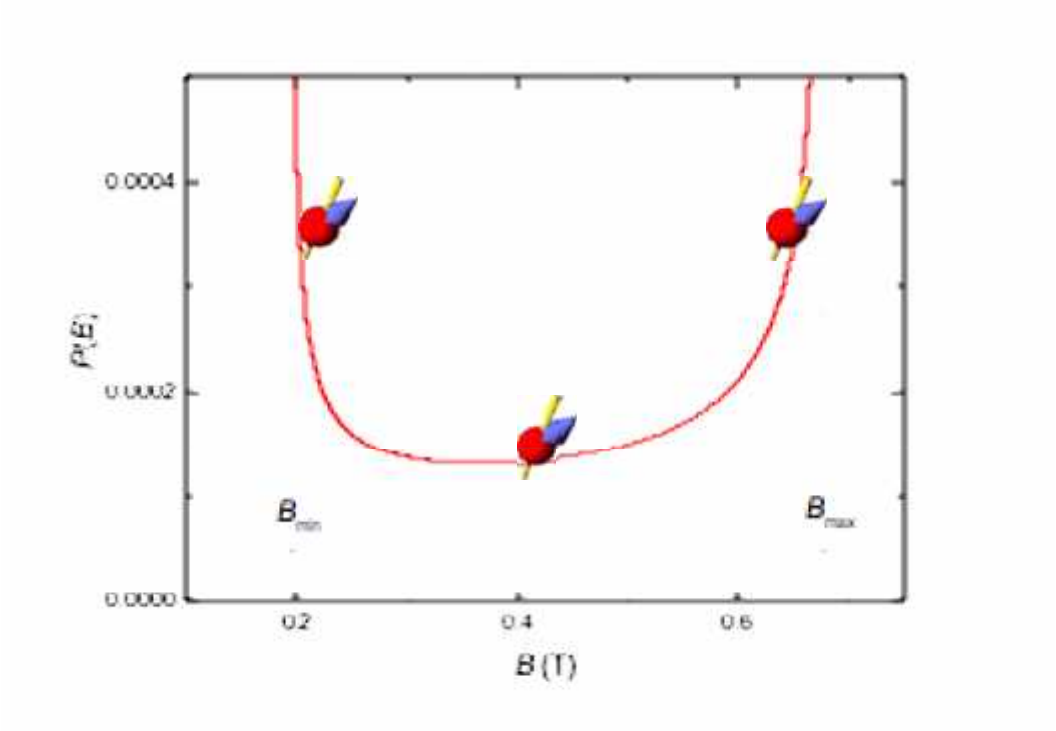

$$P(B) = \frac{2}{\pi} \frac{B}{\sqrt{(B^2 - B_{min}^2)(B_{max}^2 - B^2)}}$$

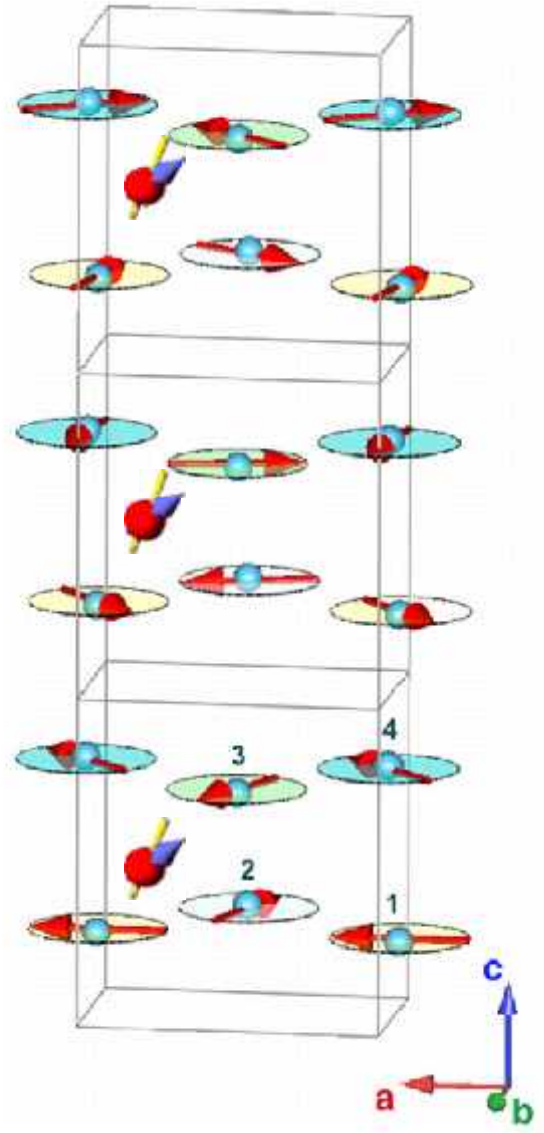

Helical magnetic order

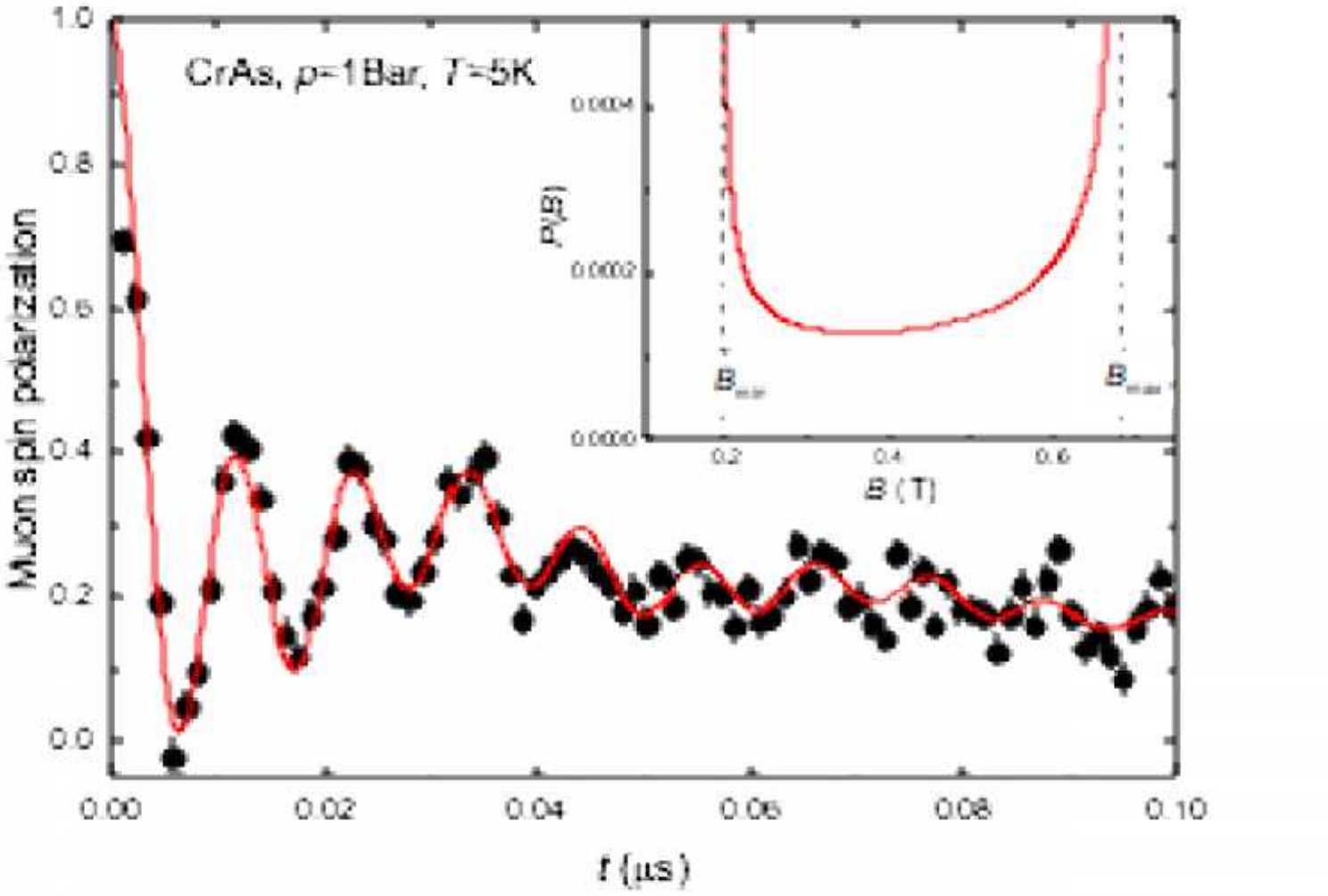

Confirmation of helical type of magnetic order in CrAs

PAUL SCHERRER INSTITUT

PSI

Example:
Microscopic Coexistence of Superconductivity and Magnetism in Fe-based superconductors

PAUL SCHERRER INSTITUT

PSI

FeSe (11-family)

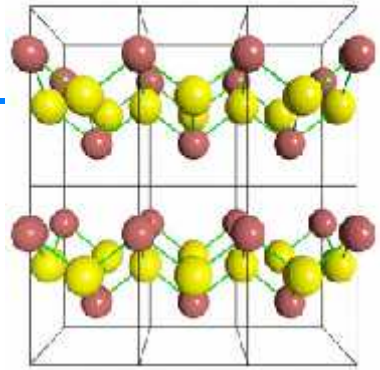

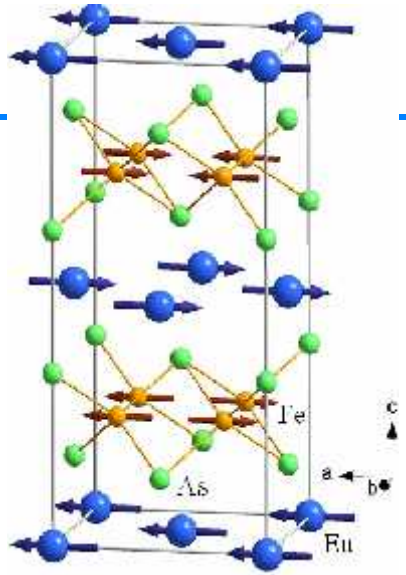

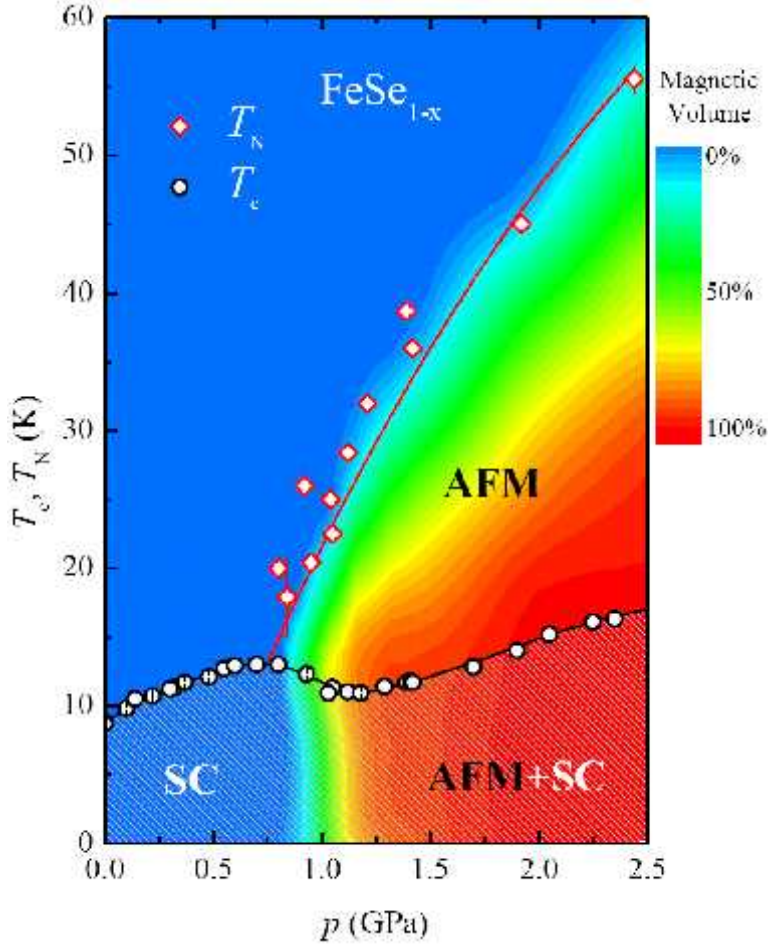

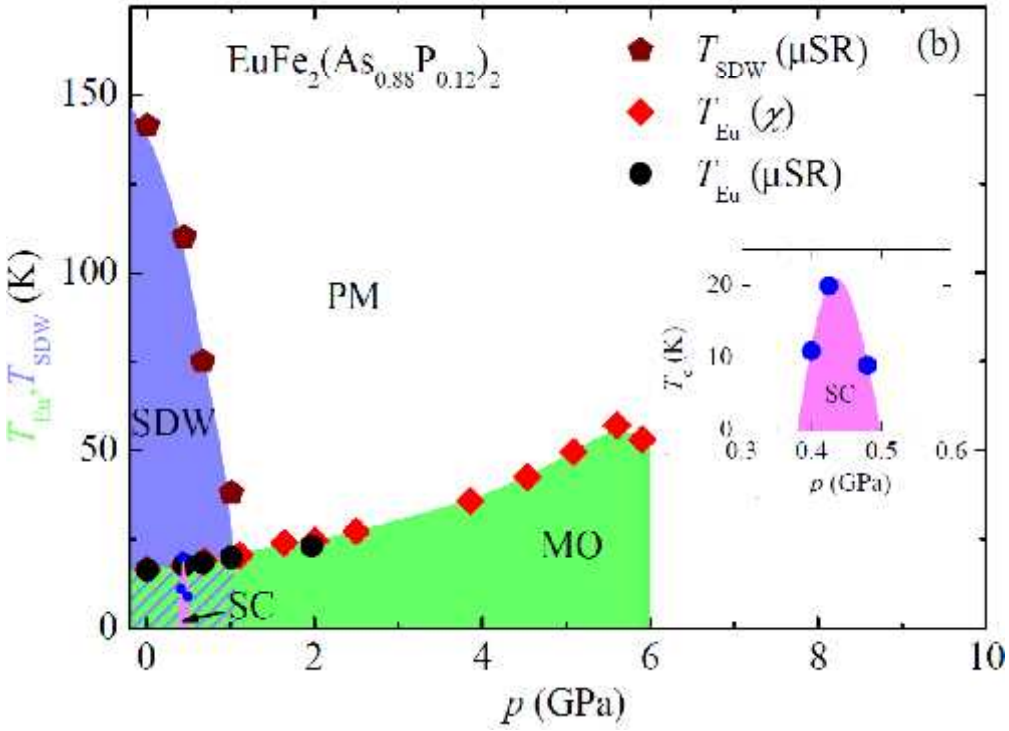

$RuSr_2GdCu_2O_8$

Resistivity:
(**superconductivity**)

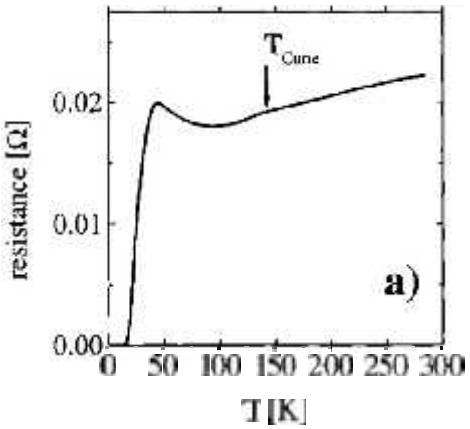

Magnetization:
(**ferromagnetism**)

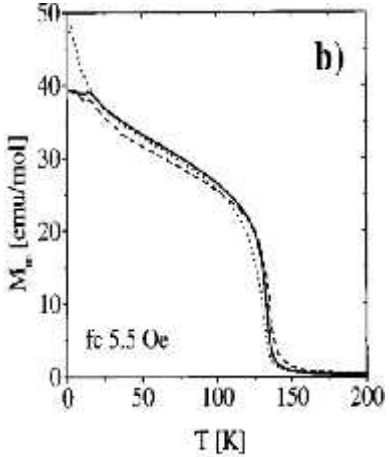

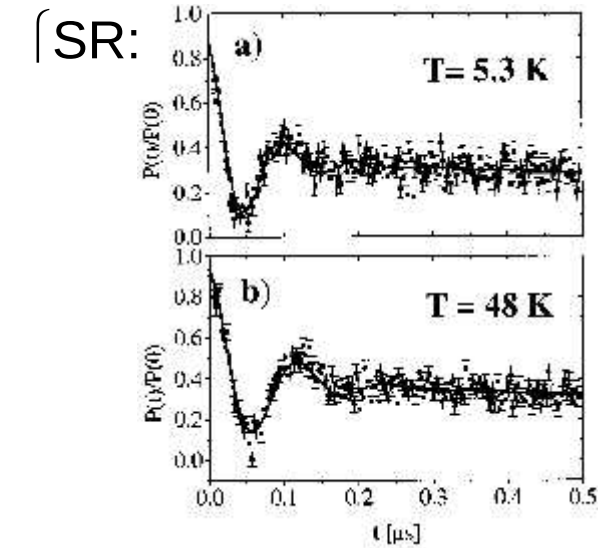

C. Bernhard et al., Phys. Rev. B 59 (1999) 14099

~100%
Magnetic volume

Mikroscopic coexistence of superconductivity and magnetism

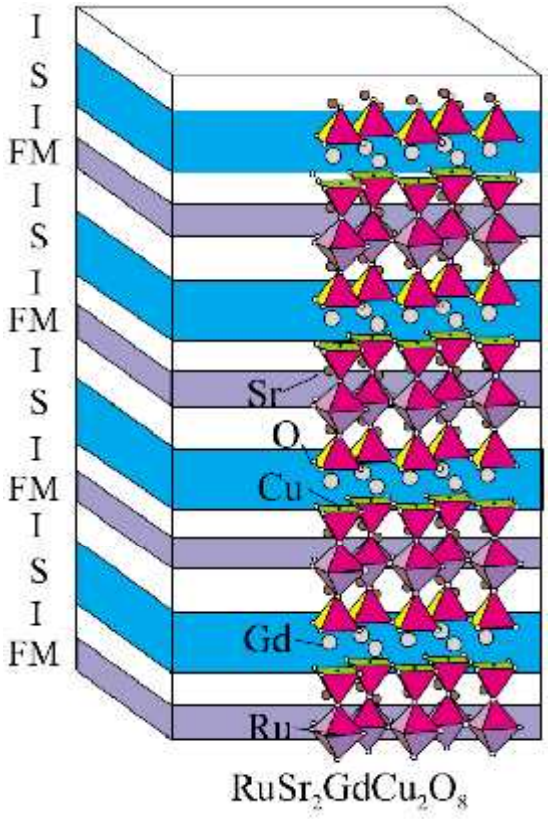

Structure:
T. Nachtrab et al., Phys. Rev. Lett. **92** (2004) 117001

Static Magnetism Probed by ZF

Single Crystals – Magnet

$$P_z(t) = \exp\left[-\frac{1}{2}\gamma_\mu^2\langle\Delta B_\mu{}^2\rangle t^2\right]\cos(\gamma_\mu B_\mu t)$$

- **Frequency:**
  Size of the magnetic moments
- **Damping:**
  Inhomogeneity
- **Amplitude:**
  Magnetic volume fraction

Polycrystals – Magnet

$$P_z(t) = \frac{1}{3} + \frac{2}{3}\exp\left[-\frac{1}{2}\gamma_\mu^2\langle\Delta B_\mu{}^2\rangle t^2\right]\cos\left[\gamma_\mu\langle B_\mu\rangle t\right]$$

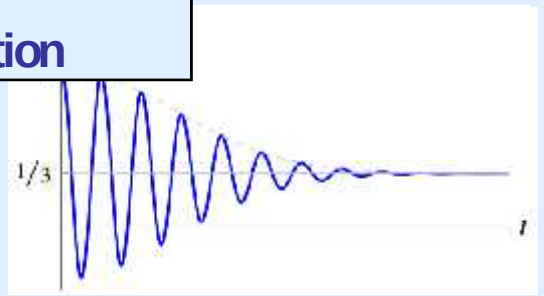

Randomly oriented static moments

$$P_z(t) = \frac{1}{3} + \frac{2}{3}\left[1 - \gamma_\mu^2\langle\Delta B_\mu^2\rangle t^2\right]\exp\left[-\frac{\gamma_\mu^2\langle\Delta B_\mu^2\rangle t^2}{2}\right]$$

PAUL SCHERRER INSTITUT

PSI

Muon Spin Rotation on Superconducting Materials

Zurab Guguchia

Superconductivity -- Introduction

Discovery by **Kamerlingh Onnes** in 1911 in mercury

Received the Nobel Prize in 1913 for "*his investigations on the properties of matter at low temperatures which led, inter alia, to the production of liquid helium*".

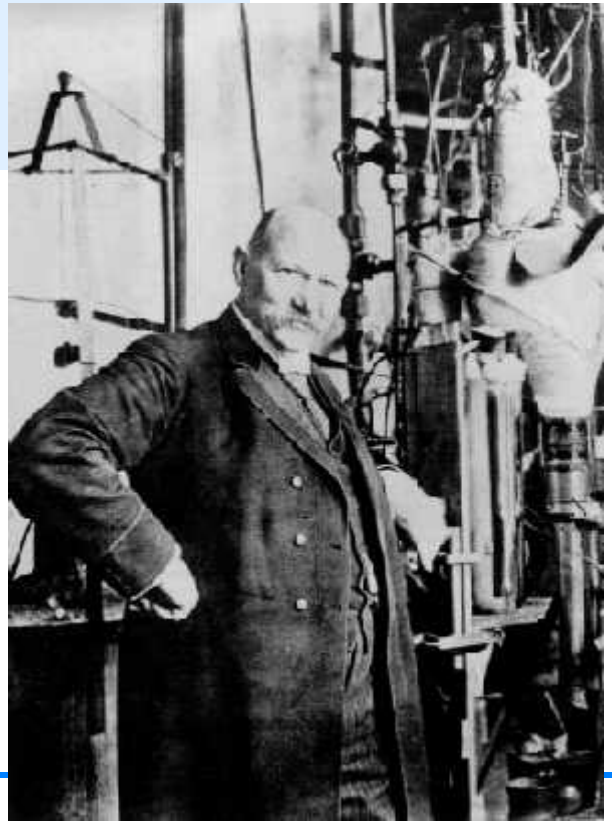

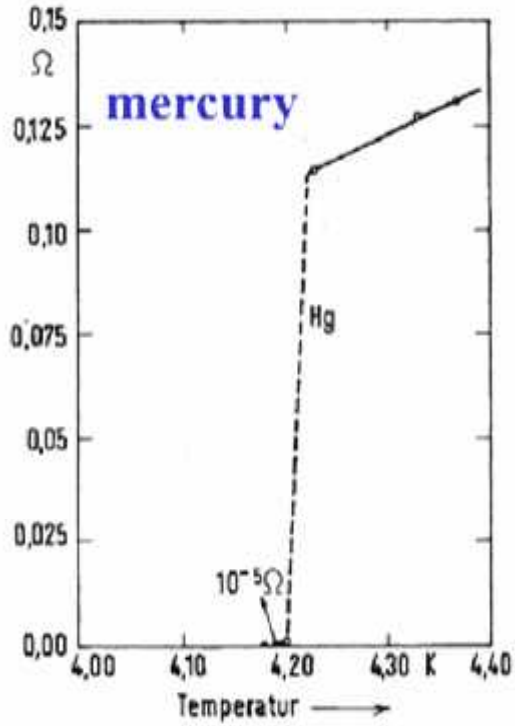

Temperature dependence of the resistance of a Hg sample

Superconductivity -- Introduction

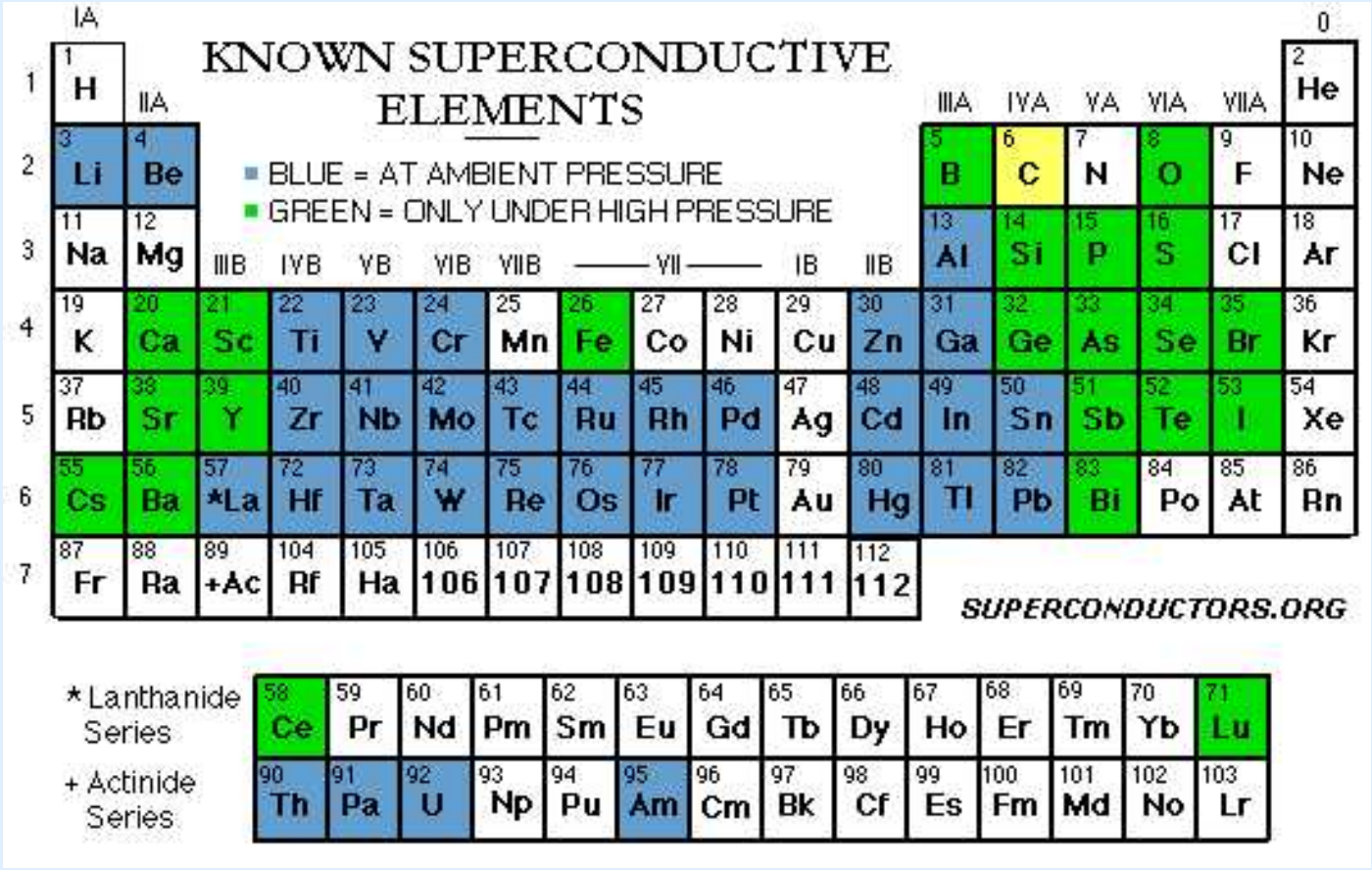

Superconductivity -- Timeline

1908 **Kammerling Onnes**: production of liquid helium 

1911 **Kammerling Onnes**: discovery of zero resistance

1933 **Meissner and Ochsenfeld**: superconductors expell applied magnetic fields (MOE)

1935 **F. and H. London:** MOE is a consequence of the minimization of the electromagnetic free energy carried by superconducting current

1950 **Ginzburg and Landau**: phenomenological theory of superconductors 

1950 **Maxwell and Reynolds et al.**: isotope effect

1957 **Abrikosov**: 2 types of superconductors (magnetic flux) 

1957 **Bardeen, Cooper, and Schrieffer**: BCS theory -- superconducting current as a superfluid of Cooper pairs 

1962 **Josephson**: Joesephson effect 

1986 **Berdnorz and Müller**: High-Tc's superconductors 

Main Characteristics:

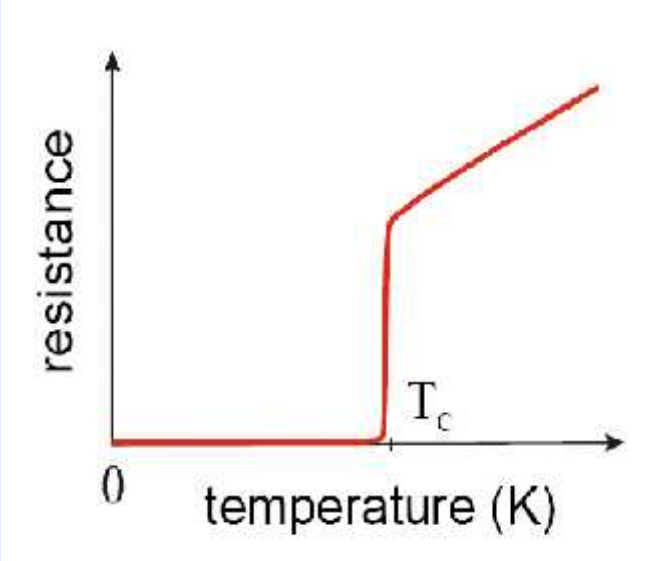

Kamerlingh Onnes

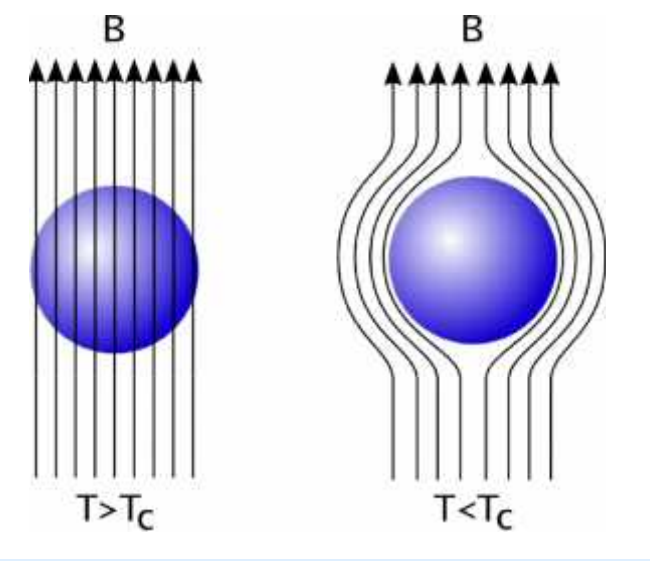

Meissner and Ochsenfeld

Is a superconductor "just" an ideal conductor?

New thermodynamic state of matter!

Ideal Conductor

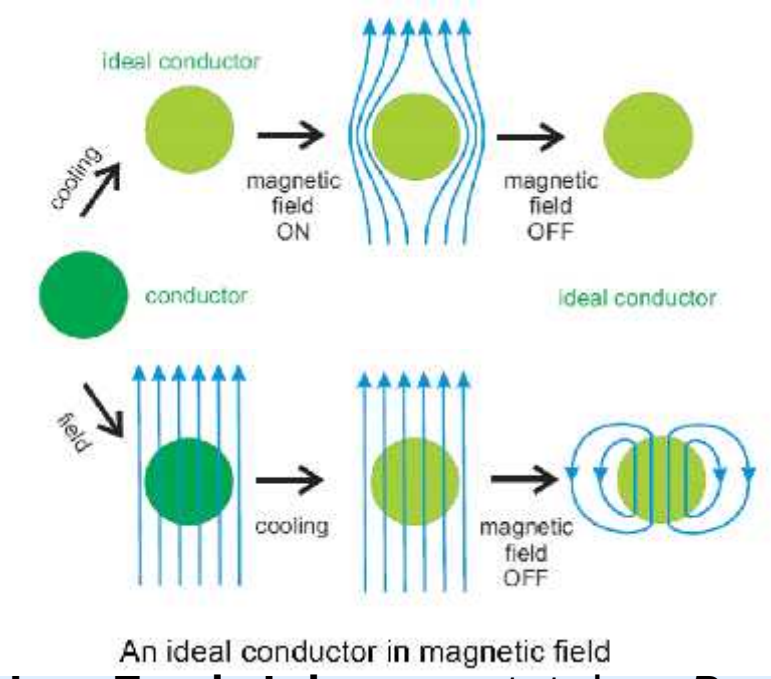

An ideal conductor in magnetic field

Lenz-Faraday's law: currents to keep *B* constant inside of the sample

Superconductor

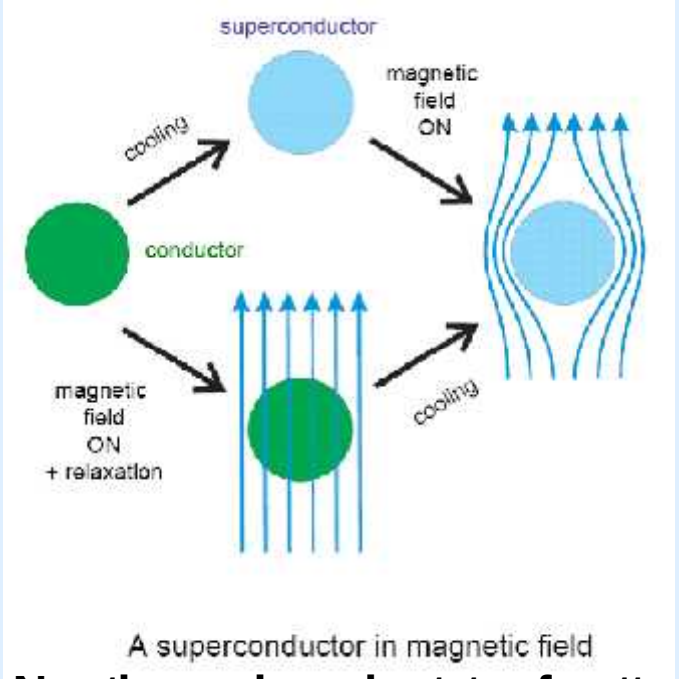

A superconductor in magnetic field

New thermodynamic state of matter

From: Lecture on Superconductivity, Alexey Ustinov, Uni. Erlangen, 2007

PAUL SCHERRER INSTITUT

PSI

Nanometer scale parameters

Magnetic penetration depth: λ

Coherence length: ξ

Phenomenological London's equations

In a sample without resitance, the electrons will feel a force:

$$\mathbf{F} = -e\mathbf{E} = m\frac{\partial\langle\mathbf{v}\rangle}{\partial t}$$

F. and H. London,
Proc. Roy. Soc. **A149**, 71 (1935)

Recalling that the current density is: $\mathbf{j} = -n_s e\langle\mathbf{v}\rangle$

one obtains the first London equation (*acceleration equation*):

$$\Lambda\frac{\partial\mathbf{j}}{\partial t} = \mathbf{E} \quad \text{with} \quad \Lambda = \frac{m}{n_s e^2}$$

Taking the curl of this equation

using the 3rd and 4th Maxwell equations

$$\nabla\times\mathbf{E} = -\frac{\partial\mathbf{B}}{\partial t}$$

$$\nabla\times\mathbf{B} = \mu_0\mathbf{j} \qquad (\text{assuming } \frac{\partial\mathbf{E}}{\partial t} = 0)$$

$$\nabla\times\nabla\times\vec{B} = \nabla\left(\nabla\bullet\vec{B}\right) - \nabla^2\vec{B}$$

one obtains:

$$\Delta\frac{\partial\mathbf{B}}{\partial t} = \frac{1}{\lambda^2}\frac{\partial\mathbf{B}}{\partial t}$$

$$\Delta\frac{\partial\mathbf{j}}{\partial t} = \frac{1}{\lambda^2}\frac{\partial\mathbf{j}}{\partial t}$$

with: $\lambda^2 = \frac{\Lambda}{\mu_0} = \frac{m}{\mu_0 e^2 n_s}$

$$\Delta\mathbf{B} = \frac{1}{\lambda^2}\mathbf{B}$$

$$\Delta\mathbf{j} = \frac{1}{\lambda^2}\mathbf{j}$$

with: $\lambda^2 = \frac{\Lambda}{\mu_0} = \frac{m}{\mu_0 e^2 n_s}$

1st Nano-scale Param.: London Penetration Depth

$$\Delta \mathbf{B} = \frac{1}{\lambda^2}\mathbf{B}$$

$$\Delta \mathbf{j} = \frac{1}{\lambda^2}\mathbf{j}$$

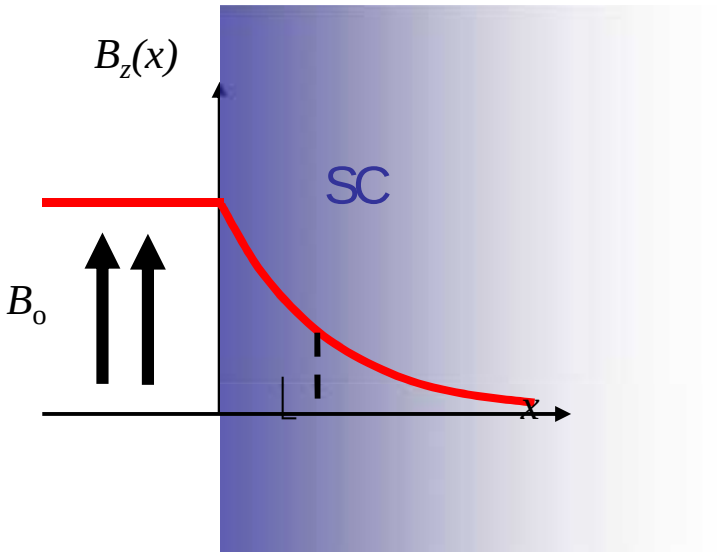

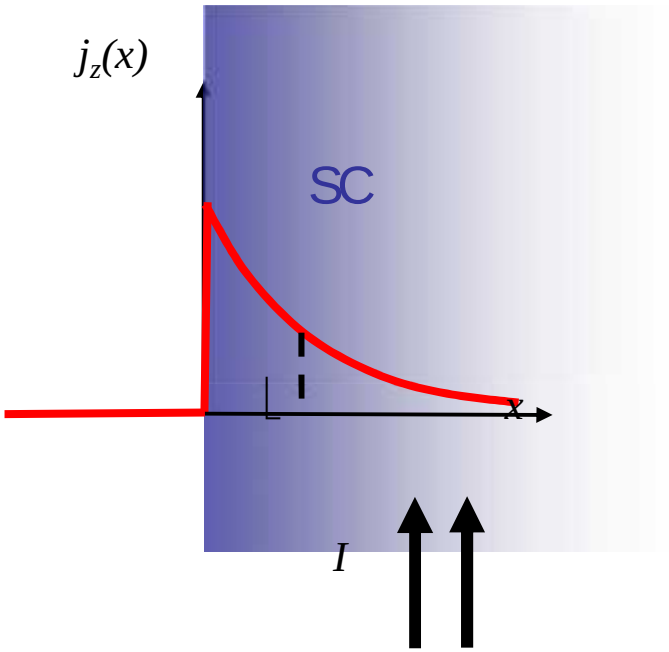

$$B_z(x) = B(0)\exp(-x/\lambda)$$

$$j_z(x) = \frac{I}{2\pi R\lambda}\exp(-x/\lambda)$$

$$\lambda = \sqrt{\frac{m^*}{\mu_0 e^2 n_s}}$$

Ginzburg-Landau Equations (1950)

Powerful phenomenological theory, based on the Landau theory of second order transition.

Pseudowave-function ψ acting as order parameter (in the normal phase $= 0$, in the superconducting phase $\neq 0$).

ψ describes the superconducting electrons and their density

$$n_s = |\psi(\mathbf{r})|^2$$

The free energy density f_s can be expanded in a series:

$$f_s = f_n + \alpha|\psi|^2 + \frac{\beta}{2}|\psi|^4 + \frac{1}{2m}|(-i\hbar\nabla - 2e\mathbf{A})\psi|^2 + \frac{|\mathbf{B}|^2}{2\mu_0}$$

The order parameter and the vector potential are obtained by minimizing the Ginzburg-Landau formula with respect to ψ and $\mathbf{A}$.

2nd Nano-scale Param.: Coherence Length

$$f_s = f_n + \alpha|\psi|^2 + \frac{\beta}{2}|\psi|^4 + \frac{1}{2m}|(-i\hbar\nabla - 2e\mathbf{A})\psi|^2 + \frac{|\mathbf{B}|^2}{2\mu_0}$$

Let assume a situation without field and at an interface

vaccuum/superconductor.

Minimizing the free energy with respect to ψ

$$\alpha\psi + \beta|\psi|^2\psi - \frac{\hbar^2}{2m}\nabla^2\psi = 0$$

Taking into account that $\psi(0) = 0$ and that $\psi(x \gg 0) = \psi_\infty$

$$\psi(x) = \psi_\infty \tanh\left(\frac{x}{\sqrt{2}\,\xi}\right)$$

with: $\xi = \sqrt{\dfrac{\hbar^2}{2m|\alpha|}}$ $\qquad \psi_\infty^2 = -\dfrac{\alpha}{\beta}$

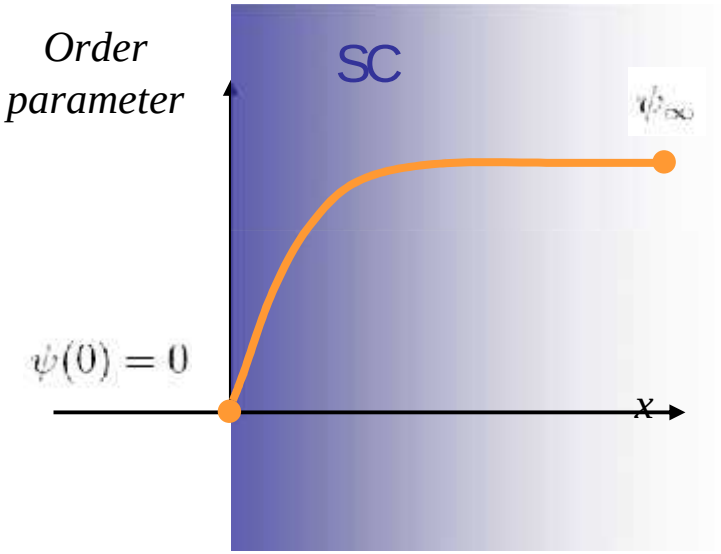

$$\xi = \frac{\hbar v_F}{\pi\Delta}$$

Type I and Type II Superconductors

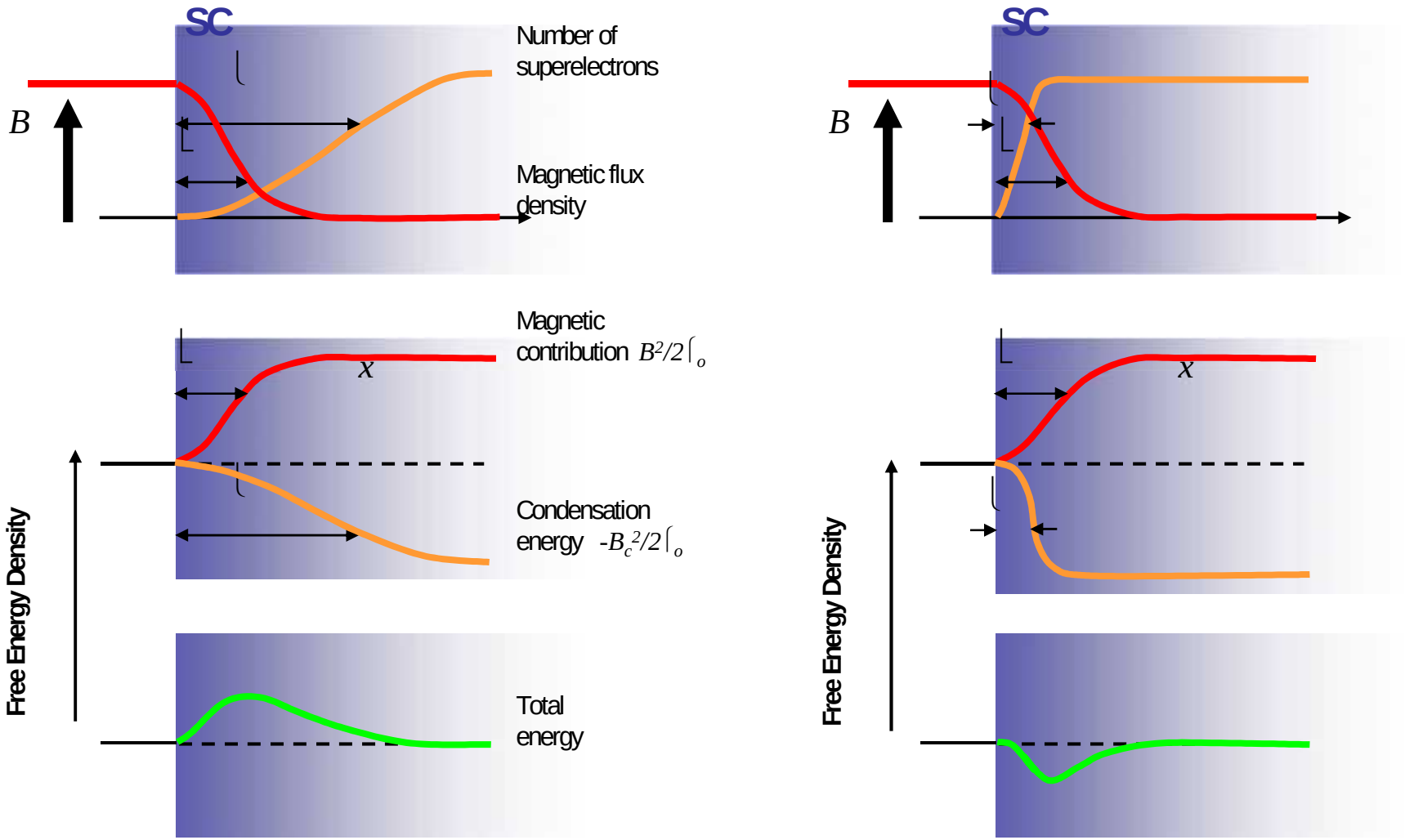

Type I (ξ < λ) Ty

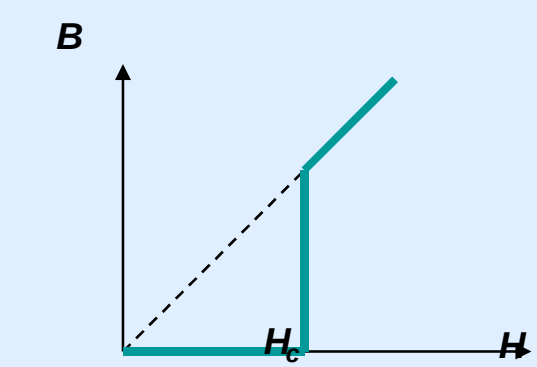
B
H_c
H

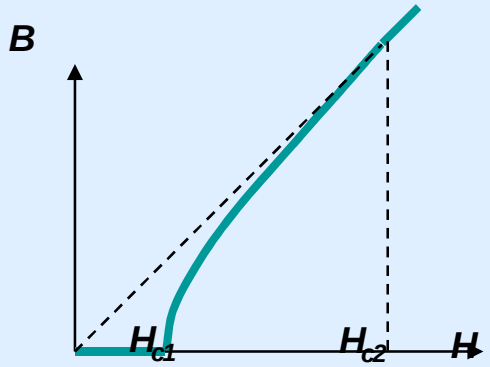
B
H_{c1}
H_{c2}
H

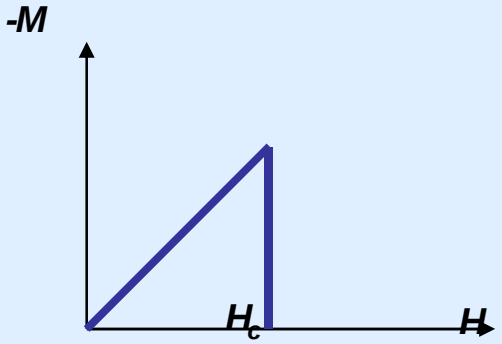
-M
H_c
H

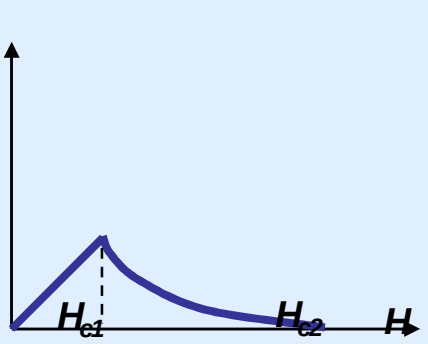
-M
H_{c1}
H_{c2}
H

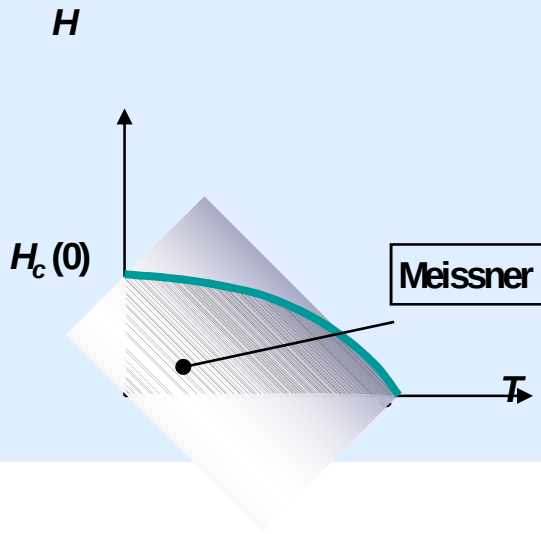
H
H_c (0)
Meissner phase
T

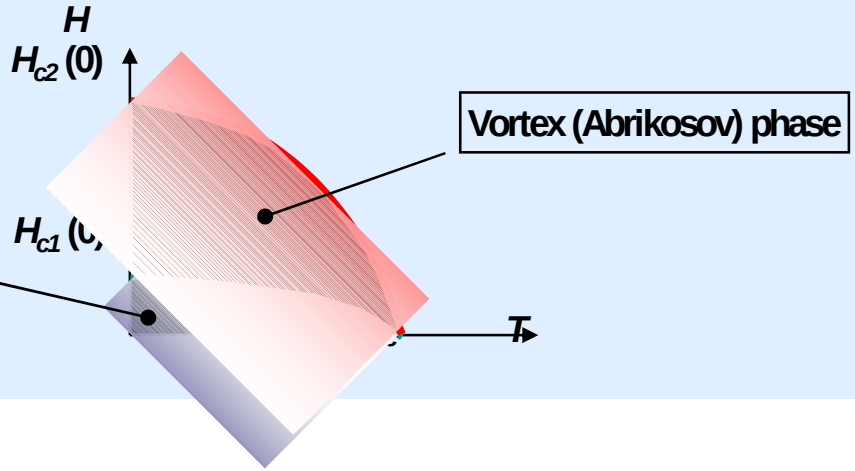
H
H_{c2} (0)
Vortex (Abrikosov) phase
H_{c1} (
T

Vortex (Abrikosov) phase

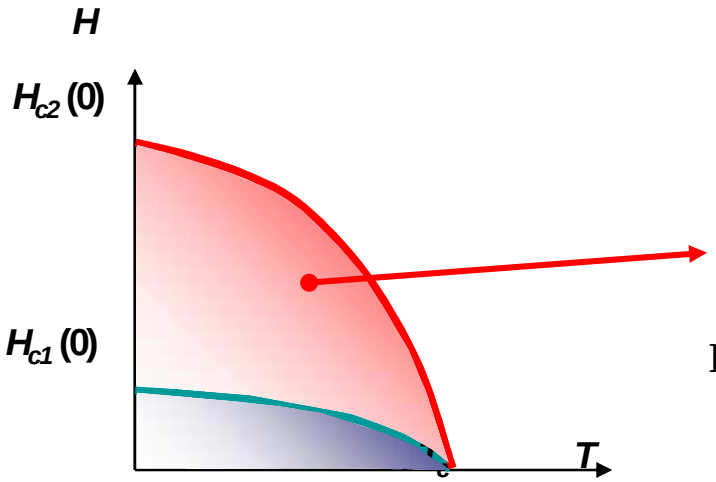

"Flux Line Lattice"

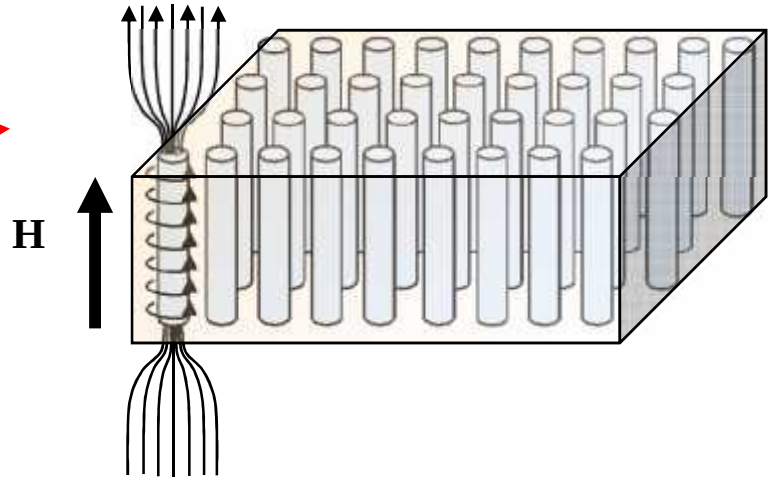

Magnetic flux quantum

$\Phi_0 = h/2e = 2.067 \cdot 10^{-15}$ Wb

Bitter Decoration
Pb-4at%In rod, 1.1K, 195G
U. Essmann and H. Trauble, Phys. Lett 24A, 526 (1967)

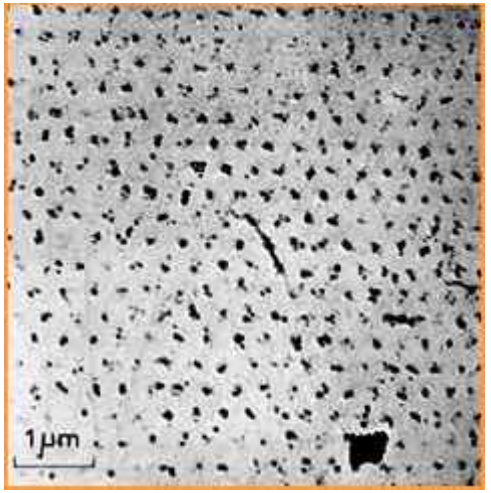

Muons and Field Distribution in Type II S.C.

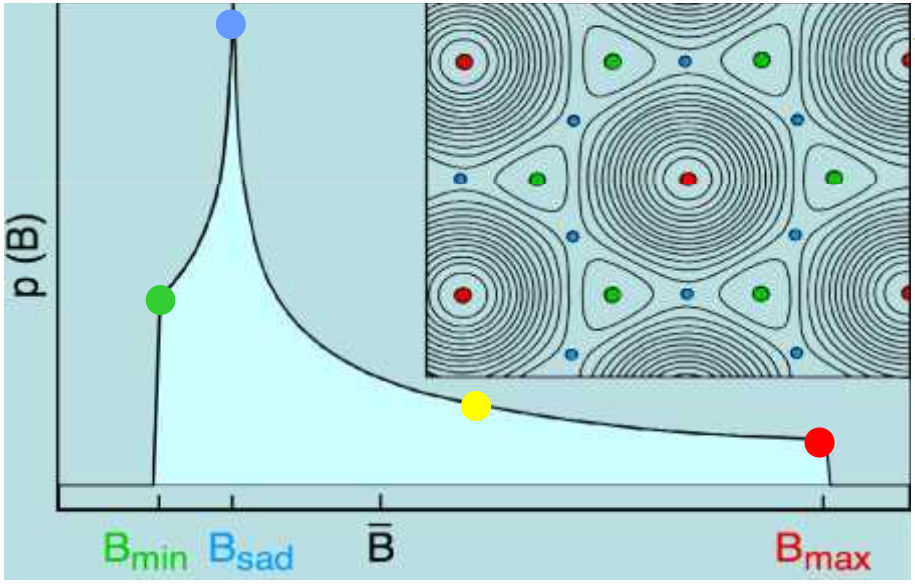

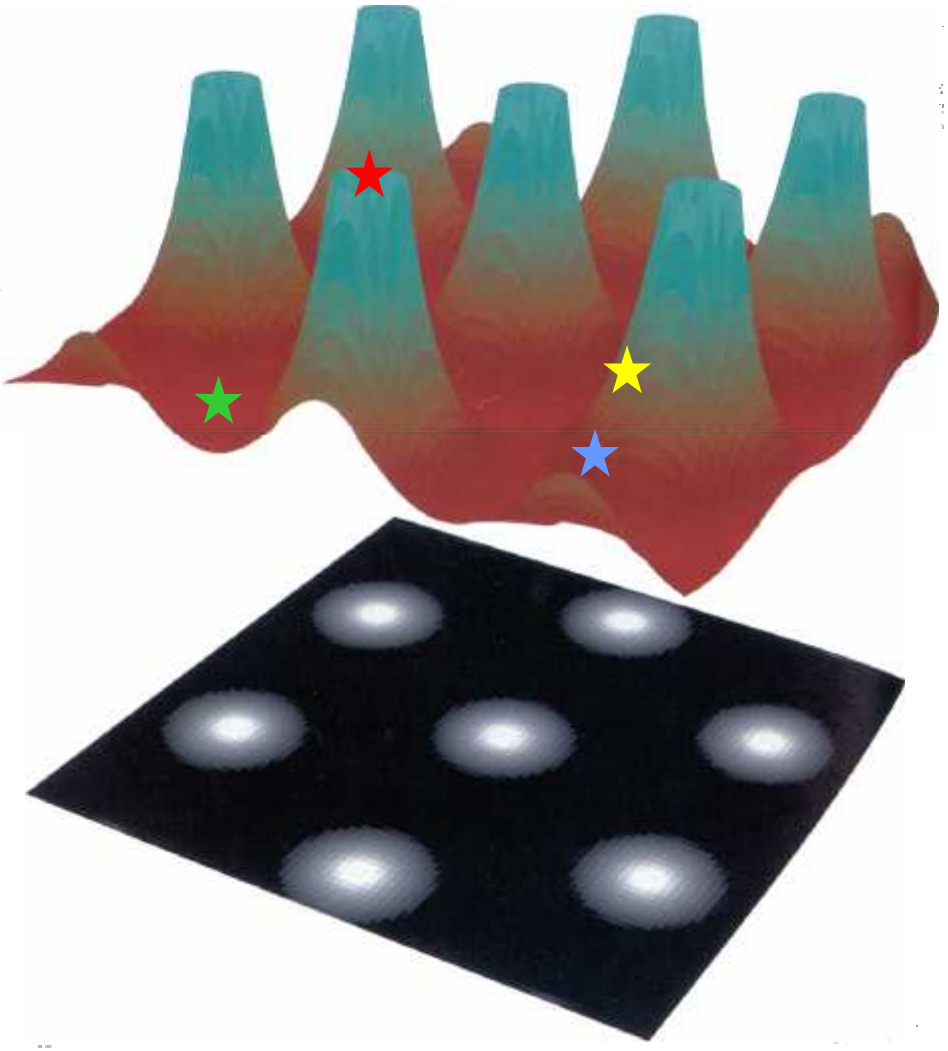

*Bishop et al., Scientific American **48** (1993)*

PAUL SCHERRER INSTITUT

PSI

Using Bulk Muon Spin Rotation to Study Superconducting Materials

Zurab Guguchia

Flux-line lattice (Abrikosov lattice)

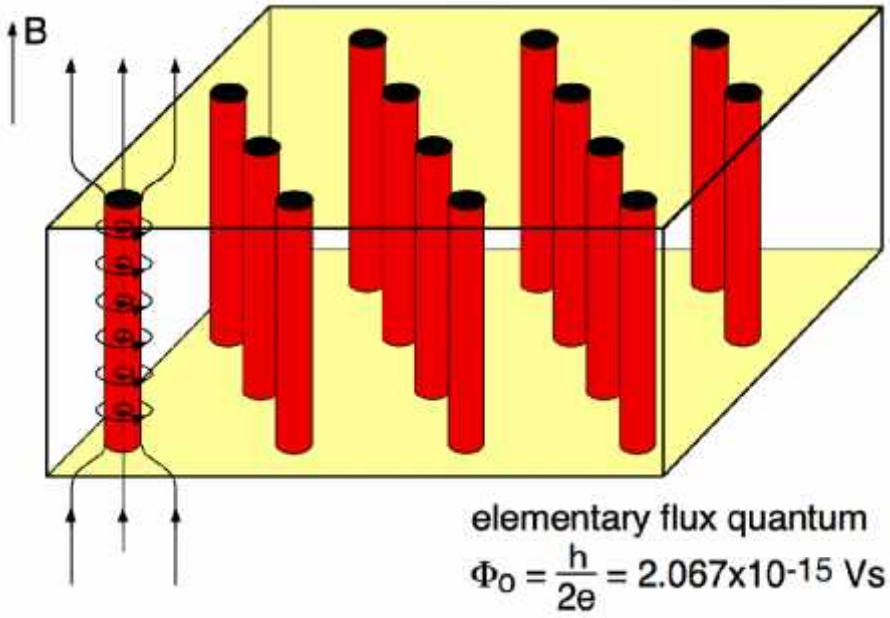

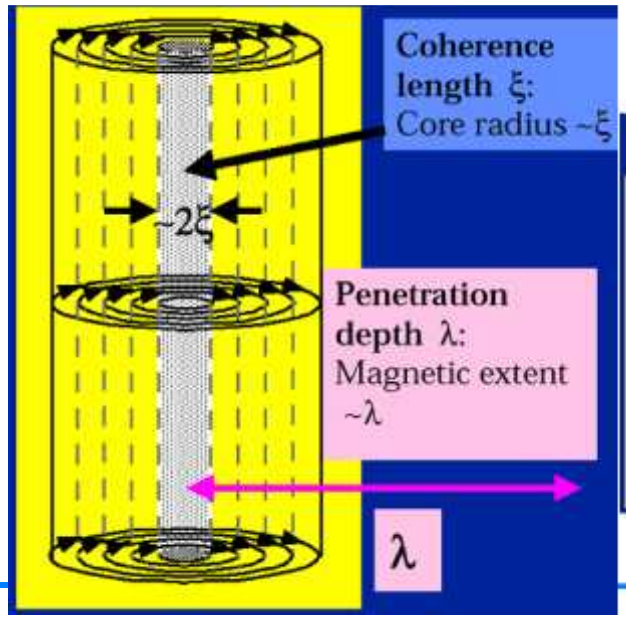

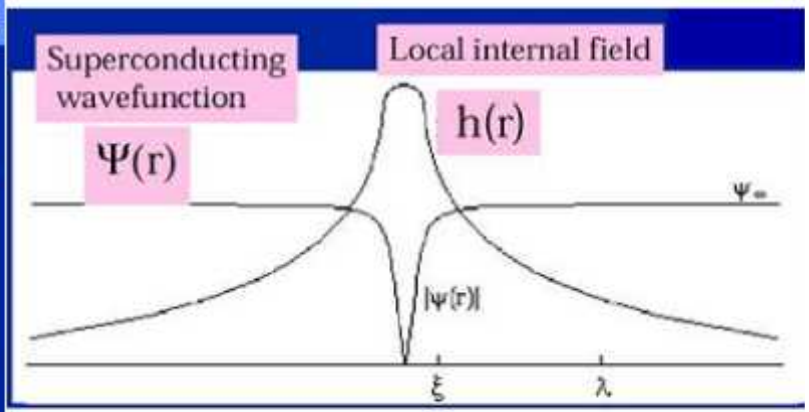

Field Distribution in a Type II S.C.

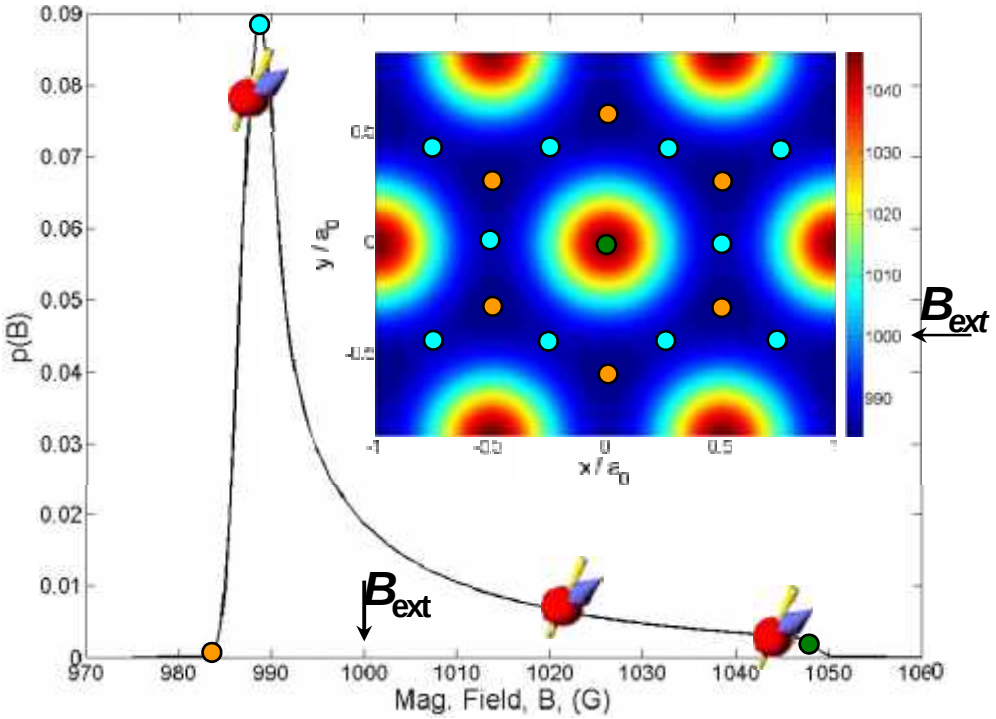

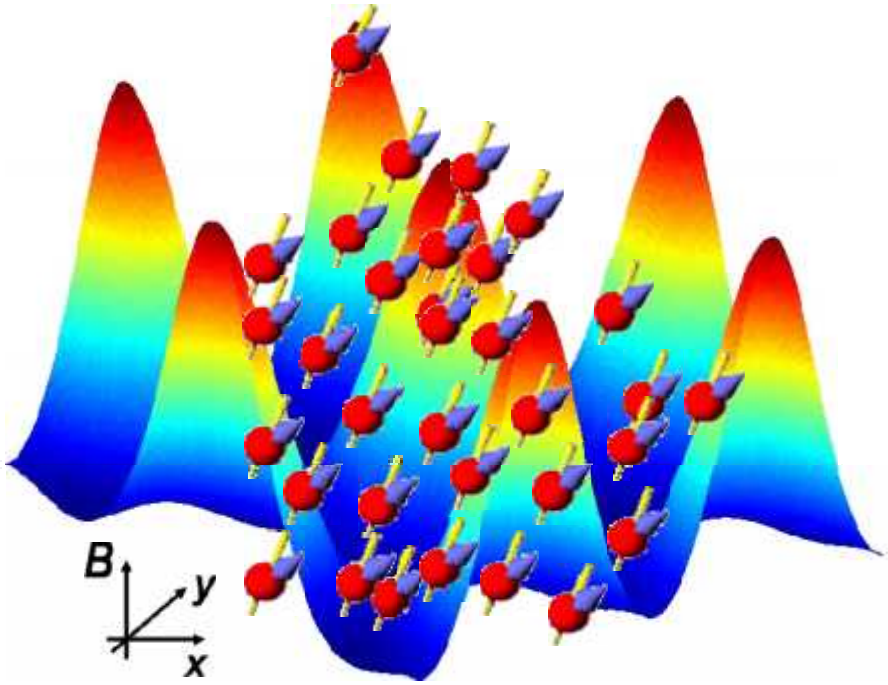

Since the muon is a local probe, the μSR relaxation function is given by the weighted sum of all oscillations:

$$G(t) = \int f(\mathbf{B}_\mu)\cos(\gamma_\mu B_\mu t)d\mathbf{B}_\mu$$

SR a Type II Superconductor

$T > T_c$

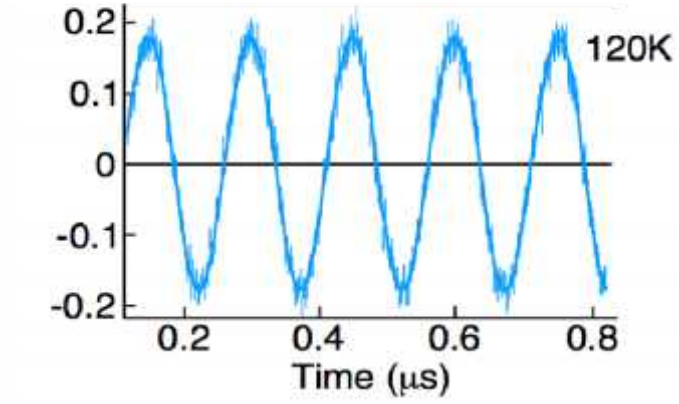

$YBa_2Cu_3O_{6.97}$
*Pümpin et al., Phys. Rev. B **42**, 8019 (1990)*

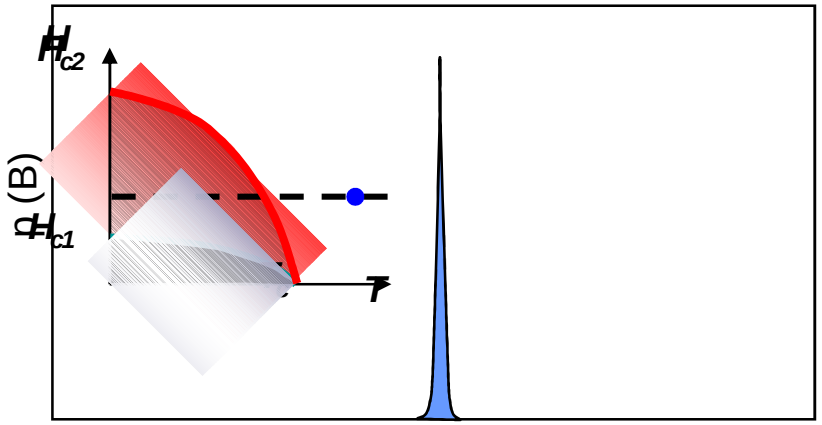

SR a Type II Superconductor

$T < T_c$

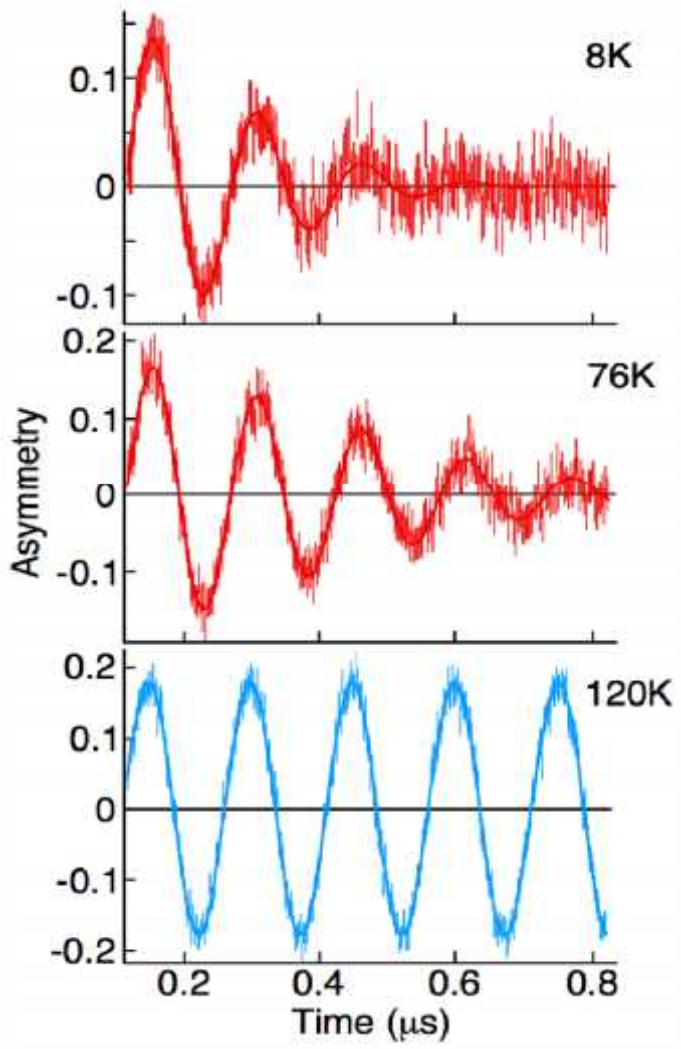

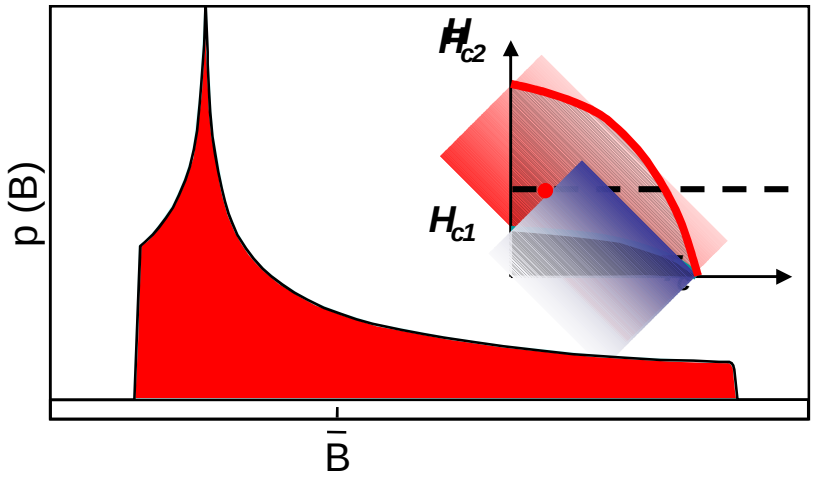

$T > T_c$

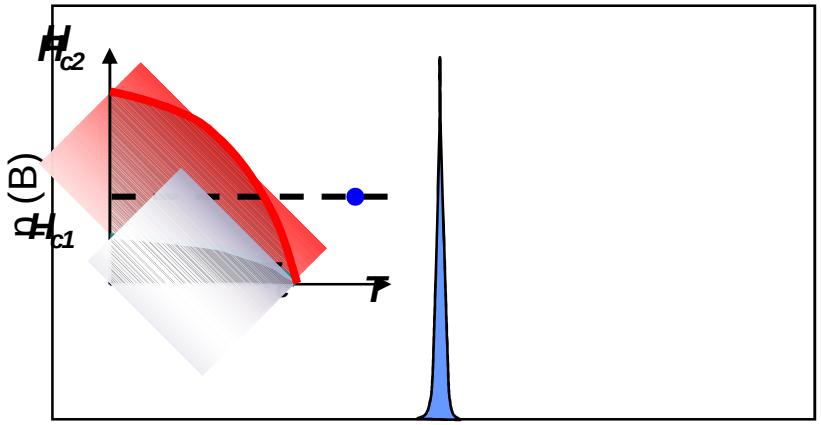

$YBa_2Cu_3O_{6.97}$
*Pümpin et al., Phys. Rev. B **42**, 8019 (1990)*

Field Distribution in "Extreme" Type II S.C.

- Ginburg-Landau parameter $\kappa = \frac{\lambda}{\xi} \gg 1$
- Large range of fields (up to $B_{c2}/4$) where London model applies
- Vortex cores well separated and do not interact
- Vortex fields superimpose linearly

$$S = d^2 \frac{\sqrt{3}}{2}$$

$$\phi_0 = S \cdot B$$

$$\Rightarrow d = \sqrt{\frac{2\phi_0}{B\sqrt{3}}}$$

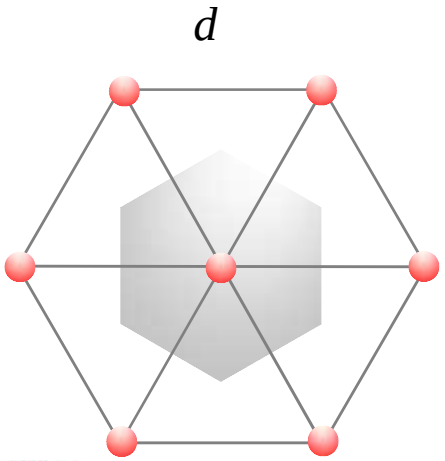

In an ideal vortex state the vectors $\vec{r}_n$ form a periodic two dimensional lattice. Therefore [7-4] can be solved in Fourier space ($\vec{k}$ space).

For an hexagonal lattice:

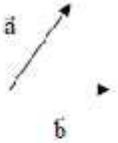

$$|\vec{a}| = |\vec{b}| = d, \quad \vec{a} \cdot \vec{b} = \cos 60^\circ$$

Reciprocal vectors:

$$\vec{a}^* = 2\pi \frac{\vec{b} \times \vec{c}}{\vec{a} \cdot (\vec{b} \times \vec{c})} \qquad \vec{b}^* = 2\pi \frac{\vec{c} \times \vec{a}}{\vec{a} \cdot (\vec{b} \times \vec{c})}$$

$$|\vec{a}^*| = 2\pi \frac{|\vec{b}|}{|\vec{a} \cdot \vec{b}|} = \frac{4\pi}{\sqrt{3}d} = |\vec{b}^*|$$

$$\vec{k}_{m,n} = m\vec{a}^* + n\vec{b}^*$$

(also hexagonal symmetry)

$$\vec{B}(\vec{r}) = \sum_{\vec{k}} b_{\vec{k}} e^{i\vec{k}\vec{r}} \qquad [7\text{-}5]$$

With Fourier components:

$$b_{\vec{k}} = \frac{1}{S} \int \vec{B}(\vec{r}) e^{-i\vec{k}\vec{r}} d^2\vec{r}$$

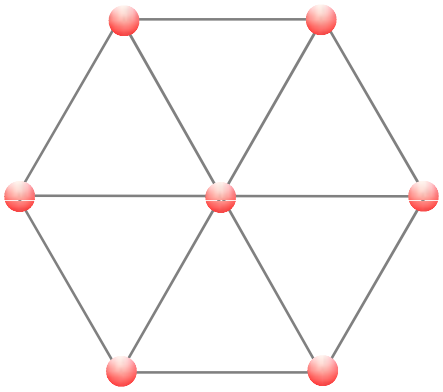

Field distribution: $\mathbf{B}(\mathbf{r})$?

$\mathbf{B}(\mathbf{r})$ must fulfill the modified London equation:

$$\mathbf{B}(\mathbf{r}) - \lambda^2 \Delta \mathbf{B}(\mathbf{r}) = \phi_0 \sum_n \delta(\mathbf{r} - \mathbf{r}_n)\hat{z}$$

We expect a periodic magnetic field

and therefore can use:

$$\mathbf{B}(\mathbf{r}) - \sum_{\mathbf{K}} \mathbf{B}(\mathbf{K}) \exp(i\mathbf{K}\mathbf{r})$$

with Fourier components:

$$\mathbf{B}(\mathbf{K}) = \frac{1}{S} \int \mathbf{B}(\mathbf{r}) \exp(-i\mathbf{K}\mathbf{r}) d^2\mathbf{r}$$

The modified London equation becomes

(fields only along $\hat{z}$):

$$\sum_{\mathbf{K}} (\mathbf{B}(\mathbf{K}) + \lambda^2 K^2 \mathbf{B}(\mathbf{K})) \exp(i\mathbf{K}\mathbf{r}) = N\phi_0 \sum_{\mathbf{K}} \exp(i\mathbf{K}\mathbf{r})$$

and one finds:

$$B_z(\mathbf{K}) = \frac{B}{1 + \lambda^2 K^2}$$

With: $B_z(\mathbf{r}) = \sum_{\mathbf{K}} \frac{B}{1+\lambda^2 K^2} \exp(i\mathbf{K}\mathbf{r})$

The second moment $\langle \Delta B_z^2 \rangle = \langle B_z^2 \rangle - \langle B_z \rangle^2$

of the field distribution is given by:

$$\langle \Delta B_z^2 \rangle = \sum_{\mathbf{K} \neq 0} |B_z(\mathbf{K})|^2$$

Taking into account the perfect triangular lattice where:

$K^2 = K_{m,n}^2 = \frac{16\pi^2}{3d^2}(m^2 + mn + n^2)$ and that $K^2\lambda^2 \gg 1$

$$< \Delta B_z^{\,2} > = \frac{3\Phi_0^{\,2}}{64\pi^4\lambda^4} \sum_{(m,n)\neq(0,0)} \frac{1}{(m^2 - mn + n^2)^2}$$

$$\langle \Delta B_z^2 \rangle = 0.00371 \frac{\phi_0^2}{\lambda^4}$$

- By measuring the second moment of the field distribution (for example by μSR), we directly determine the London penetration

Extract Information from the ⌈SR data

Theory

Maisuradze et al., (2008)

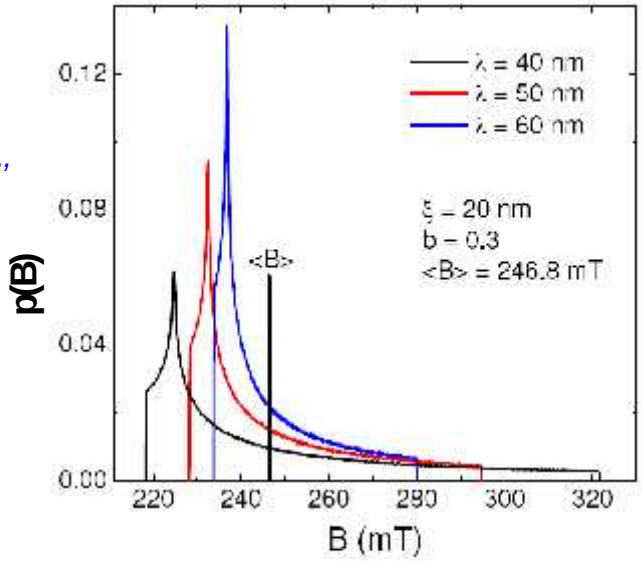

Pd-In alloy

*Charalambous et al., Phys. Rev. B **66**, 054506 (2002)*

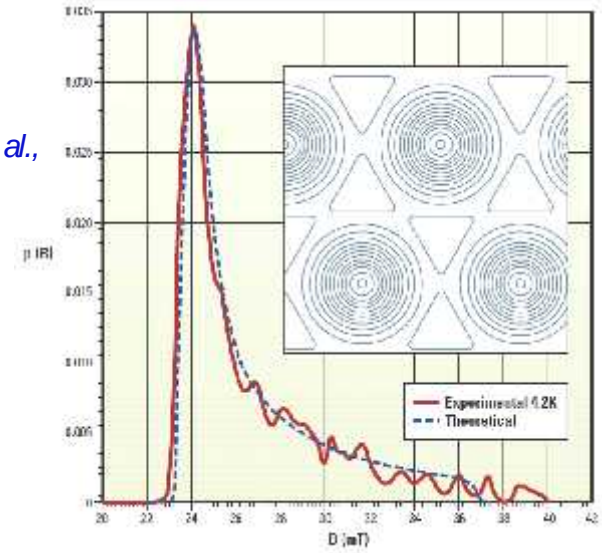

Field distribution depends on the microscopic parameters of superconductivity ⌊ and ⌊

Theoretical models of the flux line lattice to fit the ⌈SR data

▼

Structure, symmetry of the flux line lattice

Vortex motion

Characteristic lengths: magnetic penetration depth ⌊, radius of the vortex core - coherence length ⌊

Classification scheme of superconductors

Extract Information from t… data

Single crystals

- Anisotropy field distribution

Polycrystals or sintered sample

- Disorder of pinning sites
- Strong smearing of the field distribution

*Pümpin et al., Phys. Rev. B **42** 8019 (1990)*

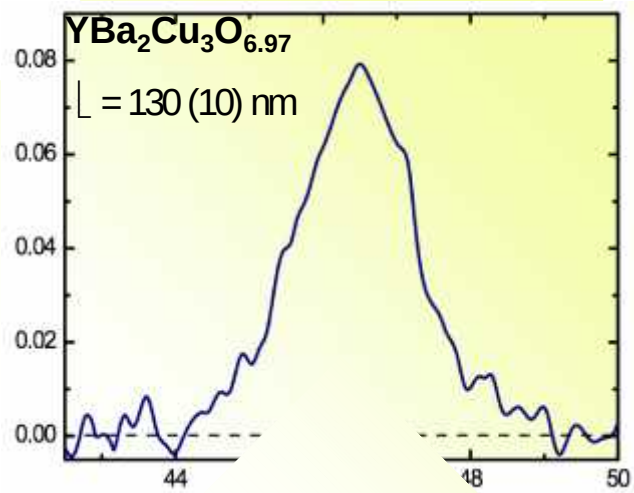

Pd-In alloy

*Charalambous et al., Phys. Rev. B **66**, 054506 (2002)*

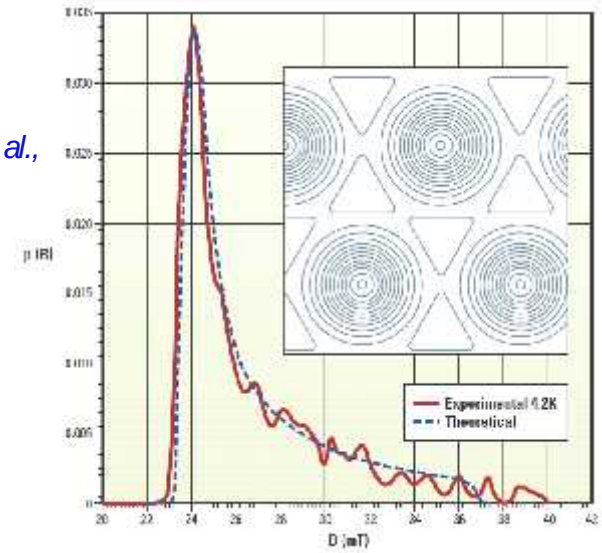

*Sonier et al., PRL **83**, 4156 (1999)*

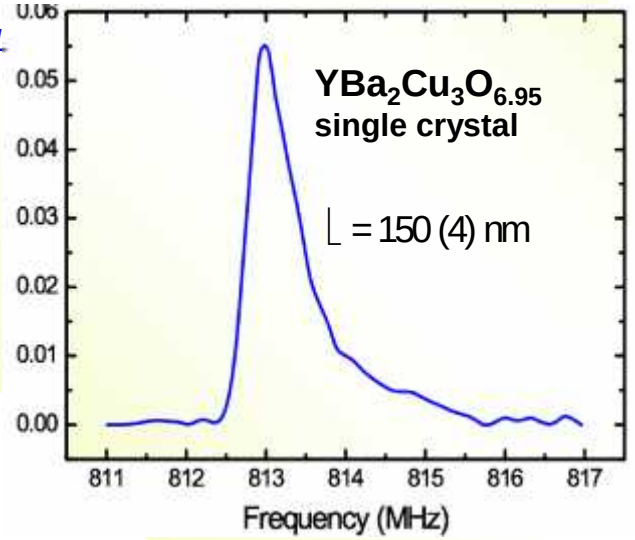

Extract Information from t… data

$$G(t) = \underbrace{\exp(-\frac{1}{2}\sigma^2 t^2)}_{\text{depolarization}} \times \underbrace{\cos(\gamma_\mu \langle B_\mu^z \rangle t)}_{\text{oscillations}}$$

where: $\sigma^2 = \gamma_\mu^2 \langle \Delta B_\mu^{z\,2} \rangle$

Pümpin et al., Phys. Rev. B 42 8019 (1990)

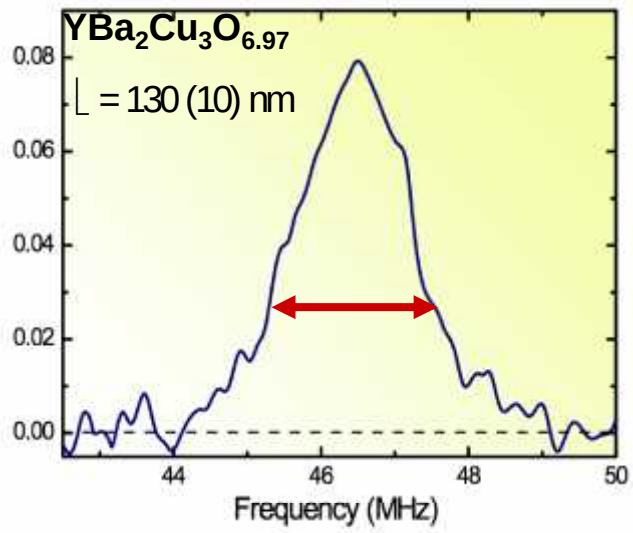

Ginzburg-Landau model

$$\langle \Delta B_z^2 \rangle = 0.00371 \frac{\phi_0^2}{\lambda^4}$$

London model

$$\lambda = \sqrt{\frac{m}{\mu_0 e^2 n_s}}$$

$$\Rightarrow \quad \sigma \propto \frac{1}{\lambda^2} \propto \frac{\mu_0 e^2}{m} n_s$$

A μSR measurement of the second moment of the field distribution allows to determine the London penetration depth λ.

The damping of a TF-μSR spectrum is proportional to the super fluid density n_s (number of Cooper pairs).

Classification of SCs: Uemura Plot

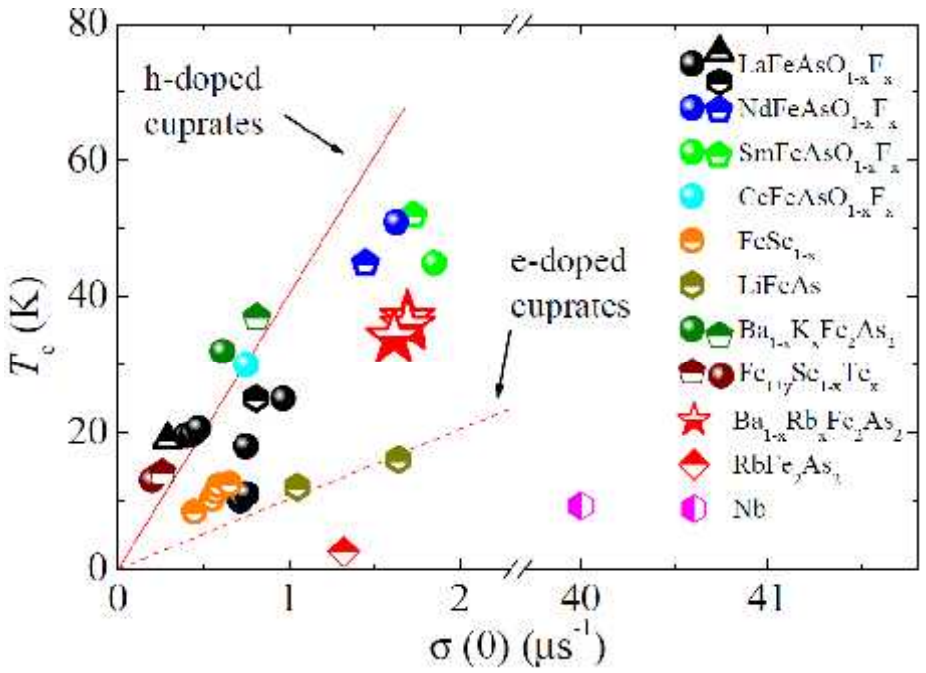

$$T_c \text{ versus } T_F \propto \sigma \propto \frac{1}{\lambda^2} \propto \frac{\mu_0 e^2}{m} n_s$$

- Conventional superconductors have low T_C and high superfluid density
- Unconventional superconductors have relatively low superfluid density ("dilute superfluid")

Z. Guguchia, et al., Phys. Rev. B 84, 094513 (2011)

Pairing Symmetry in Cuprates

Wave function of two electrons:

$$\Psi(\mathbf{r}_1, s_1; \mathbf{r}_2, s_2) = \psi(\mathbf{r}_1, \mathbf{r}_2)\chi(s_1, s_2)$$

where:

$\psi(\mathbf{r}_1, \mathbf{r}_2)$: space part

$\chi(s_1, s_2)$: spin part

spin singlet: $\chi = \frac{1}{\sqrt{2}}(|\uparrow\downarrow\rangle - |\downarrow\uparrow\rangle)$

$\Rightarrow S = 0 \rightarrow$ space part must be even.

$\Rightarrow$ s-wave (l = 0), d-wave (l = 2) etc...

BCS **High-Tc's**

spin triplet: $\chi = \frac{1}{\sqrt{2}}(|\uparrow\downarrow\rangle + |\downarrow\uparrow\rangle, \ldots)$

$\Rightarrow S = 1 \rightarrow$ space part must be odd.

$\Rightarrow$ p-wave (l = 1), f-wave (l = 3), etc...

Gap function: $\Delta(\mathbf{k})$ has a lower symmetry than the Fermi surface

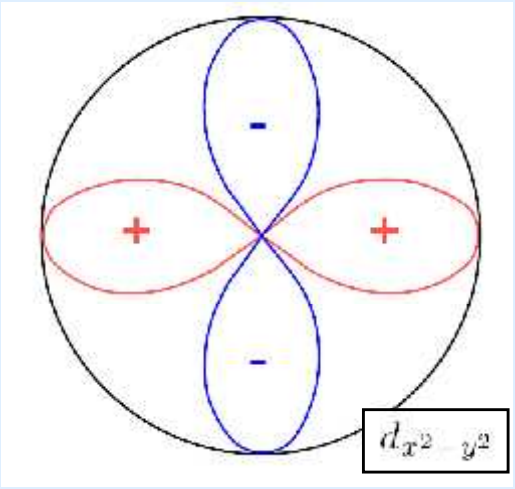

As the gap disappears along some directions of the Fermi surface ("nodes"), extremely-low-energy quasiparticles excitations (and therefore significant pair-breaking) may occur at very low temperature

s-wave Superconducting Gap

- BCS conventional pairing: isotropic *s*-wave pairing

s-wave gap

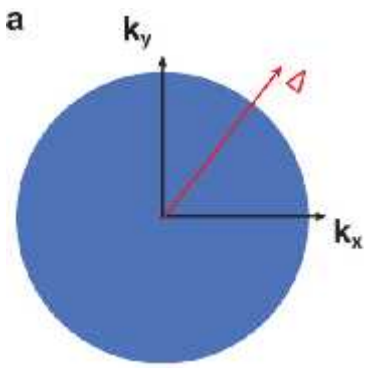

From μSR:

$$\sigma_\mu \propto \frac{1}{\lambda^2} = \frac{\mu_0 e^2}{m} n_S$$

$$n_S(T) = n_S(0)\left(1 - \frac{2}{k_B T}\int_0^\infty f(\varepsilon,T)[1-f(\varepsilon,T)]\,d\varepsilon\right)$$

and for an isotropic energy gap (s-wave):

$$n_S(T) = n_S(0)\left(1 - \sqrt{\frac{2\pi\Delta(0)}{k_B T}}\exp\left[-\frac{\Delta(0)}{k_B T}\right]\right)$$

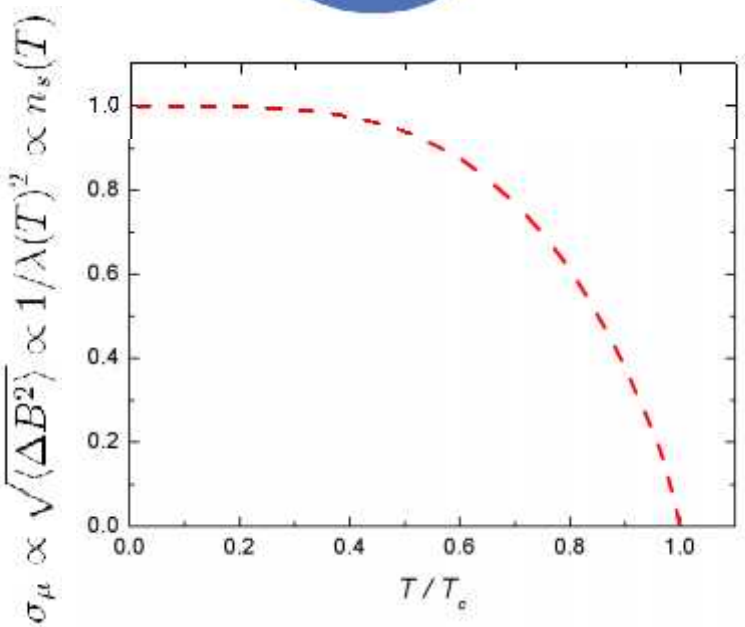

B. Mühlschlegel, Z. Phys. 155, 313 (1959)

d-wave Pairing Symmetry

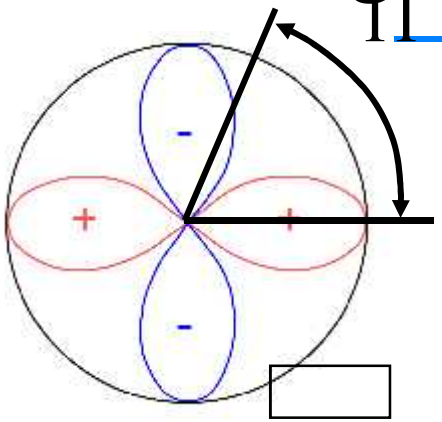

d-wave SC state:

$$n_s(T) = n_s(0)\left(1 - \frac{1}{\pi k_B T}\int_0^{2\pi}\int_0^{\infty} f(\epsilon,T)\,[1-f(\epsilon,T)]\,d\varphi\,d\epsilon\right)$$

with:

$$f(\epsilon,T) = \left(1+\exp\left[\sqrt{\epsilon^2 + |\Delta_s(T)\cos(2\varphi)|^2}/k_B T\right]\right)^{-1}$$

remembering that:

$$\lambda = \sqrt{\frac{m}{\mu_0 e^2 n_s}}$$

one gets: (for $T \ll T_c$)

$$n_s(T) \propto n_s(0)\left(1 - 2C\frac{T}{\Delta_s(0)}\right)$$

$$\lambda(T) \propto \lambda(0)\left(1 + C\frac{T}{\Delta_s(0)}\right)$$

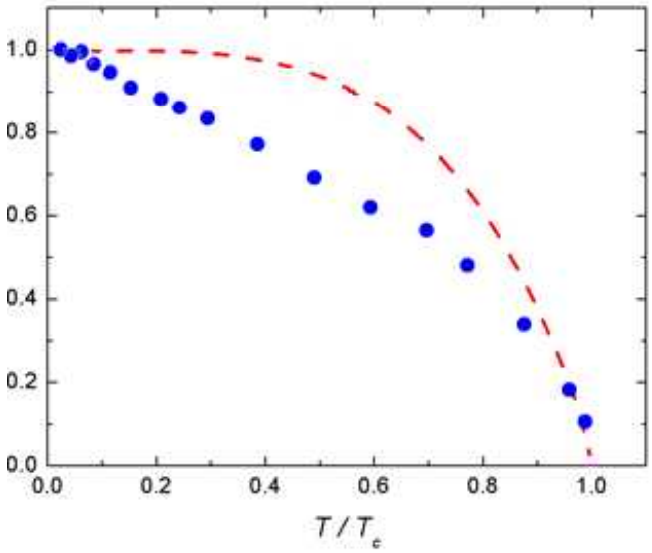

Single crystal $YBa_2Cu_3O_{6.95}$

*J.E. Sonier et al, PRL **72**, 744 (1994)*

Multiband Superconductivity

ARPES on $Ba_{1-x}K_xFe_2As_2$:

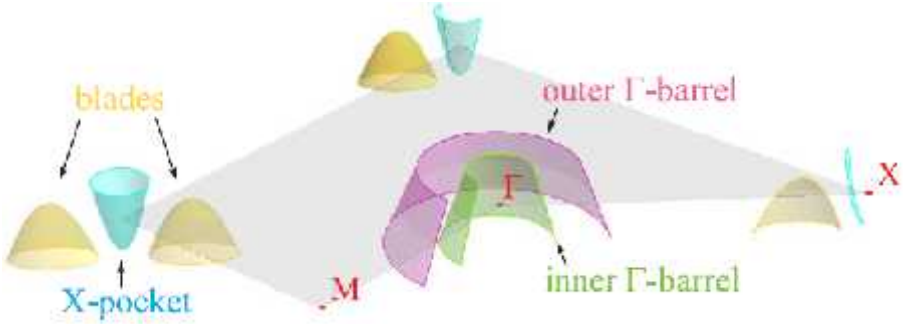

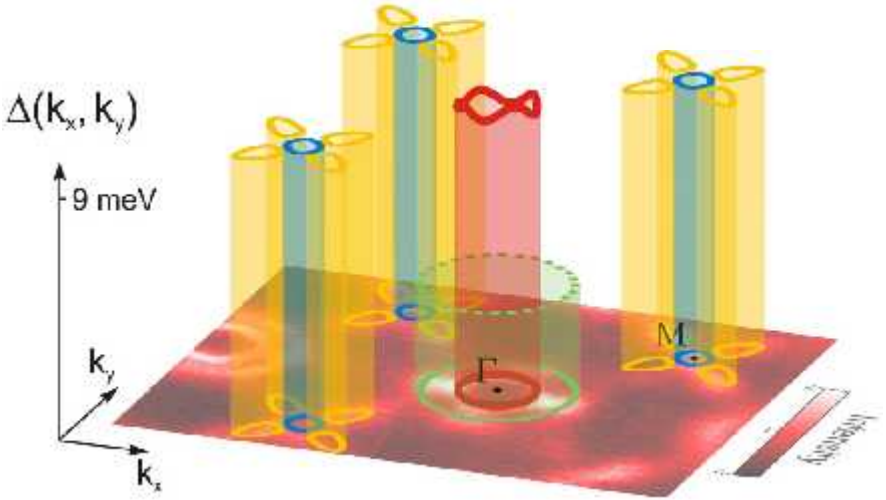

- Multiband superconductivity
- Nodeless gaps

$$\frac{\lambda^{-2}(T)}{\lambda^{-2}(0)} = \omega_1 \frac{\lambda^{-2}(T,\Delta_{0,1})}{\lambda^{-2}(0,\Delta_{0,1})} + \omega_2 \frac{\lambda^{-2}(T,\Delta_{0,2})}{\lambda^{-2}(0,\Delta_{0,2})}$$

V. B. Zabolotnyy *et al.*, Nature **457**, 569 (2009).
D. V. Evtushinsky *et al.*, Phys. Rev. B **79**, 054517 (2009).
D. V. Evtushinsky *et al.*, New J. Phys. **11**, 055069 (2009).

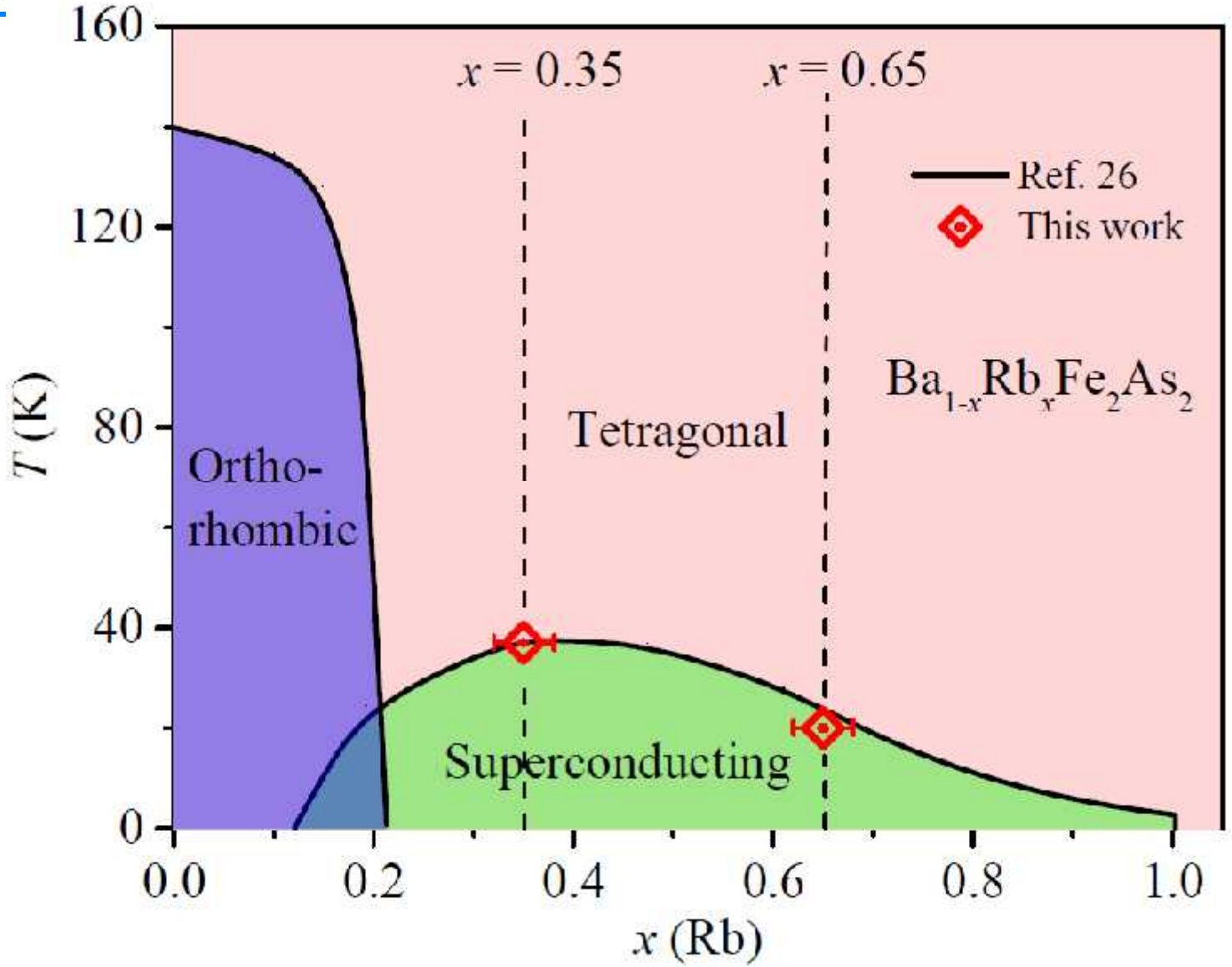
160
120
80
40
0
T (K)
0.0
0.2
0.4
0.6
0.8
1.0
x (Rb)
x = 0.35
x = 0.65
Ref. 26
This work
Ba1-xRbxFe2As2
Ortho-
rhombic
Tetragonal
Superconducting

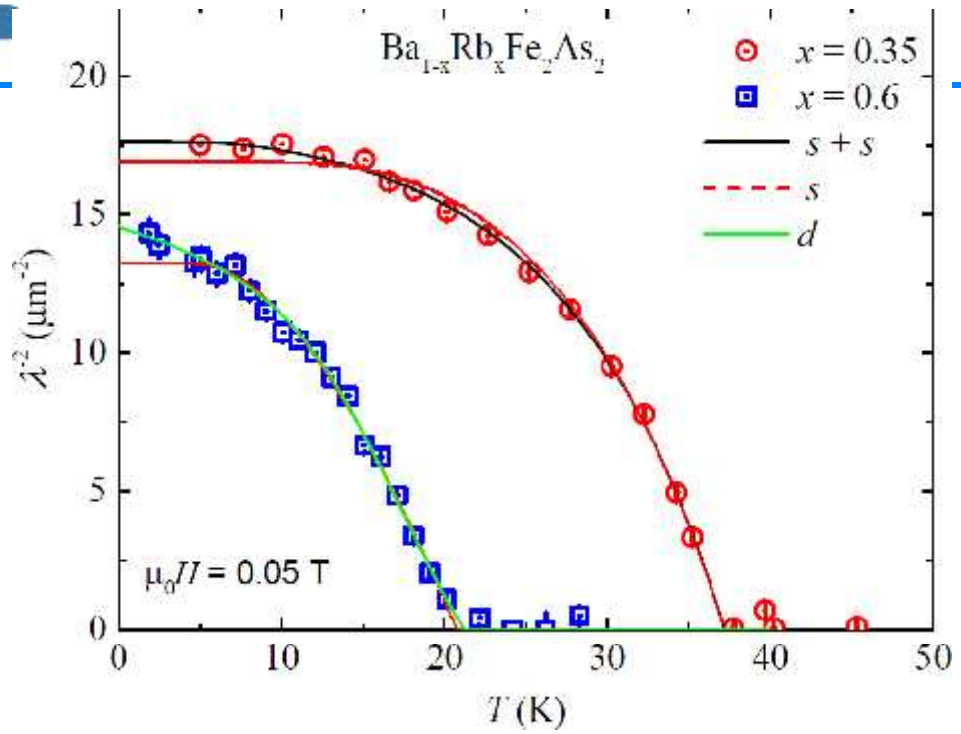

s-wave gap

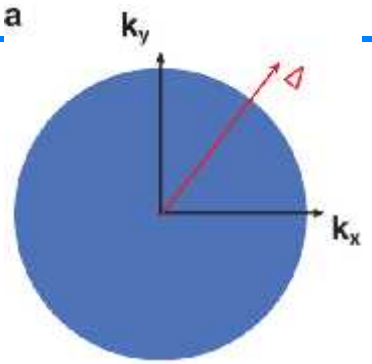

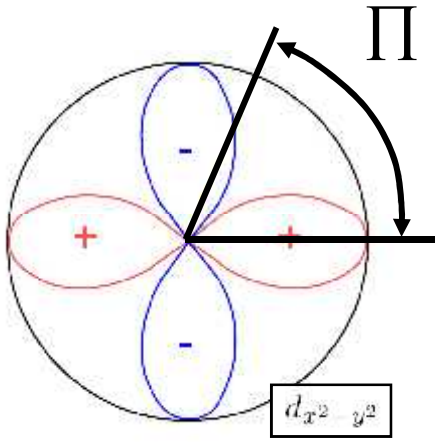

$$\rho_{tot}(T) = w\rho_1(T) + (1-w)\rho_2(T)$$

$$\rho_i(T) = \lambda_{ab}^{-2}(T, \Delta_{0,i}) / \lambda_{ab}^{-2}(0, \Delta_{0,i}),\ i = 1, 2$$

$$\Delta_{0,1} = 9.06(2)\text{mcV},\ \Delta_{0,2} = 1.50(2)\text{mcV},\ w = 0.51(2)$$

$\Delta_{0,1}$=1.1(3) meV, $\Delta_{0,2}$=7.5(2) meV, ω = 0.15(3).

Guguchia *et al.*, Phys. Rev. B **84,** 094513 (2011).

Melting of the vortex lattice

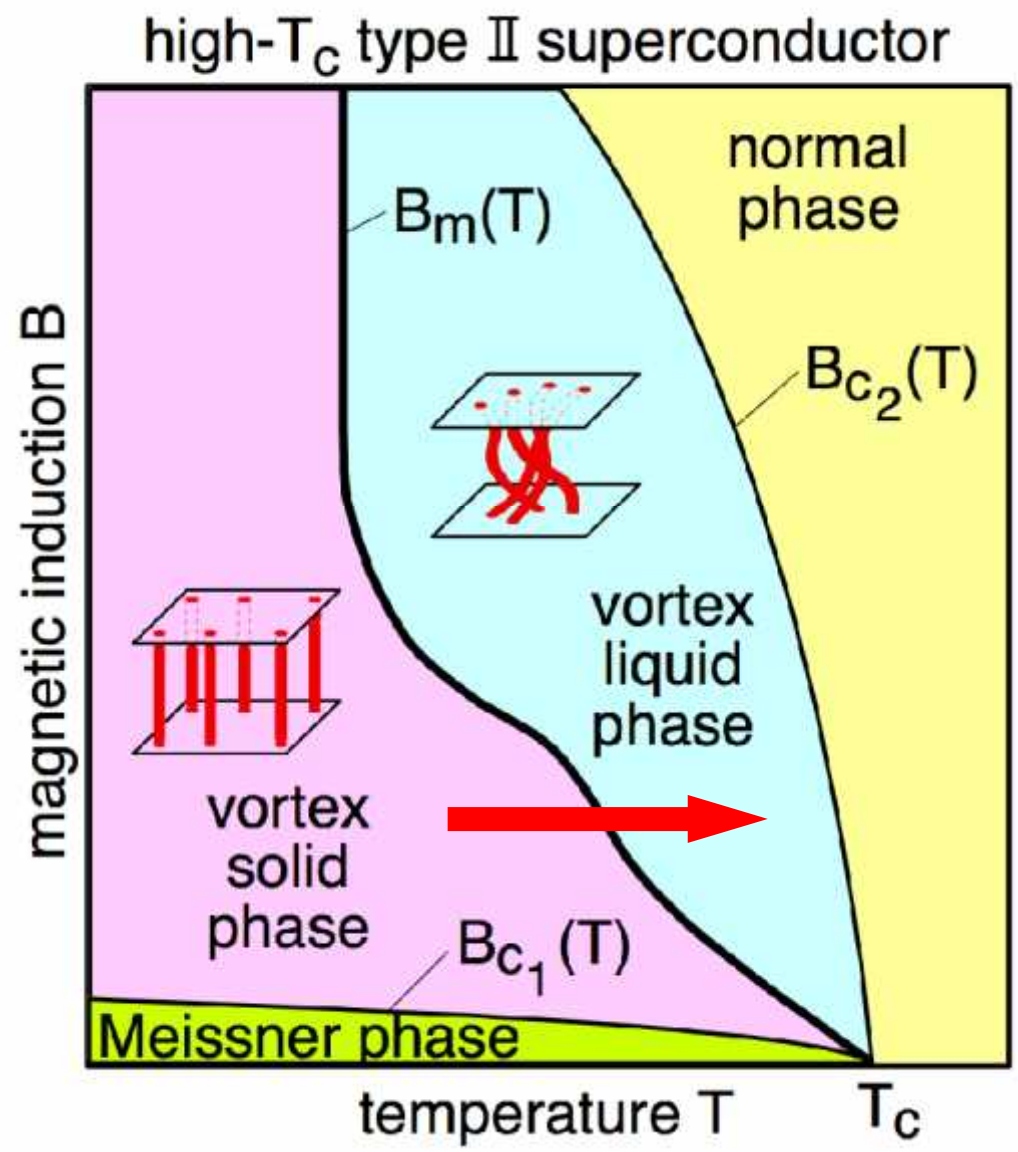

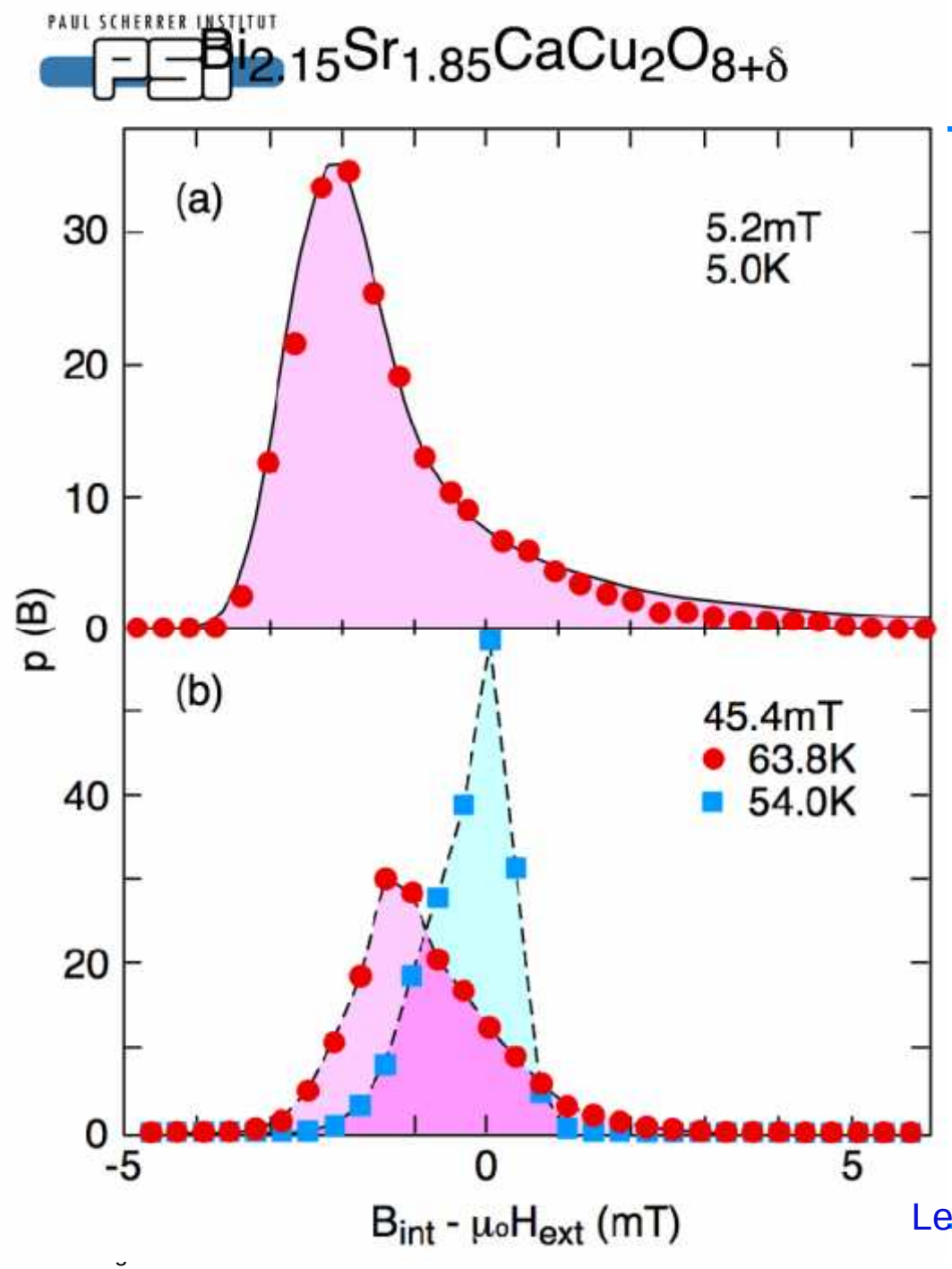

Vortex lattice melting

Lee *et al.*, Phys. Rev. Lett. **71**, 3862 (1993)

Lineshape asymmetry parameter α
“skewness parameter”

$$\alpha = \langle (\Delta B)^3 \rangle^{1/3} / \langle (\Delta B)^2 \rangle^{1/2}$$

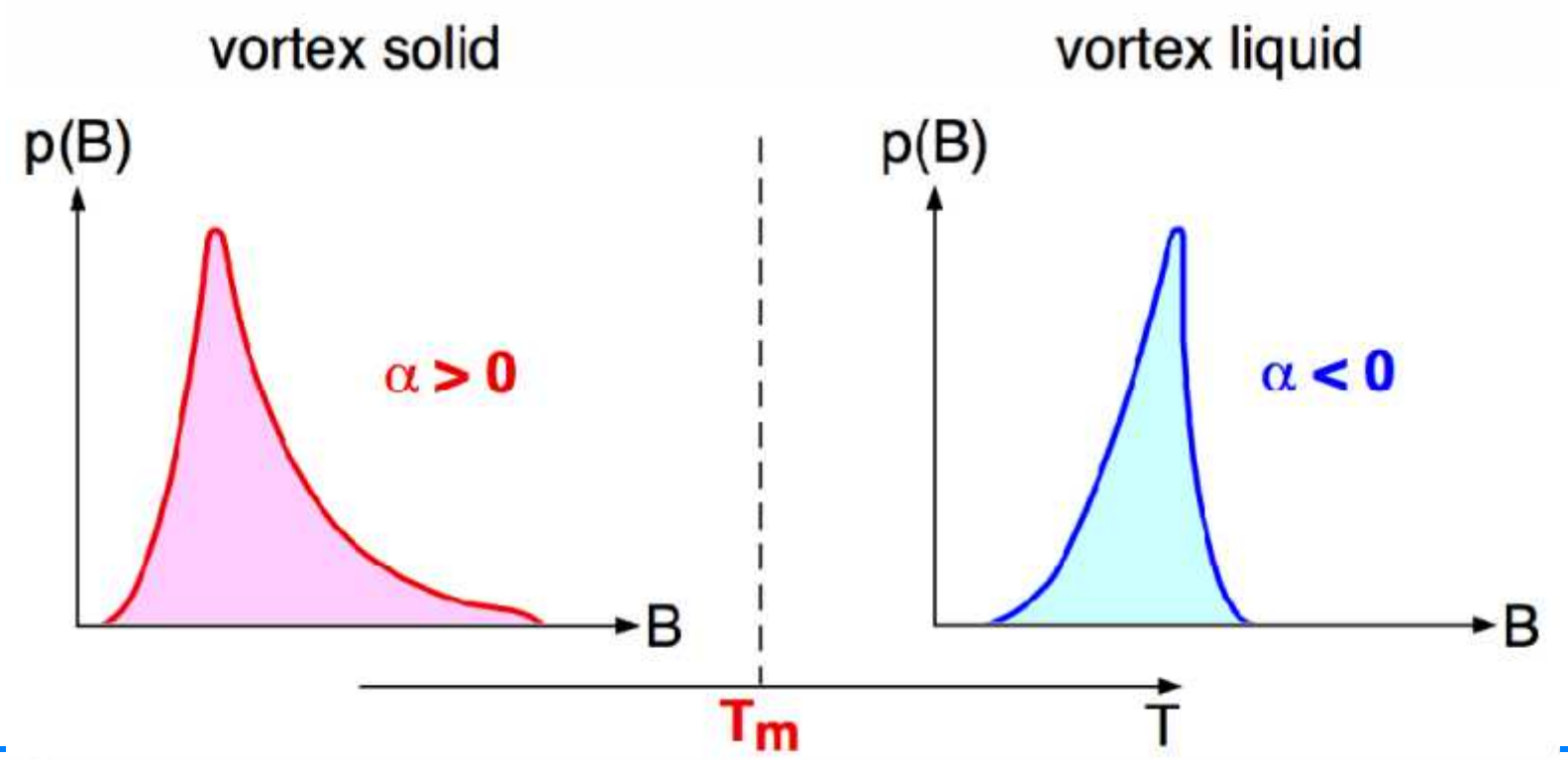

Vortex lattice melting

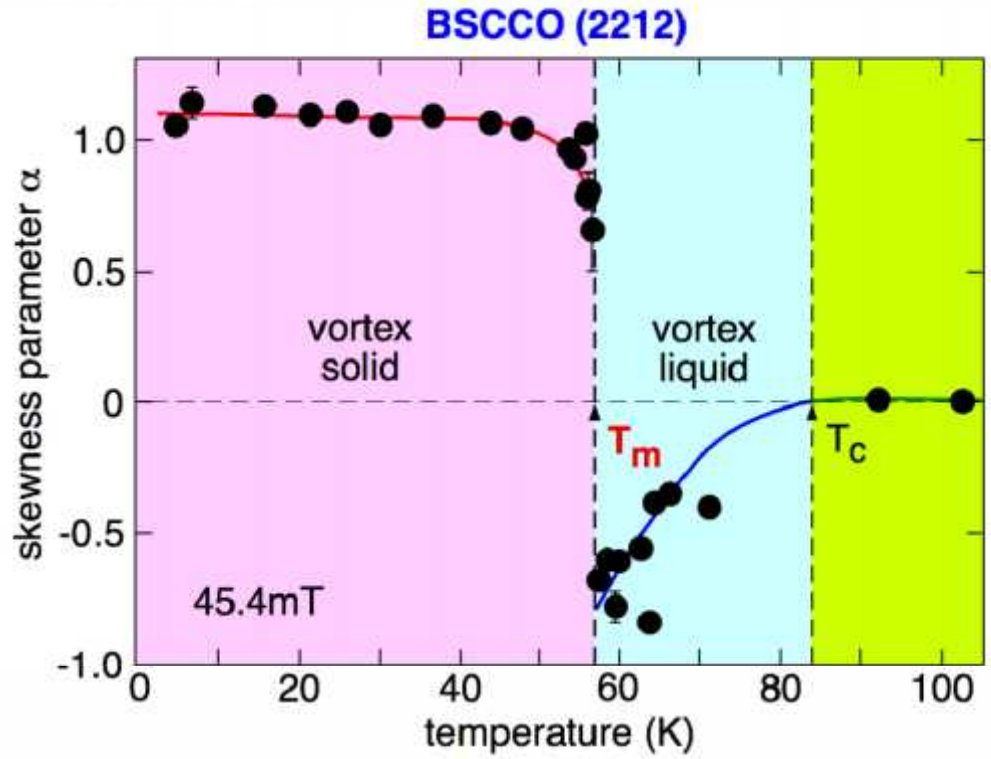

$$\alpha = \langle (\Delta B)^3 \rangle^{1/3} / \langle (\Delta B)^2 \rangle^{1/2}$$

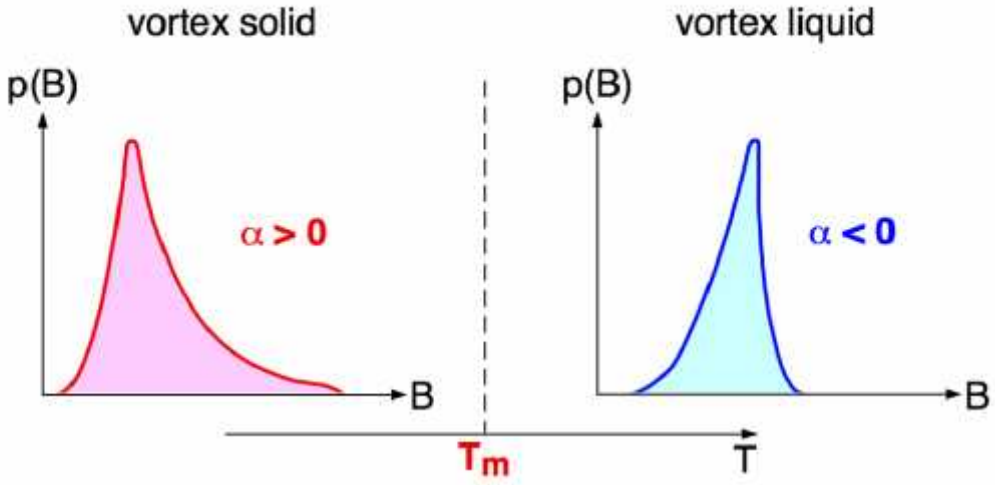

Lee *et al.*, Phys. Rev. Lett. **71**, 3862 (1993)

PAUL SCHERRER INSTITUT

PSI

Using Low Energy Muon Spin Rotation to Study Superconducting Materials

Zurab Guguchia

Low Energy μSR

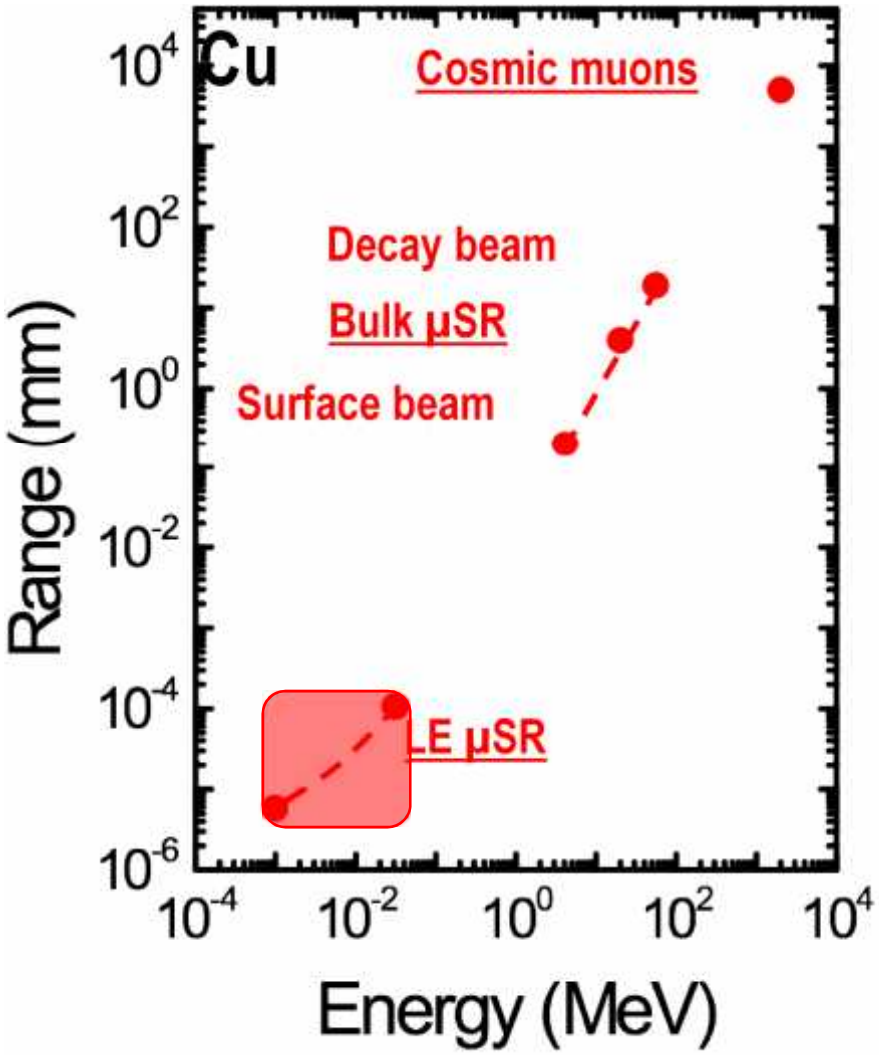

Variable muon energy: 0 – 30 keV

▼

Depth-sensitive local magnetic spin probe on the nm length scale

- Thin films
- Near-surface regions
- Multilayers
- Buried interfaces

Low Energy ⁺SR Apparatus

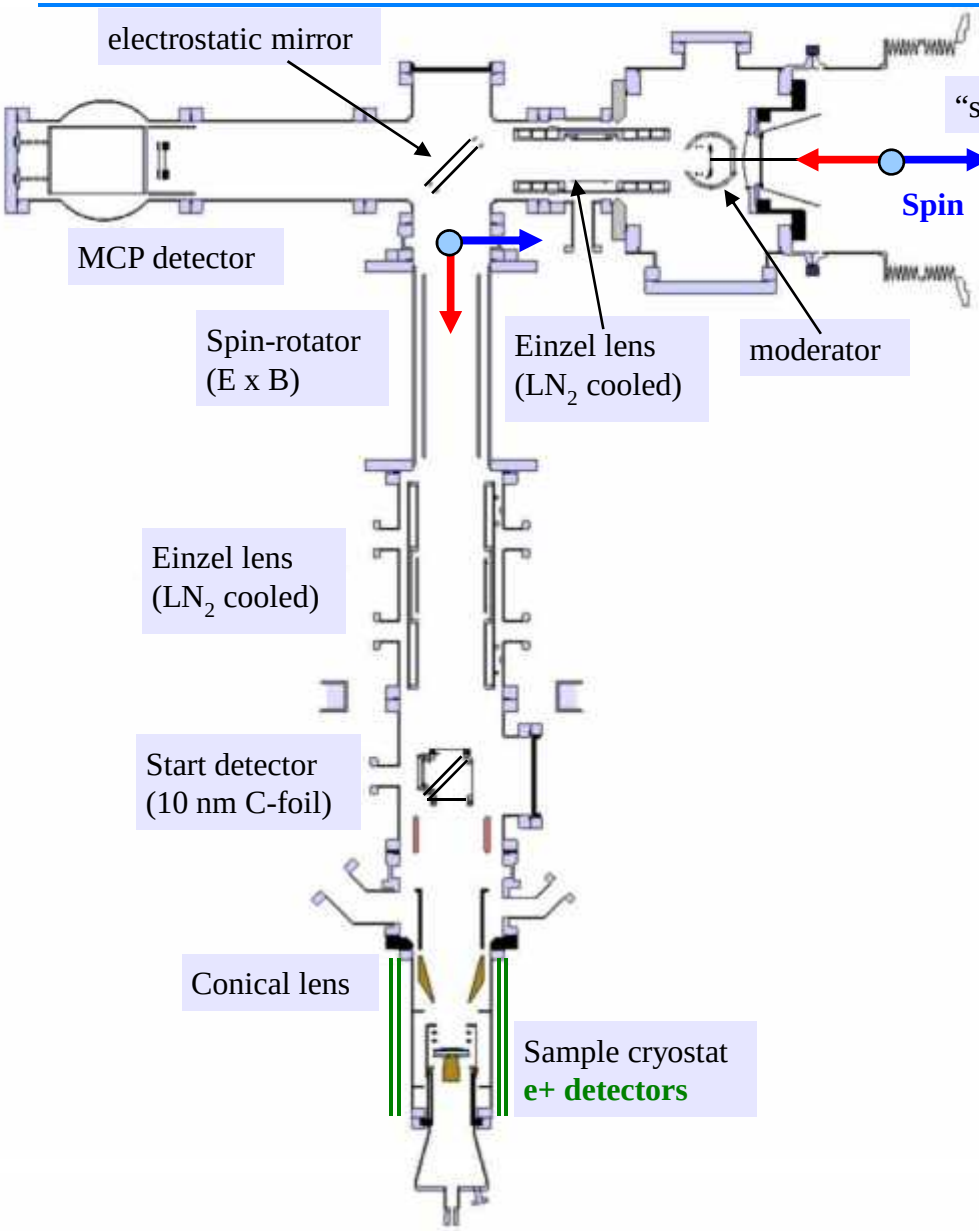

"surface" $^{+}$ beam, ~4 MeV

Spin

UltraHighVacuum

~ 10^{-10} mbar

Low Energy ⁺SR Apparatus

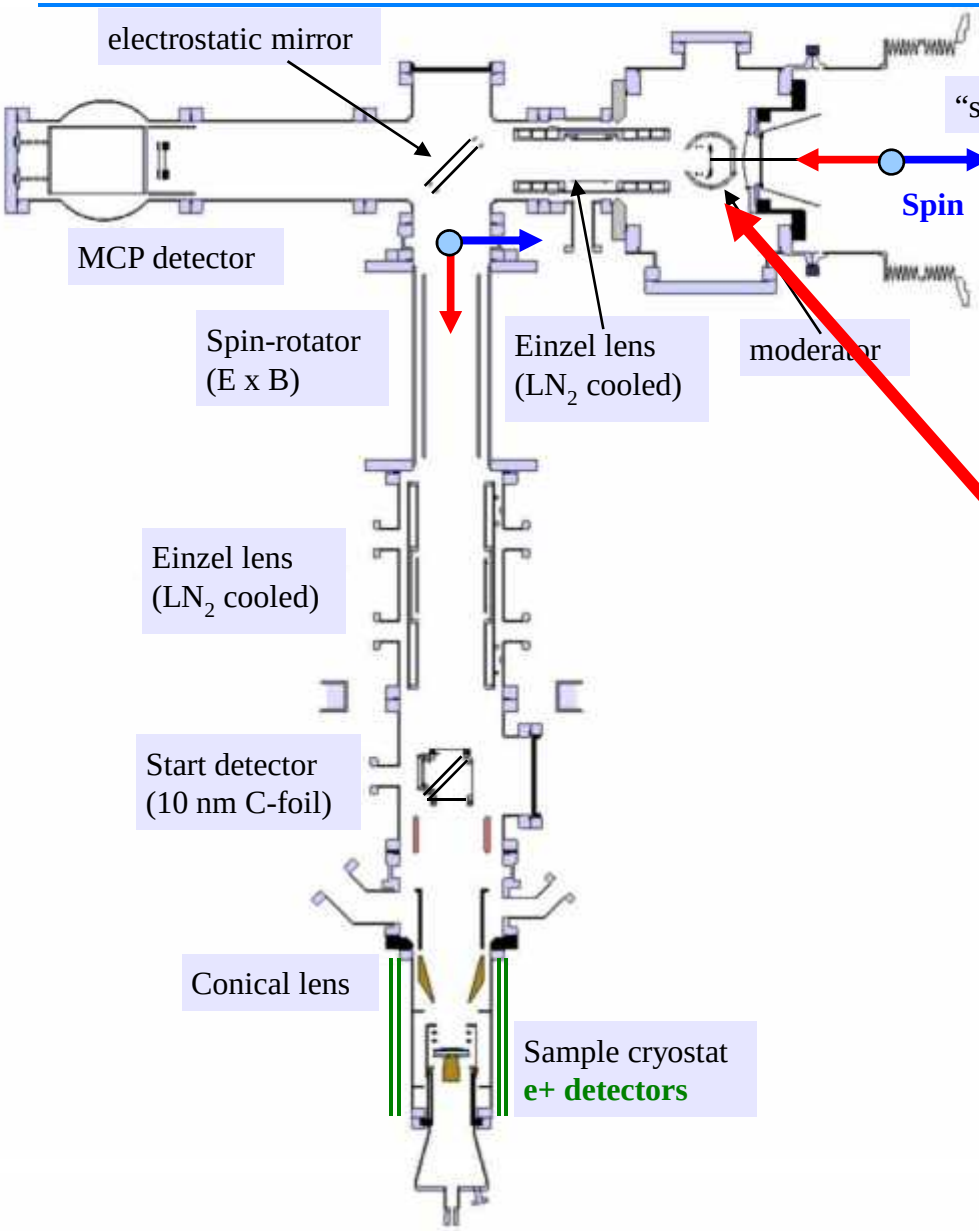

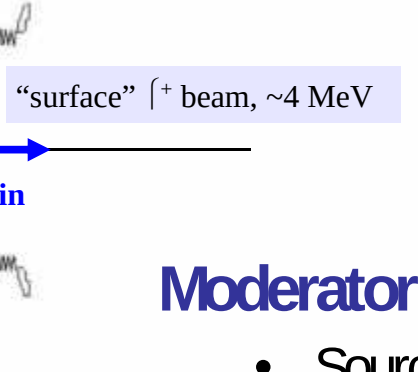

Moderator

- Source of low energy muons

Low Energy ⌠SR Apparatus

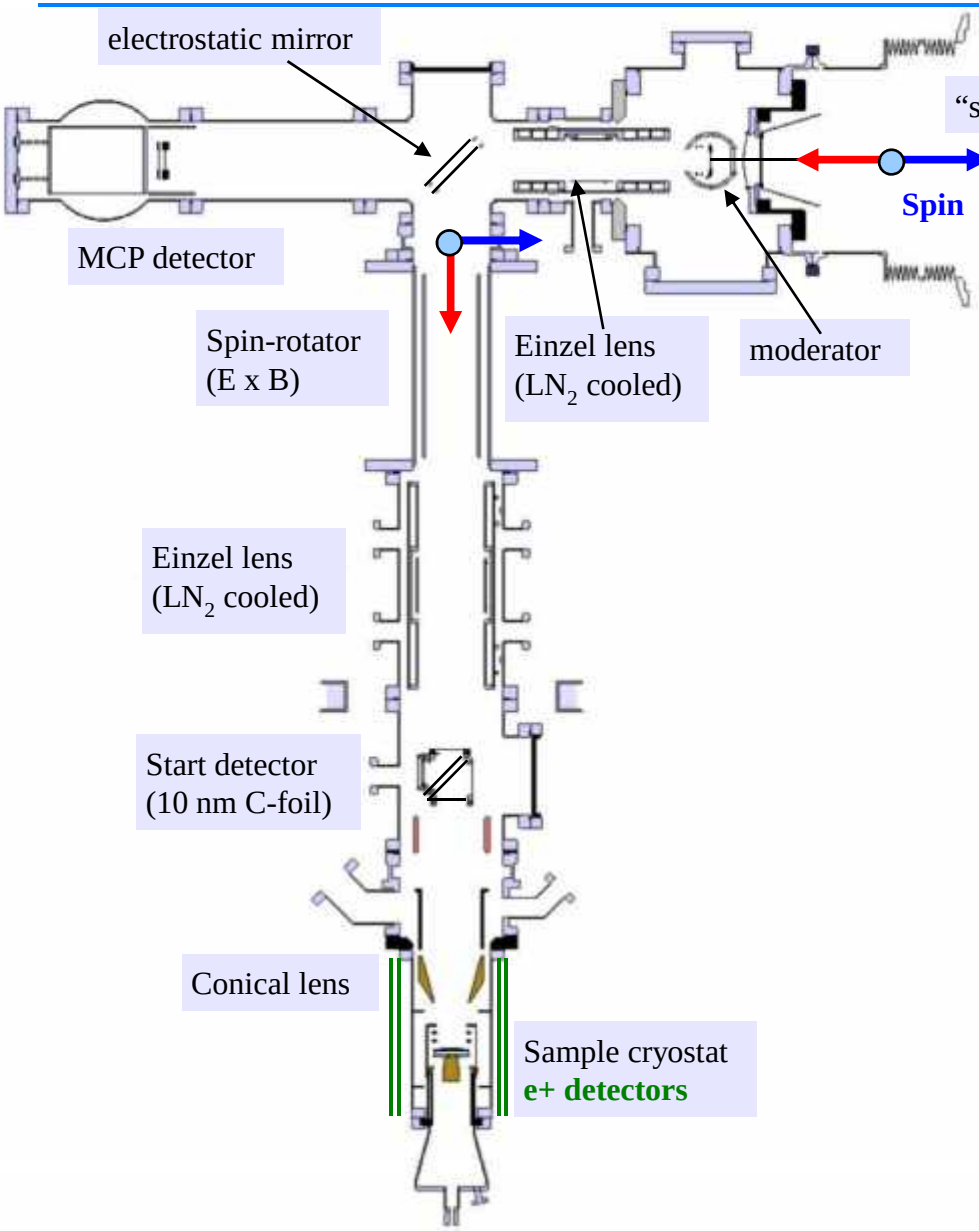

Moderator

15 eV ⌠+ 4 MeV ⌠+

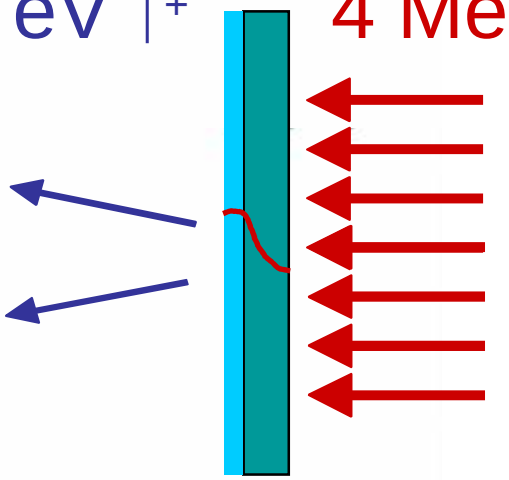

<500 nm <100 ⌠m

s-Ne, s- Ar, Ag at 6K

s-N_2

✦ Efficiency ~ 10^{-4} – 10^{-5}

Low Energy ⌠SR Apparatus

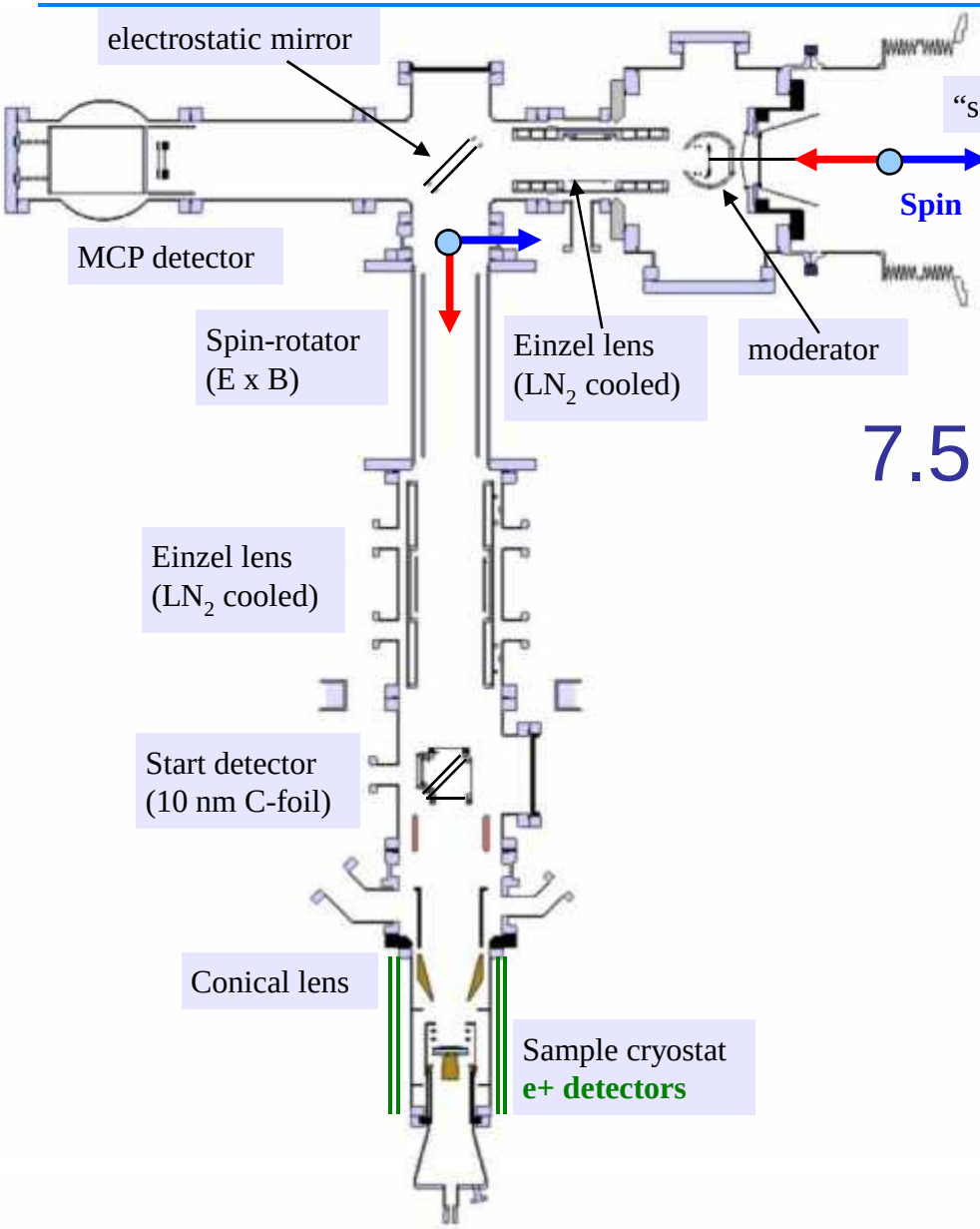

"surface" ⌠+ beam, ~4 MeV

Spin

Moderator

7.5 – 20 keV ⌠+

4 MeV ⌠+

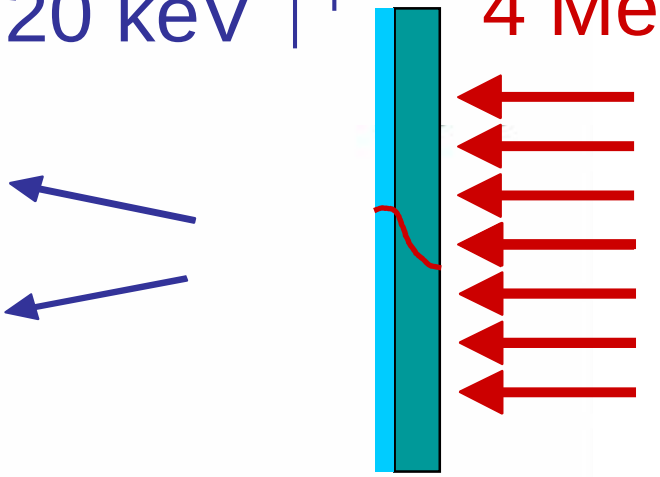

<500 nm <100 ⌠m

s-Ne, s- Ar, Ag at 6K

s-N_2

✦ Efficiency ~ 10^{-4} – 10^{-5}

Low Energy ⁺SR Apparatus

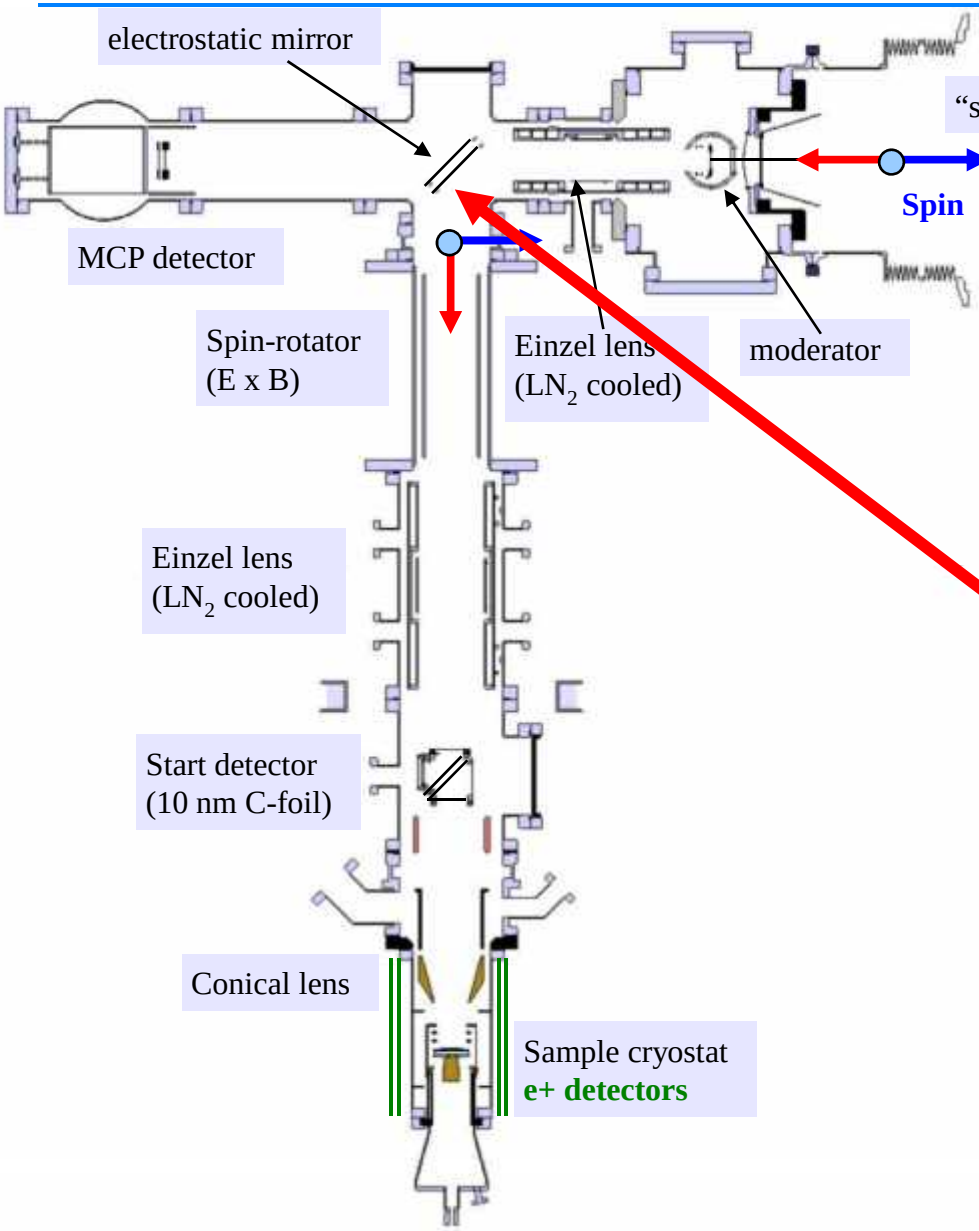

Electrostatic mirror

- Deflection of the low energy muons

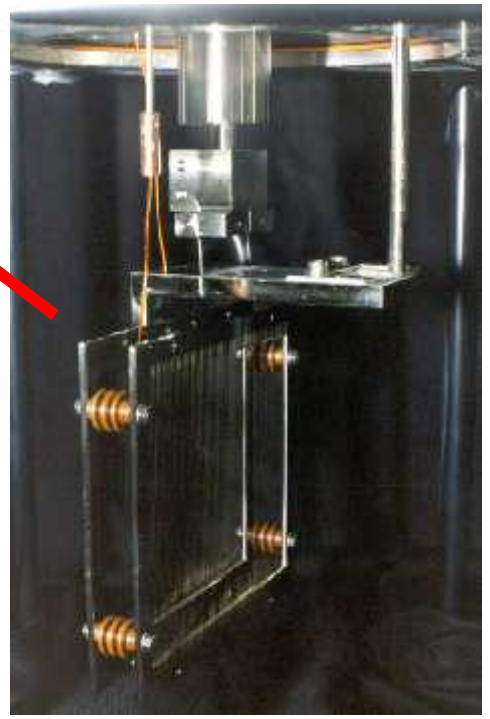

Low Energy ⁺SR Apparatus

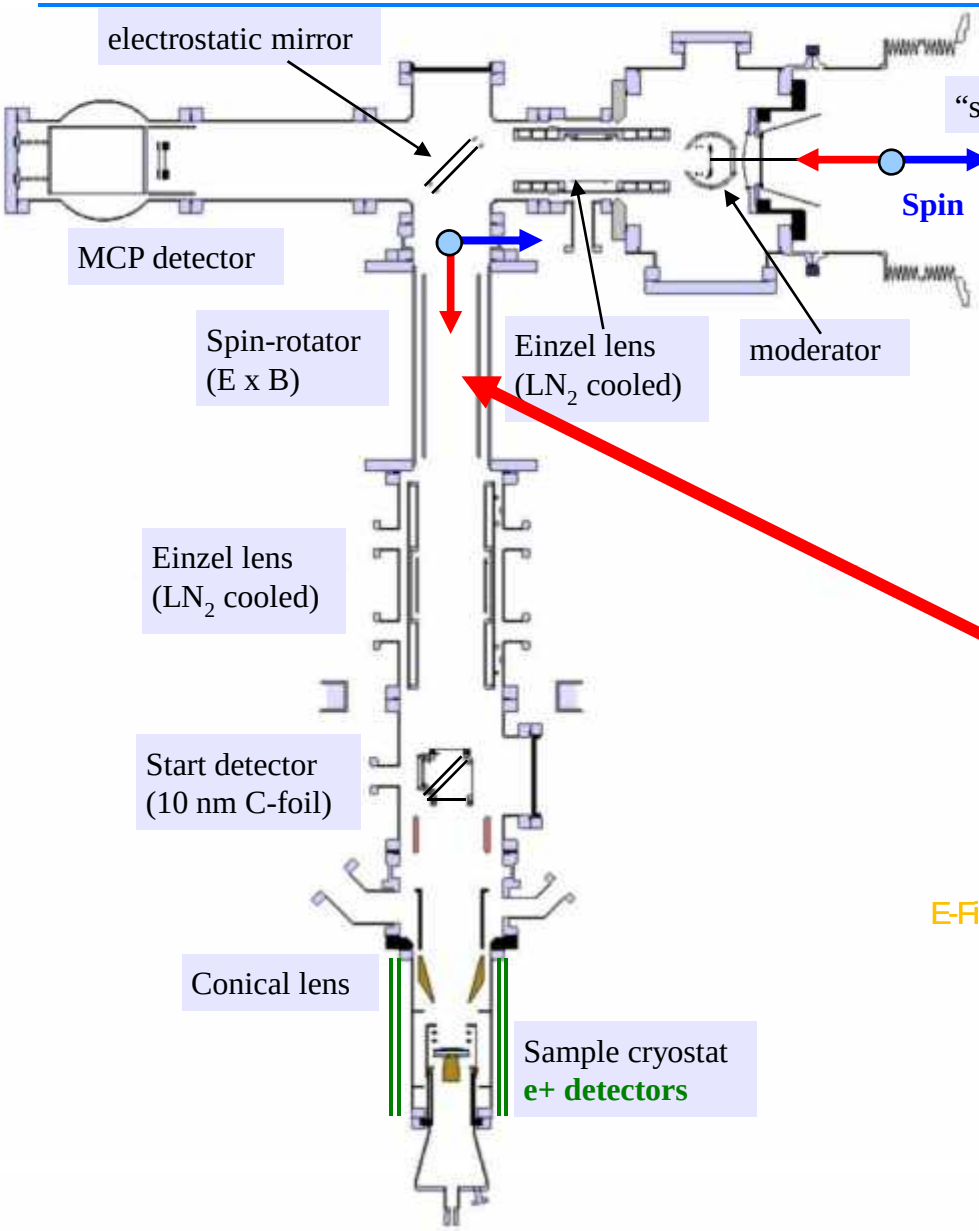

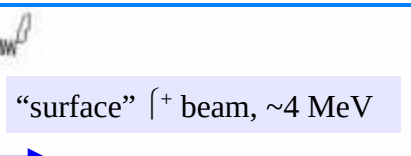

Spin Rotator

Rotates muon spin for different experimental conditions

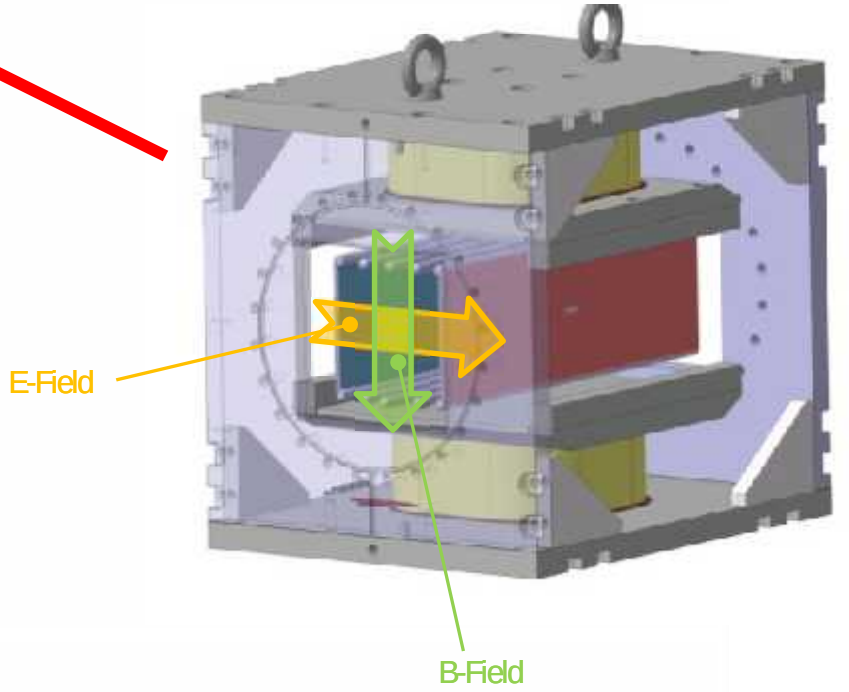

Low Energy ⁺SR Apparatus

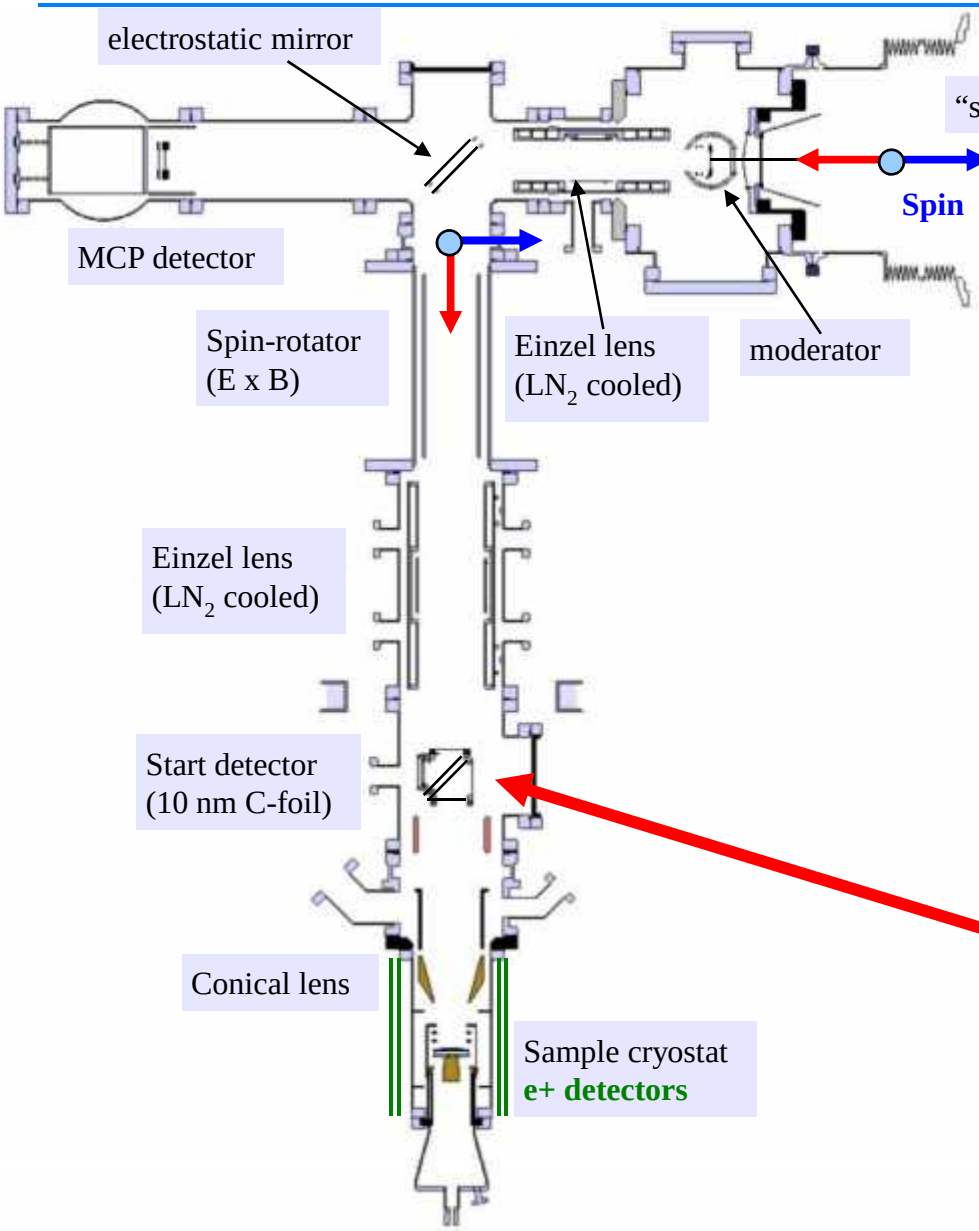

Trigger detector

- Start of the LE-⁺SR measurement
- Time-of-flight measurements

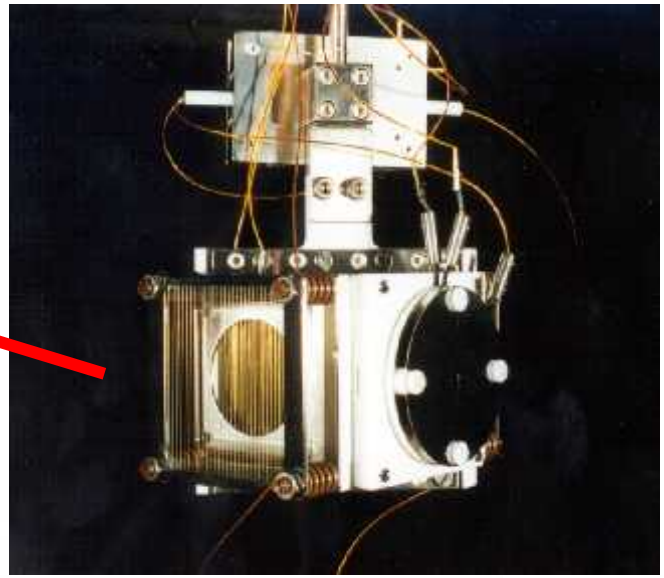

Low Energy ⌠SR Apparatus

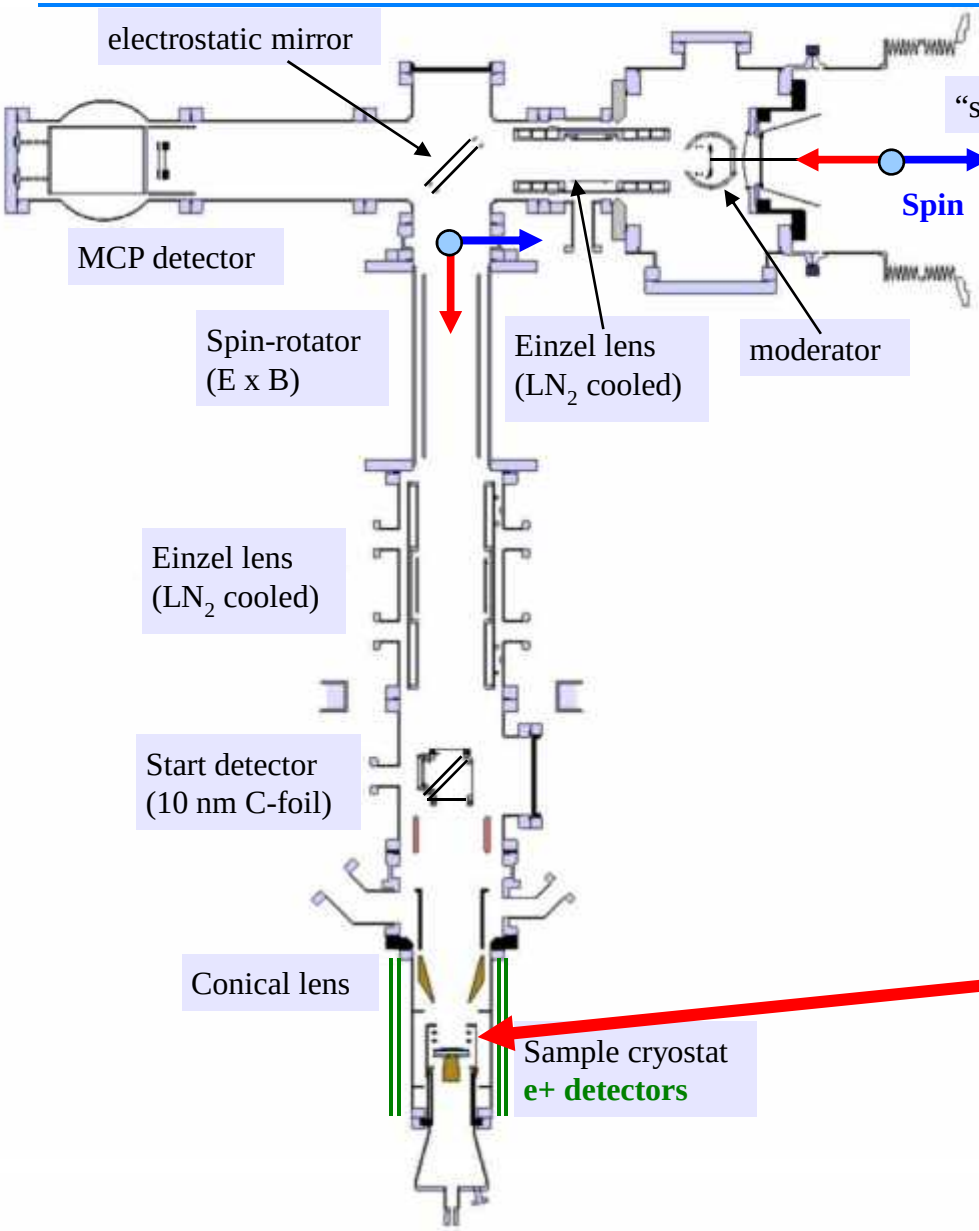

Sample cryostat

- Deceleration and acceleration of the ⌠+

Low Energy ⁺SR Apparatus

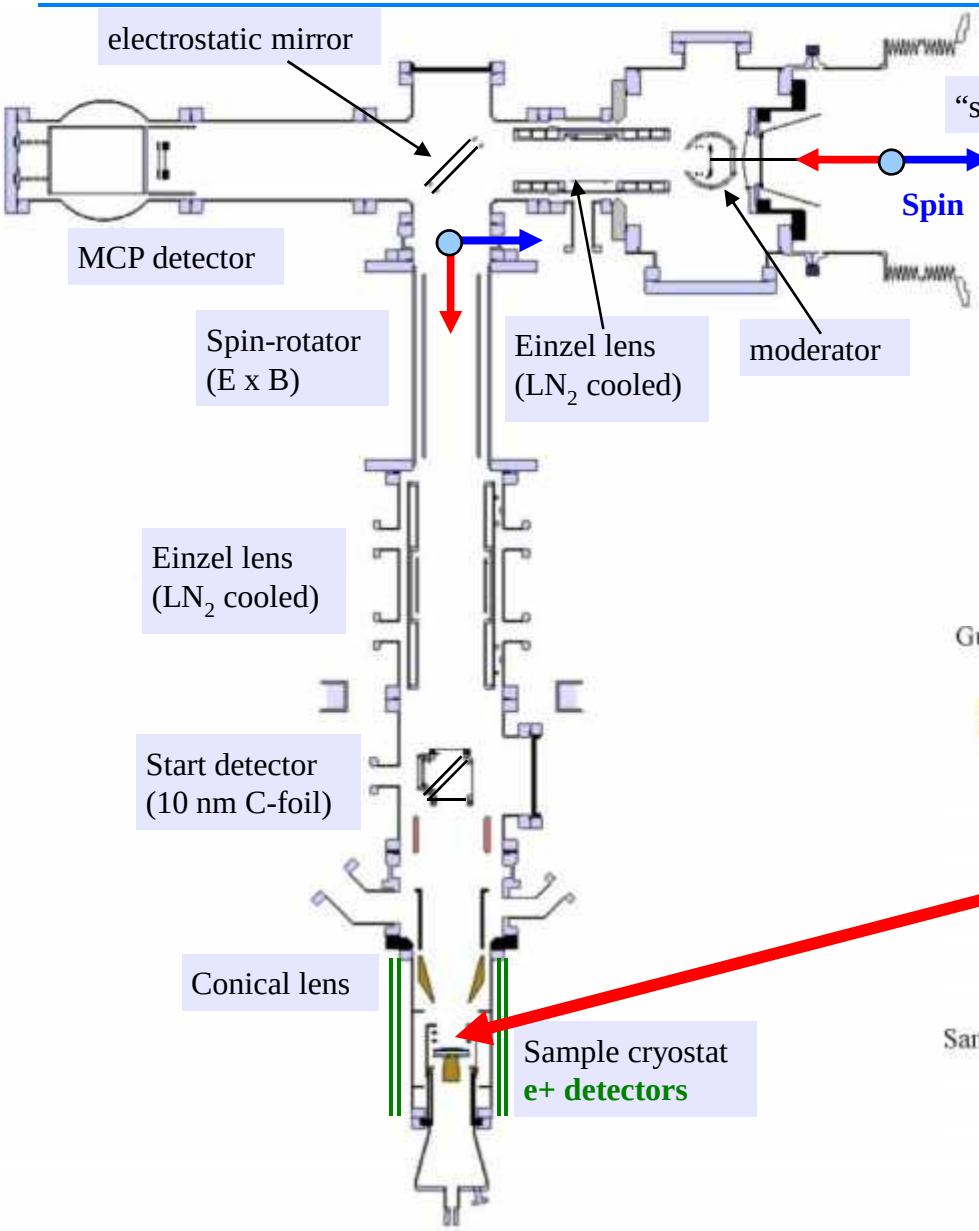

Sample cryostat

- Deceleration and acceleration of the ⁺

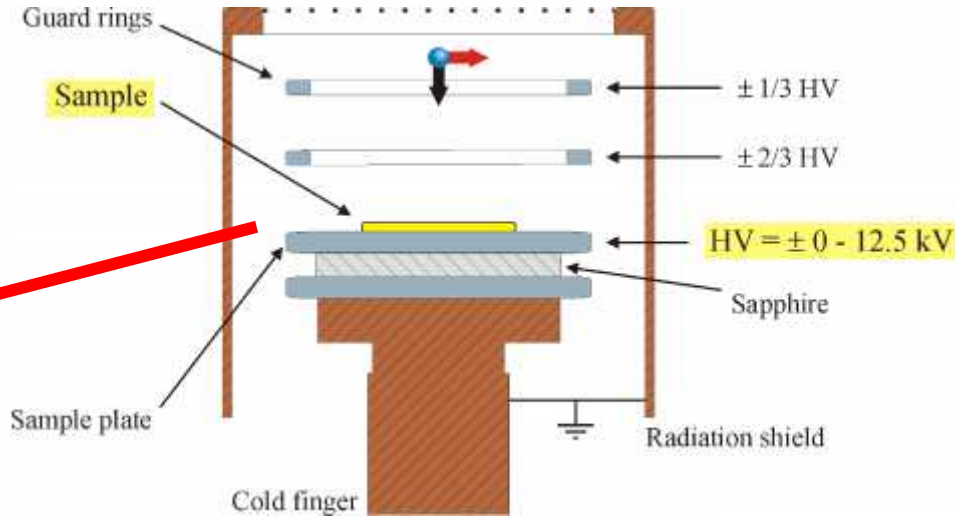

PAUL SCHERRER INSTITUT

Example:
Magnetic field profile in type-I and type-II superconductors

Depth dependent μSR measurements

$$B(z) = B_{ext} \exp(-z/\lambda)$$

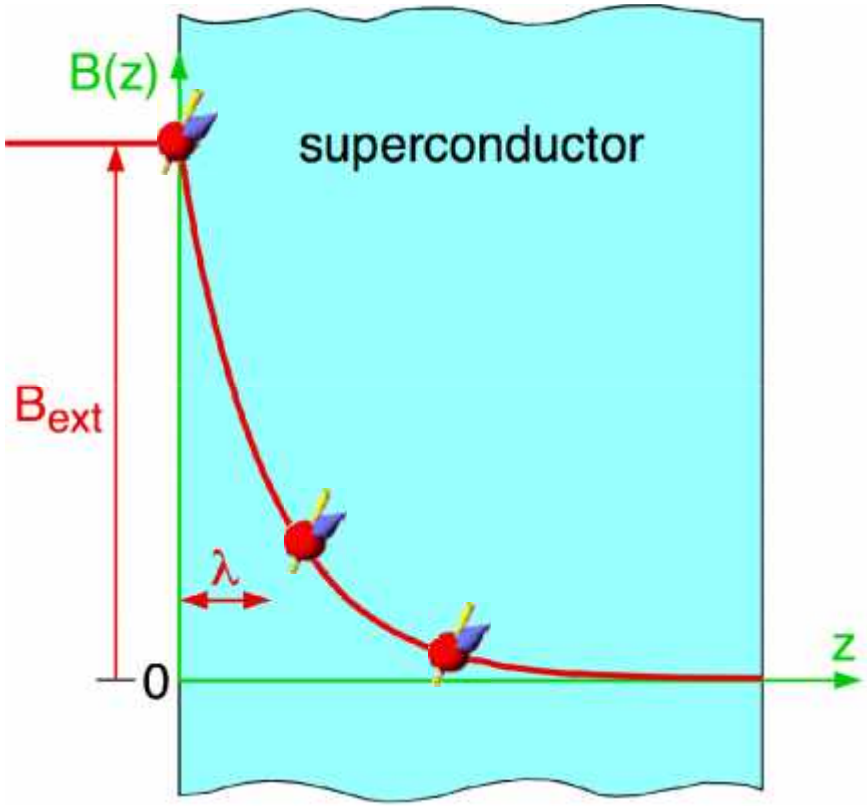

$$\omega_\mu(z) = \gamma_\mu B_{loc}(z)$$

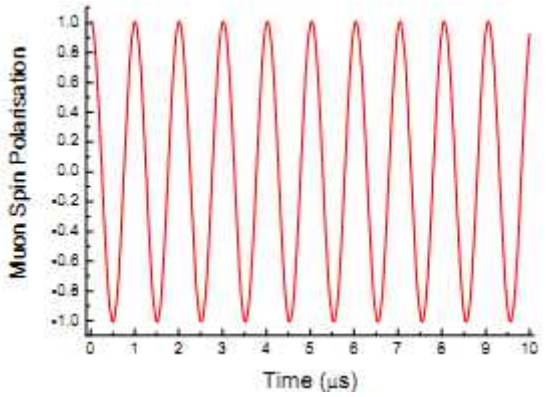

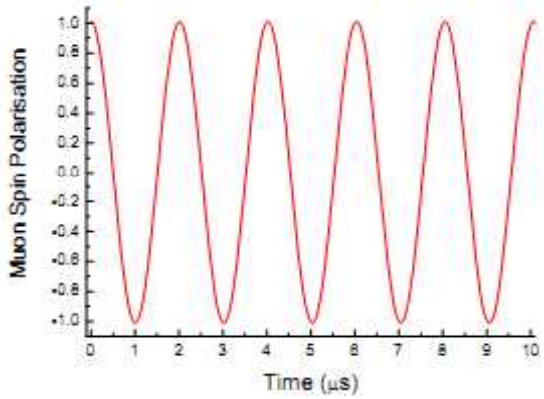

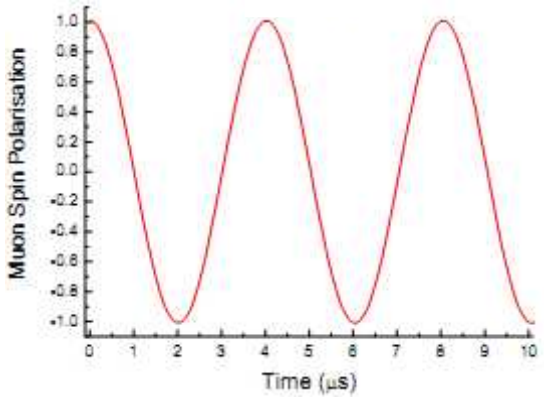

Jackson *et al*., Phys. Rev. Lett. **84**, 4958 (2000)

PAUL SCHERRER INSTITUT

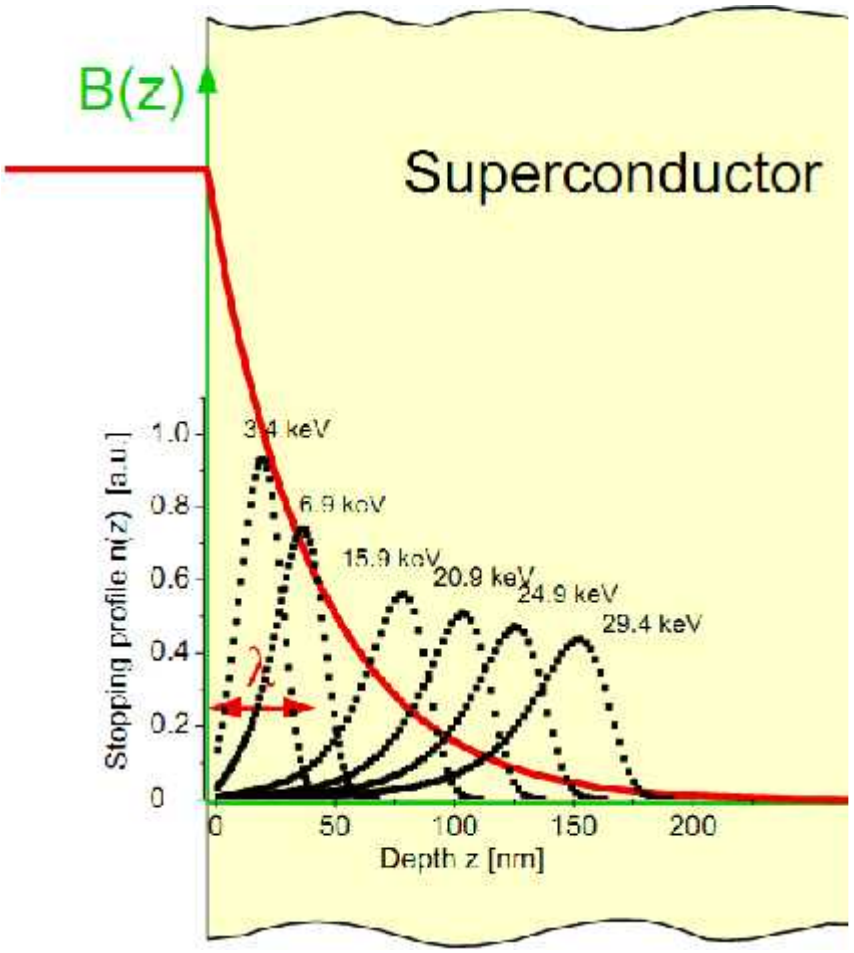

→ Magnetic field profile B(z) over nm scale

n(z,E): muon implantation profile for a particular muon energy E

μSR experiment ⇒ magnetic field probability distribution p(B, E) sensed by the muons

$$n(z,E)\,\mathrm{d}z = p(B,E)\,\mathrm{d}B$$

$$\int_0^z n(\zeta,E)\,\mathrm{d}\zeta = \int_{B(z)}^{\infty} p(\beta,E)\,\mathrm{d}\beta$$

⇒ B(z)

Jackson *et al.*, Phys. Rev. Lett. **84**, 4958 (2000)

Direct measurement of the magnetic penetration depth

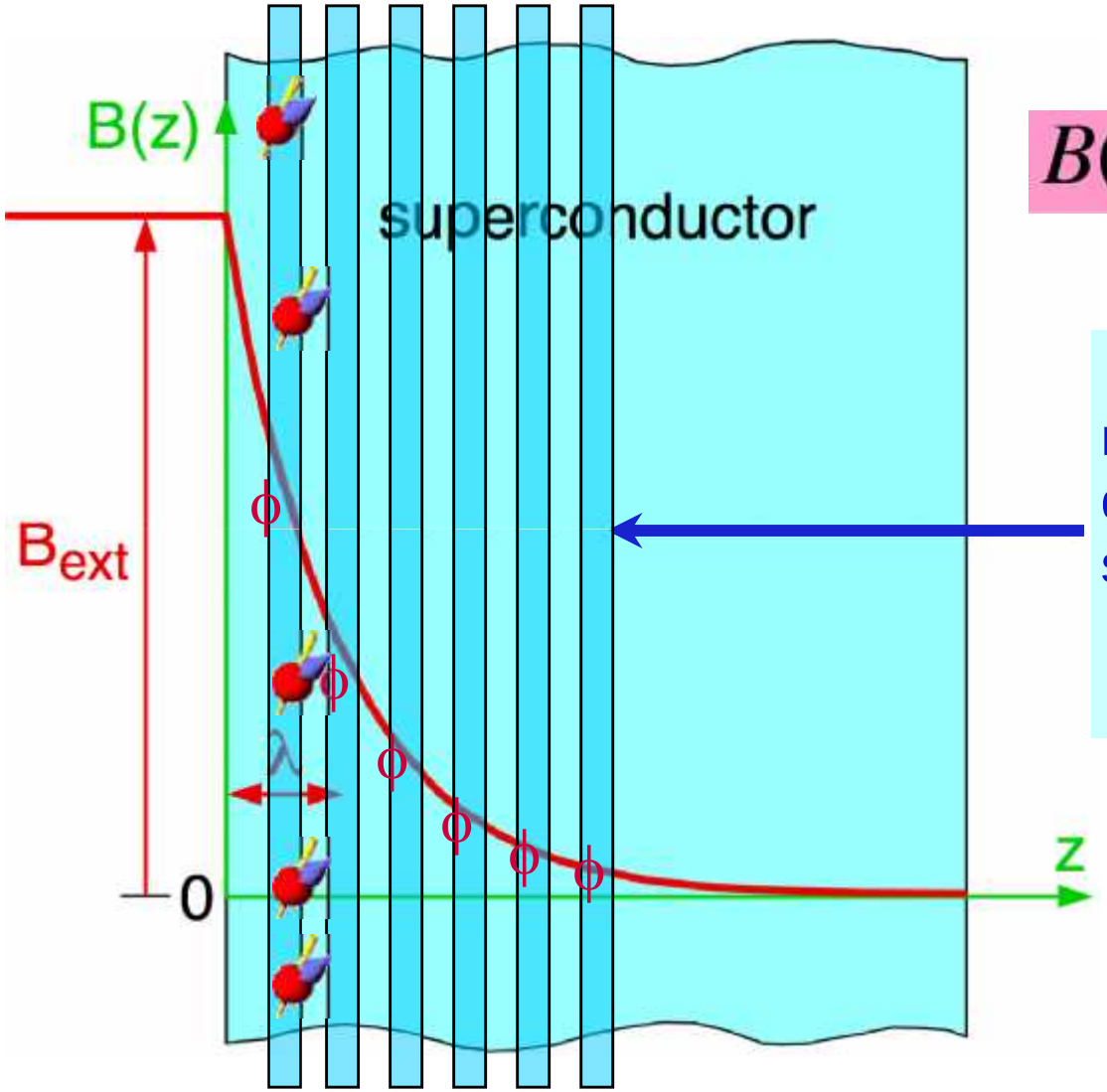

$$B(z) = B_{ext} \exp(-z/\lambda)$$

⌠SR experiment ® magnetic field probability distribution p(B) at the muon site

® p(B) ® B(z)

Jackson *et al.*, Phys. Rev. Lett. **84**, 4958 (2000)

Direct measurement of λ in a $YBa_2Cu_3O_{7-\delta}$ film

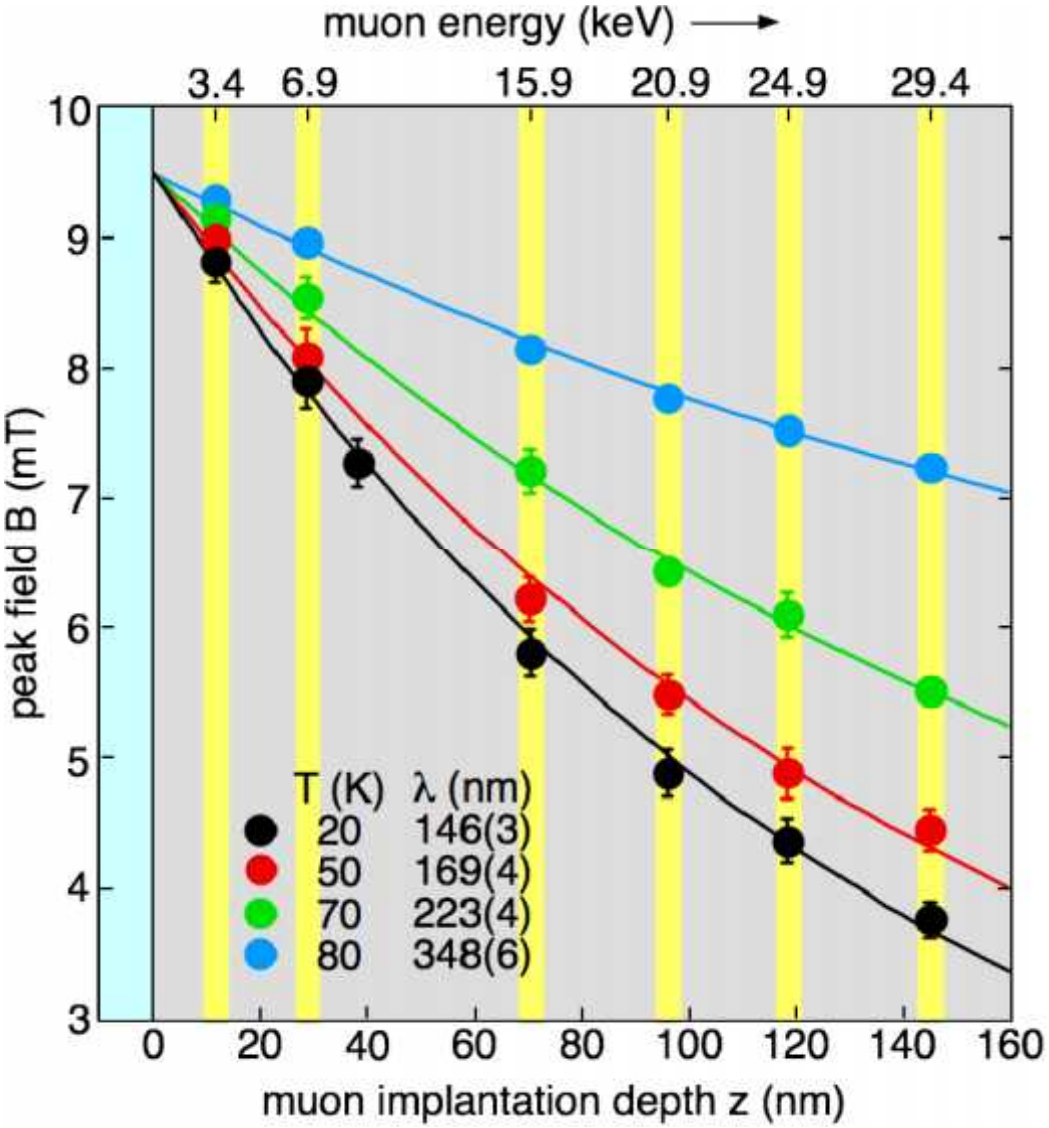

Jackson *et al.*, Phys. Rev. Lett. **84**, 4958 (2000)

PAUL SCHERRER INSTITUT

Summary

Muon Spin Rotation / Relaxation (⌠SR)

Magnetism:

- **Local probe**
  - Magnetic volume fraction
- **⌠SR frequency**
  - Magnetic order parameter (10^{-3} – 10^{-4} ⌠$_B$)
  - Temperature dependence
- **⌠SR relaxation rate**
  - Homogeneity of magnetism
- **Magnetic fluctuations**
  - Time window: 10^5 – 10^9 Hz

Superconductivity:

- **Field distribution of vortex lattice**
  - Penetration depth
  - Coherence length
  - Vortex dynamics
- **Absolute determination of penetration depth ⌡(0)**
- **Temperature dependency of**
  - Penetration depth, ⌡ ^{4} <⊗B^2>^{2} ⌠^{2}
  - Superfluid density n_s/m^* <⊗B^2> ⌠
  - → Symmetry of the SC gap function

Literature

BOOKS

•A. Yaouanc, P. Dalmas de Réotier, MUON SPIN ROTATION, RELAXATION and RESONANCE (Oxford University Press, 2010)

•A. Schenck, MUON SPIN ROTATION SPECTROSCOPY, (Adam Hilger, Bristol 1985)

•E. Karlsson, SOLID STATE PHENOMENA, As Seen by Muons, Protons, and Excited Nuclei, (Clarendon, Oxford 1995)

•S.L. Lee, S.H. Kilcoyne, R. Cywinski eds, MUON SCIENCE: MUONS IN PHYSICS; CHEMISTRY AND MATERIALS, (IOP Publishing, Bristol and Philadelphia, 1999)

•INTRODUCTORY ARTICLES

•S.J. Blundell, SPIN-POLARIZED MUONS IN CONDENSED MATTER PHYSICS, Contemporary Physics 40, 175 (1999)

•P. Bakule, E. Morenzoni, GENERATION AND APPLICATIONN OF SLOW POLARIZED MUONS, Contemporary Physics 45, 203-225 (2004).

REVIEW ARTICLES, APPLICATIONS

•P. Dalmas de Réotier and A. Yaouanc, MUON SPIN ROTATION AND RELAXATION IN MAGNETIC MATERIALS, J. Phys. Condens. Matter 9 (1997) pp. 9113-9166

•A. Schenck and F.N. Gygax, MAGNETIC MATERIALS STUDIED BY MUON SPIN ROTATION SPECTROSCOPY, In: Handbook of Magnetic Materials, edited by K.H.J. Buschow, Vol. 9 (Elsevier, Amsterdam 1995) pp. 57-302

•B.D. Patterson, MUONIUM STATES IN SEMICONDUCTORS, Rev. Mod. Phys. 60 (1988) pp. 69-159

•A. Amato, HEAVY-FERMION SYSTEMS STUDIED BY μSR TECHNIQUES, Rev. Mod. Phys., 69, 1119 (1997)

•V. Storchak, N. Prokovev, QUANTUM DIFFUSION OF MUONS AND MUONIUM ATOMS IN SOLIDS, Rev. Mod. Physics, 70, 929 (1998)

•J. Sonier, J. Brewer, R. Kiefl, ⌈SR STUDIES OF VORTEX STATE IN TYPE-II SUPERCONDUCTORS, Rev. Mod. Physics, 72, 769 (2000)

•E. Roduner, THE POSITIVE MUON AS A PROBE IN FREE RADICAL CHEMISTRY, Lecture Notes in Chemistry No. 49 (Springer Verlag, Berlin 1988)